Master's thesis

NTNU
Norwegian University of Science and Technology
Faculty of Natural Sciences
Department of Materials Science and Engineering

Emma Solhaug

Methods for K-impregnation of carbon materials and their effect on the CO_2 reactivity

Master's thesis in Material Science and Engineering
Supervisor: Merete Tangstad
Co-supervisor: Maria Wallin
June 2022

NTNU
Norwegian University of
Science and Technology

Emma Solhaug

Methods for K-impregnation of carbon materials and their effect on the CO_2 reactivity

Master's thesis in Material Science and Engineering
Supervisor: Merete Tangstad
Co-supervisor: Maria Wallin
June 2022

Norwegian University of Science and Technology
Faculty of Natural Sciences
Department of Materials Science and Engineering

NTNU
Norwegian University of
Science and Technology

Preface

This report investigates the effect of potassium on the CO_2 reactivity of carbon materials in the manganese alloy production. The work is a part of the subject TMT4905 Materials Technology, Master´s thesis at the department of Materials Technology and Engineering at the Norwegian University of Science and Technology, during the spring of 2022. This work is also a part of the NTNU´s contribution to the project named "KPN Reduced CO_2 emissions in metal production". The project aims to develop a basis for reduced climate effects from the production of Si, FeSi, Mn-alloy and TiO_2 slag to obtain 30% lower CO_2 emission in 2030 and zero CO_2 emission in 2050 [1].

It has been interesting to work on this project, and I would like to express my sincerest gratitude to my supervisors, Professor Merete Tangstad and Maria Wallin for their guidance. I am very grateful for the knowledge they have shared and time they have used to help me through this project. Another person I utterly thankful for is Hamideh Kaffash, her contribution to my experimental training and knowledge about carbon materials have been invaluable.

I would also like to thank all the technical staff from the Department of Material Science and Engineering. There are also some contributors from SINTEF that I would like to show my sincerest gratitude. Without them there would have been much more difficult to solve technical problems on the equipment during the experimental work.

Finally, I would like to acknowledge the people that have helped me on a personal level. My fellow students for supporting me and making the time as a student a time to remember. The students in my study hall also deserves some gratitude for always being a discussion partner or someone to drink coffee with. I also want to thank my family for always have supported me, and cheered on me. I would not come this far if it had not been for them.

Abstract

A large part of the Norwegian CO_2 emissions comes from fossil carbon sources used as reduction materials in the metallurgical industry. In the Norwegian manganese alloy production, coke is the most used carbon material for reducing the manganese ores. This thesis considers charcoal as a possible renewable substitute for coke. In earlier research it were found that there are several differing material properties between the two carbon materials, and this thesis studies the effect of the potassium present in the Mn-production and how the potassium affects the CO_2 reactivity of the carbon materials.

The experimental work in this thesis is based on two methods for increasing the potassium content in the carbon materials; gas K-impregnation and wet K-impregnation. Both methods resulted in increased potassium content compared to the raw materials, but the wet K-impregnation increased the potassium content the most with 8.71 and 10.53 $\%K_2O$ for impregnating using 5 molar solution. Later the samples were studied using SEM and CT, where several differences with the placement and size of the potassium particles were found. It turned out that the differences did not affect the CO_2 reactivity of the samples. For all the impregnated samples the CO_2 reactivity increased, and for the potassium levels above $3.5\%K_2O$ there is found that the CO_2 reactivity for all the carbon materials were between 0.030 to 0.045 %FixC/s. This means that both coke and charcoal will react with CO_2 with almost the same rate, which will make other material properties be more important when studying a change from coke to charcoal for the manganese production.

Sammendrag

En veldig stor andel av det norske CO_2 utslippet kommer som en følge av bruk av fossile karbon materialer i metall produksjon. I den norske mangan (Mn) produksjonen er koks mest brukt til å redusere manganmalmen. Denne masteroppgaven ser på trekull som en mulig fornybar karbon-kilde til å erstatte koks. En utfordring med å erstatte koks med trekull er at materialene har flere ulike egenskaper som vil påvirke driften av ovnen under produksjon. Denne oppgaven studerer karbon materialenes CO_2 reaktivitet og hvordan reaktiviteten blir påvirket av kaliumet som finner sted inne i ovnen.

Den eksperimentelle delen av arbeidet er basert på to impregnerings metoder for å øke innholdet av kalium i karbon materialene. De to metodene er gass K-impregnering og våt K-impregnering. Begge metodene resulterte i at karbon materialene fikk økt kalium innhold, og innholdet økte mest hos våt K-impregnering. Det høyeste kalium innholdet ble oppnådd ved å bruke en 5 molar løsning i våt impregneringen med resulterende 8.71 og 10.53 $\%K_2O$. Alle prøvene ble etterhvert både analysert i SEM og CT, hvor flere forskjeller mellom kalium partiklene på prøvene ble funnet. Disse forskjellene ble vist til å ikke påvirke CO_2 reaktiviteten i materialene. Til slutt ble CO_2 reaktiviteten på de impregnerte materialene målt, og viste at det var en økning i kalium innholdet for alle de ulike karbon materialene. For de materialene med over 3.5 $\%K_2O$, stabiliserte CO_2 reaktiviteten for alle de ulike karbon materialene seg på verdier mellom 0.030 og 0.045 %FixC/s. I praksis vil dette bety at for kalium verdiene som finnes inne i Mn-ovnen, vil både koks og trekull reagere med CO_2 med nesten lik hastighet. Noe som igjen vil gjøre de andre material egenskapene viktige å studere når det kommer til et eventuelt bytte fra koks til trekull som reduktant i Mn-produksjonen.

Contents

List of Figures

List of Tables

1 Introduction

Global warming and climate challenges is a large problem for different industries and researchers, and will change the world as we know it, if the problem stays unsolved. To solve this problem, 200 countries signed an agreement in 2005 stating that a limit for rise in temperature globally is 2 °C at the end of this century, compared to pre-industrial times. All countries that signed the agreement is required to put their best effort in, and many of the goals has a deadline to 2030 [2], [3].

The metal industry is the largest onshore industry in Norway and the major part of the Norwegian emissions comes from fossil carbon sources [4]. Another challenge with the metal industry is that the production of metals requires large quantities of energy and raw materials. In the Mn-alloy production, carbon is needed as a reducing agent, where coke is the most used carbon material. Studies have shown that the fossil coke that is most used in the manganese alloy production can be replaced by renewable bio-carbon [4]–[6]. The challenge when replacing coke with bio-carbon is that the carbon material properties will change, possibly affecting the carbon consumption, CO_2 reactivity and energy demand in the manganese alloy production.

CO_2 reactivity determines the rate of carbon materials reacting in the furnace, where bio-carbon, here charcoal, has a higher CO_2 reactivity than coke [6], [7]. Earlier research have focused on methods for reducing the CO_2 reactivity of charcoal [8]–[10], while this project will focus on the effect the potassium in the Mn-alloy production has on the carbon materials CO_2 reactivity. At NTNU the most used method for impregnating charcoal with potassium is by gas impregnation, in this study the gas impregnation is compared to a wet impregnation method to find an impregnation method that gives charcoal with high amounts of potassium. Potassium is a known catalyst for the CO_2 reactivity, and the effect of potassium on charcoal and coke will be studied in order to see how the CO_2 reactivity changes with changed potassium content.

1.1 Manganese ferroalloy Production Process

Manganese (Mn) alloys is a carbothermic reduction process where the manganese ore is reduced in a Submerged Arc Furnace (SAF). A typical SAF is a circular furnace with three electrodes as showed in Figure 1.1. There are several manganese alloys, but are most often produced as alloys containing Mn, Fe and C, and in some cases Si. These alloys are referred to as ferromanganese (FeMn) or silicomanganese (SiMn) alloys [11] depending on the Si content. The alloys will be ferromanganese alloys if the silicon content is less than 2%. In silicomanganese alloys the silicon content typically is between 16-30% Si. The production of FeMn and SiMn is quite similar, but the SiMn will have a quartz as a raw material. In this paper, the production of SiMn will be explained.

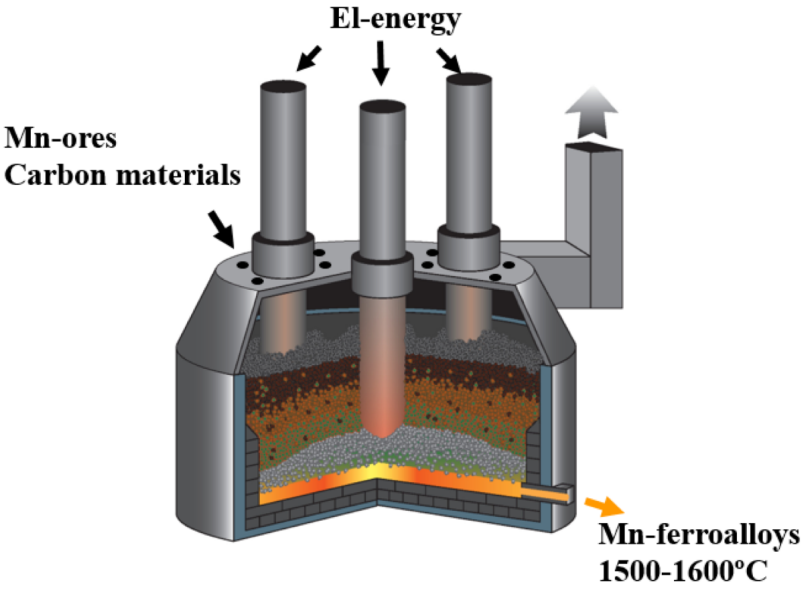

Figure 1.1: A figure showing the set up in the SAF when producing manganese alloys. [12]

The production of manganese alloys is as mentioned done by a carbothermic reduction of the manganese ore. This because Mn is in nature bound to oxygen as manganese oxides, and occur as MnO_2 and Mn_2O_3 in the manganese ores, but Mn_3O_4 in heat treated materials like e.g. sinter. The manganese ore includes other oxides like iron oxide, Fe_2O_3, calcium oxide, CaO, silicon oxide, SiO_2, aluminum oxide, Al_2O_3, and magnesium oxide, MgO, and other minor oxides. To remove the oxygen from the manganese oxide carbon materials is used as reductant in an electric furnace.

Typically, coke is used as a reductant for the Mn-alloy production, where the reduction takes place then the electrodes is submerged into the raw material and the electrode tip is in the coke bed at the bottom of the furnace. When electric energy is transported from the electrode tip, through the coke bed, the resistance in the carbon materials will generate heat which will heat up the furnace resulting in reduced oxides leading to melted metal. The electric energy used for the production in the SAF comes from electric currents in the furnace, where the current runs through the electrodes, into the solid coke and then into the metal bath at the bottom of the furnace [13]. The size of the coke bed is dependent on how much carbon material added to the SAF, but also the consumption of carbon. This makes the carbon bed size possible to adjust. The coke bed gives the carbon material a second task as a heat provider next to being the reductant.

The raw materials, or the charge, is added to the furnace from the top, and this can be seen in Figure 1.1. In this figure, there is a coke bed at the bottom near the electrode tip, and how the raw materials will be reduced while descending into the furnace [11], [14], [15]. Other raw materials than Mn-ore, carbon material and quartz normally used in the production of SiMn is fluxes. The fluxes added will end up in the slag, and is added to improve the slag properties. Typical fluxes used is limestone ($CaCO_3$) and dolomite ($(Mg, Ca)CO_3$) [15].

As the charge drifts down inside the furnace while the temperature increases as the ma-

terials descend in the SAF and the warm CO (g) ascend. The warm CO(g) heat up and reacts with the charge and the Reactions 1.1, 1.2 and 1.3 will take place with increasing temperature [13]. These three reactions make a part of the pre-reduction zone in the SAF, and since these reactions are exothermic they contribute to another temperature increase inside the furnace. All the pre-reduction zone is given as the reduction reactions above the green line in Figure 1.2. The reactions below the green line is the coke bed zone. The two zones pre-reduction zone and coke bed zone, can also be called respectively low and high temperature zone.

$$2MnO_2 + CO = Mn_2O_3 + CO_2 \qquad \Delta H^0_{298} = -99.9kJ \tag{1.1}$$

$$3Mn_2O_3 + CO = 2Mn_3O_4 + CO_2 \qquad \Delta H^0_{298} = -31.3kJ \tag{1.2}$$

$$Mn_3O_4 + CO = 3MnO + CO_2 \qquad \Delta H^0_{298} = -16.9kJ \tag{1.3}$$

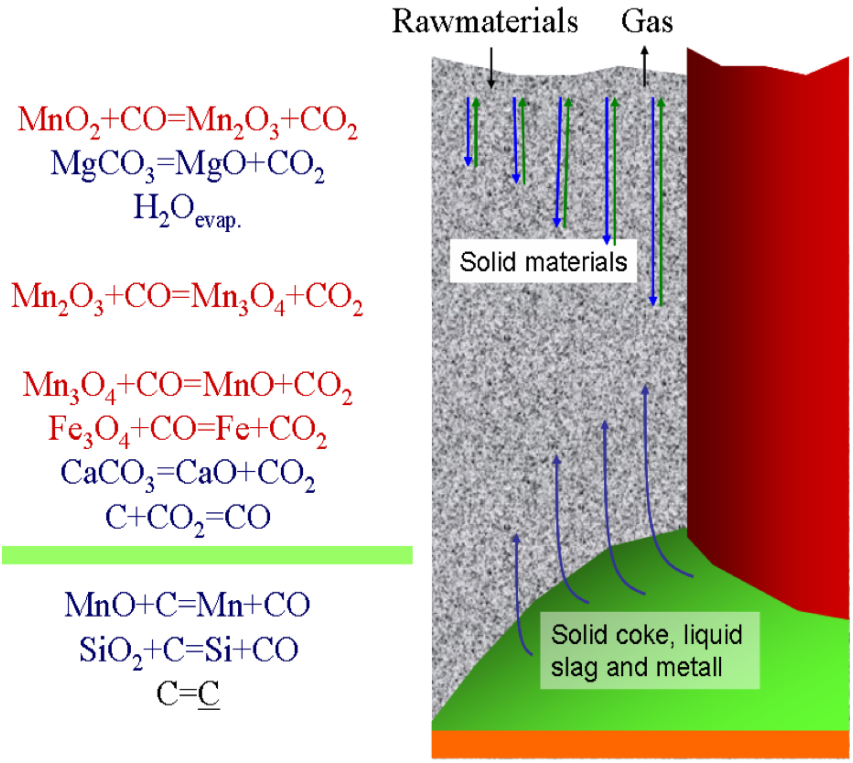

Figure 1.2: A figure showing the reactions in the SAF when producing manganese alloys. The green line shows which reactions is in the pre-reduction zone, and which is in the coke bed zone. It also shows the endothermic reactions as blue and the exothermic reactions as red [11]

The raw materials will be reduced according to Reaction 1.1 1.2 and 1.3 [13]. MnO_2 will first be reduced to Mn_2O_3 and then to Mn_3O_4. In the low temperature zone, there will also be a reduction of the fluxes, evaporation of water and reduction of Fe_2O_3. The reaction for reduction of the fluxes and iron oxide is showed in Figure 1.2.

When reducing the manganese oxides in Reaction 1.1, 1.2 and 1.3 using CO gas, there is produced CO_2 gas. The carbon material in the furnace can react with the produced CO_2 gas according to the Boudouard reaction, Reaction 1.4. The Boudouard reaction takes place when the temperature in the furnace is above 900-1000 °C, but can take place at lower temperatures, around 800 °C if there are alkalis present in the furnace [13]. The extent of the Boudouard reaction will change when changing carbon materials, and if the reaction rate increases the consumption of both carbon materials and energy will increase without increasing the amount of produced manganese alloys. A goal when producing manganese alloys is to have a minimum demand for energy and carbon materials, and therefore there is a desire for the carbon materials used in the Mn-alloy production to have a low CO_2 reactivity.

$$CO_2 + C = 2CO \tag{1.4}$$

When the temperature is increased to the point where the solid MnO phase co-exist with the liquid slag, the reduction reaction for MnO, Reaction 1.5, produces molten Mn for the Mn-alloy. This reduction takes place in the coke bed zone, where MnO reacts with the carbon in the coke bed. Reaction 1.5 produces CO (g) in the high temperature area, this gas will ascend through the furnace and be used for the reduction of the higher manganese oxides in the pre-reduction zone.

$$MnO + C = Mn(l) + CO \tag{1.5}$$

In the manganese ores, there is several oxides as explained earlier, but in the ferromanganese alloys there is a desire to have only iron and manganese in the melted metal alloy. Due to the Gibbs energy for the oxides in the manganese ore when they react with carbon, there is possible to obtain a melt with mostly iron and manganese. If considering the Gibbs energy for the different oxides in the manganese ore, it is found that iron oxide will react with carbon to pure iron, Reaction 1.6, at around 800 °C and manganese according to Reaction 1.5 at 1400 °C [13]. This makes it possible to gain a melt with almost only Fe and Mn. For the silicomanganese alloys the silicon can be reduced from silica with carbon around 1600 °C, Reaction 1.7, and then the metal alloy will contain Fe, Mn and Si. The rest of the oxides added from the manganese ore will have a higher reacting temperatures. After melting, the oxides will have a lower density than the metal, and this density difference will make it possible to separate the slag and metal while tapping from the furnace.

$$FeO + C = Fe + CO \tag{1.6}$$

$$SiO_2 + 2C = Si(l) + 2CO \tag{1.7}$$

Greenhouse gas emissions from the ferromanganese alloy production

After the industrial era began, the emission of Green House Gasses (GHG) increased. Which results in increased concentrations of GHG in the atmosphere and in the sea [16]. The GHG is found to increase the land and ocean temperatures, and the increased CO_2 uptake in the sea increase the acidity in the sea. The ferromanganese alloy production has large emissions of GHG gases from the production processes, and therefore contributes to the emissions of GHG. Typical gases which are categorized as GHG are; CO_2, CH_4, N_2O and other fluoridated gases [17]. As seen from the reduction reactions for the ferromanganese alloy production, e.g. Reaction 1.4, 1.5, 1.6 and 1.7, many produces CO gas. The CO will react with oxygen in the air and become CO_2 gas.

The ferromanganese alloy production has a production around 4.655 million tons of metal each year [18]. The generic CO_2 emissions from the ferromanganese production is given by Lindstad et al. [19] and gives 1.3 ton CO_2/ton liquid metal for the ferromanganese alloy production and 1.4 ton CO_2/ton liquid metal for the silicomanganese alloy production. For both the alloys, the CO_2 emissions are greater than the weight of the produced metal-alloy. Also since there in Norwegian furnaces is mostly used coke as carbon material, these emissions are direct fossil emissions.

2 Literature Review

In the manganese alloy production, there is important to understand how the different materials in the furnace affect each other. This thesis considers a change from coke to charcoal. When doing this, it is important to understand how the material properties of the carbon materials affects different parameters inside the furnace. First the carbon materials will be described regarding production methods, composition and material properties. Then the CO_2 reactivity of the carbon materials is explained with measures earlier research have found to change the reactivity.

2.1 Carbon materials

In Norway coke is the most used reductant in the Mn-alloy production traditionally, but countries like Brazil and South Africa uses charcoal as reductant [14]. One significant difference between Norway and Brazil´s manganese production is the furnace setup, because Norway uses a closed furnace where Brazil has an open furnace. This means that Norwegian manganese production will have to consider the off-gas system when changing the materials in the furnace, where the open furnace does not. Coke and charcoal will be the carbon materials with most focus in this section.

As mentioned earlier in this thesis, there is a desire to become more sustainable and Norway have signed an agreement to contribute to a change. In the metallurgical industry, one method could be a change from fossil carbon sources to renewable sources, like a change of carbon material from coke to charcoal. There will also be given some information about other carbon materials such as petroleum coke, anthracite and coal which are carbon materials also used for metal production, but the focus will be on metallurgical coke and charcoal.

Composition

The composition of the carbon materials is often found from a proximate analysis of the material compounds. For carbon materials, the proximate analysis is given as amount fixed carbon, volatiles and ash. The fixed carbon is the amount of carbon in the carbon material that will not go of as volatiles during heating of the material, which is also the part of the carbon material which will reach the high temperature zone in the furnace [11]. The volatiles represent hydrocarbons, the ash is mostly metal oxides and the carbon material have moisture that will evaporate at increased temperatures. Typical values for the composition is given in Table 2.1. The table shows values for industrial charcoal, metallurgical coke, petroleum coke and coal. Metallurgical coke has the highest amount of fixed carbon with an 86 - 88 %FixC and of ash with 10-12 % ash. Coal has the highest amount of volatiles with 35-40 % volatiles.

Table 2.1: Typical composition of different carbon materials. Values for industrial charcoal, metallurgical coke, petroleum coke and coal is found at [20], where anthracite is found at [21]

	Industrial charcoal	**Met. Coke**	**Pet. Coke**	**Coal**	**Anthracite**
Fixed C (%)	65 - 85	86 - 88	84 - 90	55 - 60	92 - 98
Volatiles (%)	15 - 35	1	9 - 16	35 - 40	2 - 8
Ash (%)	0.4 - 4	10 - 12	<1	1 - 4	-

For analysis of the carbon materials there is also possible to use ultimate analysis which tell which elements that are present in the compound, this is not given for the materials in this paper. However, there is given an analysis of the ash with the oxides that is found in the ash, and an example of this is given in Table 2.3. All the oxides found in the ash is given as a percentage of the total amount of ash. The oxides in the ash analysis tells which metals is present, not which oxide. Meaning that the metal oxides might appear in other forms, e.g. K_2O can appear as K_2CO_3. From Table 2.3 charcoal has a higher amount of K_2O and CaO, while there are higher amounts of Al_2O_3 and Fe_2O_3 in the metallurgical coke. Another difference between the carbon materials in Table 2.3 is that charcoal has a significantly lower amount of ash compared to coke. That means that if there will be a change from coke to charcoal, the main change will be an increase in K_2O.

Table 2.2: Ash analysis with typical values for industrial charcoal and metallurgical coke. The oxides mentioned in the table is from the ash analysis, and is given as a percentage of the total amount of ash. [20]

	Industrial Charcoal	**Metallurgical Coke**
SiO_2 (%)	5 - 25	25 - 55
Al_2O_3 (%)	1 - 13	13 - 30
Fe_2O_3 (%)	2 - 12	5 - 45
CaO (%)	20 - 60.	3 - 6
MgO (%)	5 - 12	1 - 5
K_2O (%)	7 - 35	1 - 4
P_2O_5 (%)	4 - 12	0.4 - 0.8

Production methods

For the ferromanganese alloy production, there is used different carbon materials depending on the furnace operations, availability and the cost. These raw materials and the processing of them is adapted to achieve the desired carbon material properties. The production of the carbon materials coal, coke and industrial charcoal will also vary between the different materials.

Coal is a natural carbon material and is made from a coalification process of biomass under high pressure over millions of years. The result of the coalification process is coal with a high carbon content, low volatile content and some ash [7]. Due to the long production

time for coal, the material is a fossil carbon material, and the same applies to the carbon materials made of coal, e.g. coke.

Coke is produced when coal is heated in an oxygen-free atmosphere to reduce the volatile content, this results in a carbon material consisting mainly of fixed carbon and ash. The properties of the coke that makes it suitable and preferable in metallurgical industry for producing metals like iron and ferromanganese alloys, is the high carbon content, porous structure, and high resistance to crushing or high mechanical strength [22]. This allows for the coke to go down in the furnace while reacting with the manganese ore. The porous structure and high mechanical strength form voids and channels to transport the gas out of the furnace. The main reason for a change from coke to another carbon material is that coke is a fossil carbon material.

The industrial charcoal is made from wood heated up in a pyrolysis process to remove moisture and to increase the amount of fixed carbon in the material [7]. The charcoal has a lower fixed carbon content than coke, a higher amount of volatiles and a lower amount of ash as seen in Table 2.1 [7]. Biomass and charcoal have consumed the same amount of CO_2 as the biomass releases when used in metal production, and charcoal/biomass can therefore be assumed to be CO_2 neutral as long there is a correlation between the growth and felling of timber for charcoal production. Therefore a change from coke to charcoal will lead to a decrease in specific CO_2 release [23].

One method used to change the properties of charcoal is densification of charcoal. The content of fixed carbon in charcoal are normally lower compared to coke and coal, due to the high porosity and low mechanical strength, the volumetric energy in biocarbon are lower than for coke [24]. For charcoal the densification is seen to increase the percentage of fixed carbon, decrease the CO_2 reactivity, increase the mechanical strength and decrease the porosity [6], [10], [25].

There are several methods to densify the charcoal, two methods for densification of charcoal is mechanical densification by compressing charcoal into briquettes [6] or thermochemical densification by methane purging [10]. Mechanical densification of the carbon material is achieved by pressing the charcoal to briquettes using binders to increase the properties. Thermochemical densification of the charcoal is when purging methane gas with methane cracking into carbon particles that attach to the charcoal surface and where H_2 will be produced as off-gas, according to Equation 2.1.

$$CH_4 = C + 2H_2 \tag{2.1}$$

The cracking of methane is a phenomenon that is used for production of hydrogen gas [26], carbon black production [27], [28] and for chemical densification of charcoal [10]. The reaction for cracking of methane is endothermic with $\Delta H^0 = 74.85$ kJ/mol [26]. The equilibrium for Reaction 2.1 is temperature dependent, and the kinetics can also be stimulated by other mechanisms like a catalyst. For the hydrogen gas industry, the carbon deposition is a problem, but for densification of charcoal the carbon black deposition can be utilized [10].

Carbon materials works as a catalyst during cracking of methane, and the deposited carbon will attach to the solid carbon. The temperature needed for cracking of methane

can be reduced using catalysts like wood char [29]. In densification experiments at an average temperature around 1050 °C the conversion fraction of methane is showed to be up to 22 % [30].

In earlier research, it is showed that the densification experiments while using charcoal in a crucible above 1000 °C is densifying the charcoal. Densification is here calculated as a weight increase, and according to Table 2.1 most of the experiments densified the charcoal with around 15% weight increase for purging methane for more than 60 minutes [8], [9], [25], [30], [31].

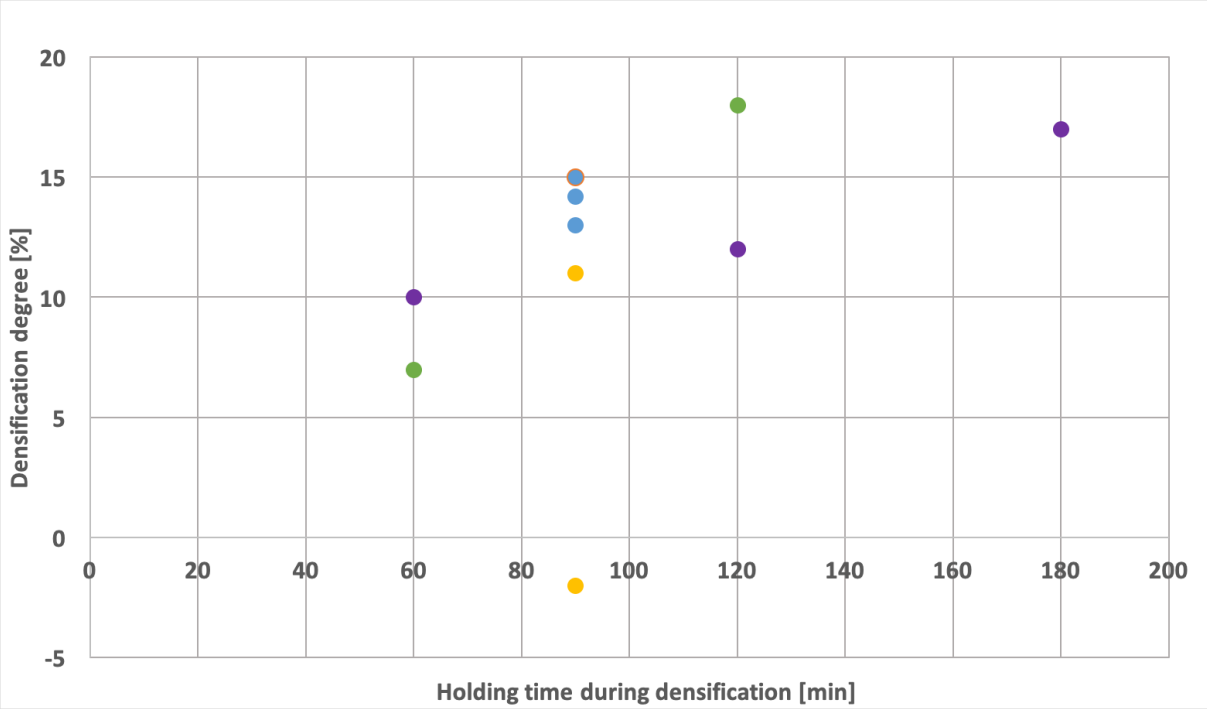

Figure 2.1: Different densification degrees from earlier densification experiments, where the obtained densification degree is given for the holding time during the densification experiments. The blue marks is densification degrees from Kaffash [25], the purple from Larsen [30], the green from Larsen [31], the yellow from authors earlier work [9] and the same for the orange [8].

Material properties

Carbon properties that is important for the carbon material in the manganese production is the electrical resistivity and CO_2 reactivity as mentioned in the section about manganese alloy production. Other important properties are density, mechanical strength, slag reactivity, thermal conductivity, porosity, pore structure and composition [7].

Table 2.3: Some important properties of coke and charcoal. The CO_2 reactivity of the materials found at 1060 °C. [10], [20].

	Industrial Charcoal	**Metallurgical Coke**
CO_2 reactivity (%FixC/s)	(2.5 - 3.5) 10^{-2}	(0.02 - 0.05) 10^{-2}
Porosity (%)	68-80	44-55
Density (g/cm^3)	0.45-0.55	0.9-1.1
Compressive strength (kg / cm^2)	10-80	130-160
Electric resistance (Ohm m)	High	Low

Carbon materials mechanical strength both before the material is loaded into the furnace and inside the furnace is important. First problem that might occur if the carbon material has a low mechanical strength is that it gets crushed into smaller particles and fines on the transport to the furnace, but also that the carbon material can break and make fines and smaller particles when loading into the furnace. Fines inside the furnace is something one would like to avoid since the fines can cause problems for the gas flow inside the furnace and the fines will clog the furnace and then the gas will form channels to escape the furnace.

Compression strength is often measured on charcoal with different pore directions. For untreated charcoal the compression strength in charcoal often is between 3 - 5 MPa [25]. There is a large variation of the strength of the charcoal, and this is because there is a large difference in the strength measuring the strength in the direction or perpendicular to the fibers in the charcoal. The metallurgical coke have a compression strength of 20-30 MPa [25]. The lower mechanical strength of charcoal is due to the lower envelope density and larger porosity.

Abrasion strength is the strength when the carbon material have reacted partly in an atmosphere with 50% CO and 50% CO_2 gas according to the Boudouard reaction, Reaction 1.4, at 1100 °C [5]. The method for testing the abrasion strength will be independent of the CO_2 reactivity since the carbon materials will have about 20% of the %FixC reacted for all samples. The abrasion test is measured by measuring the size of the samples before and after tumbling the samples. Cohesion Index (C.I.) tells the material ability to maintain strength (cohesion) after the reaction with the gas. The Thermal Stability Index (T.I.3) is testing the material ability to resist abrasion against other particles under charge pressure. Both parameters are desired to be high. In Figure 2.2 it can be seen that the Brazilian charcoals have a lower cohesion index than coke, where the charcoal has around 74-84 % and coke have around 93-97%. Some charcoals have a cohesion index more like coke, and that is charcoal from preserved wood [5].

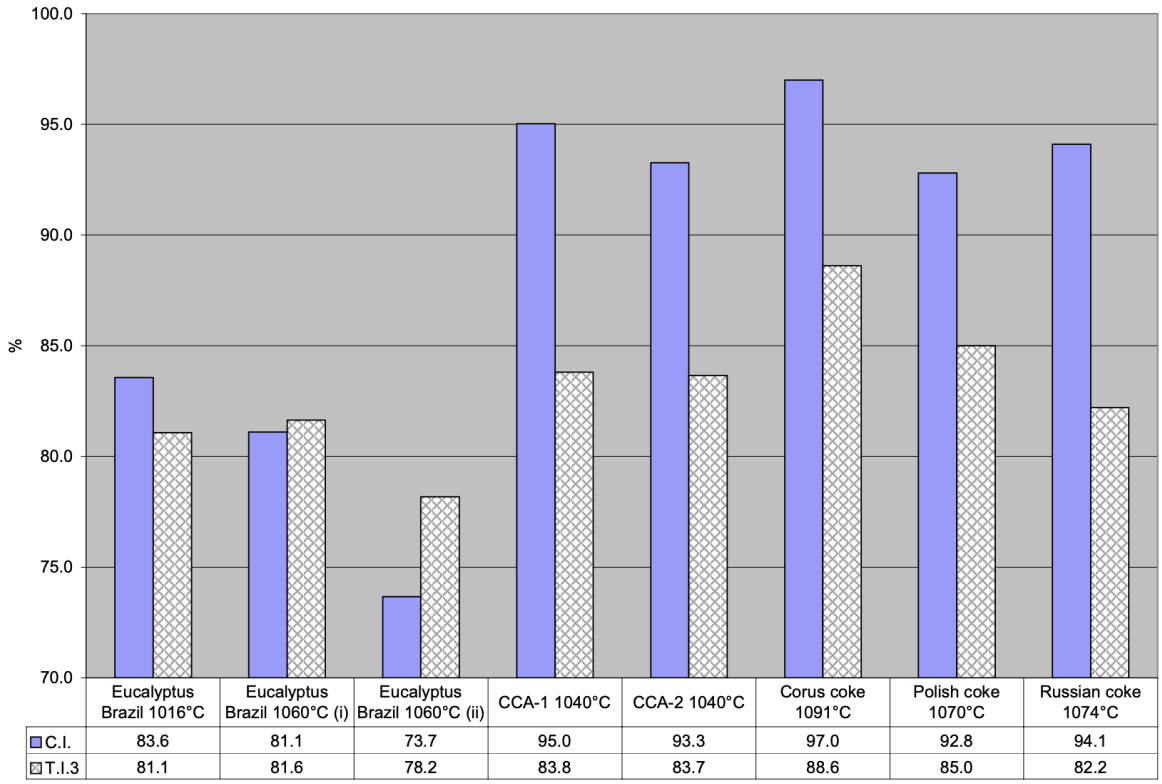

	Eucalyptus Brazil 1016°C	Eucalyptus Brazil 1060°C (i)	Eucalyptus Brazil 1060°C (ii)	CCA-1 1040°C	CCA-2 1040°C	Corus coke 1091°C	Polish coke 1070°C	Russian coke 1074°C
C.I.	83.6	81.1	73.7	95.0	93.3	97.0	92.8	94.1
T.I.3	81.1	81.6	78.2	83.8	83.7	88.6	85.0	82.2

Figure 2.2: Abrasion strength (C.I. and T.I.3) for Brazilian charcoal and charcoal from preserved wood compared to different metallurgical cokes. C.I. = Fraction larger than 4.75 mm before tumbling, T-I.3 = fraction larger than 3.33 after tumbling [5]

Porosity estimates the fraction of pores in the material, and it is assumed that a higher porosity increases the reactivity with gas and decreases the mechanical strength of the materials [7]. The reason for the change in properties with increasing porosity is due to the faster transport of gas through the pores, that allows the gas to react with a larger surface area of the carbon material, and therefore increases the gas reactivity. Typical values for charcoal lays between 65-80% while the values for metallurgical coke lays between 44-55% porosity [32]. The porosity of charcoal is large compared to coke which is due to a higher fraction of voids and open spaces in the material structure. The high porosity results in a fragile structure of the charcoal [6], [24] which gives the charcoal a low mechanical strength and the high porosity decreases the volumetric energy density. A low density means that the charcoal will occupy a larger volume.

Electrical resistivity of the carbon materials is as mentioned earlier important for the Mn-production. It is through the coke beds/carbon material resistivity the temperature in the high temperature area can increase to this level [13]. It is found that coke has a lower resistivity than petroleum coke, anthracite and charcoal. The electrical resistivity is decreasing with increasing temperature and with increasing particle size, this is showed in Figure 2.3a. Figure 2.3b shows the electrical resistivity as a function of temperature, and is can be seen that for temperatures up to 1300 °C the electrical resistivity of charcoal is higher than for coke, while for temperatures above 1300 °C coke has the same or higher electrical resistivity than charcoal.

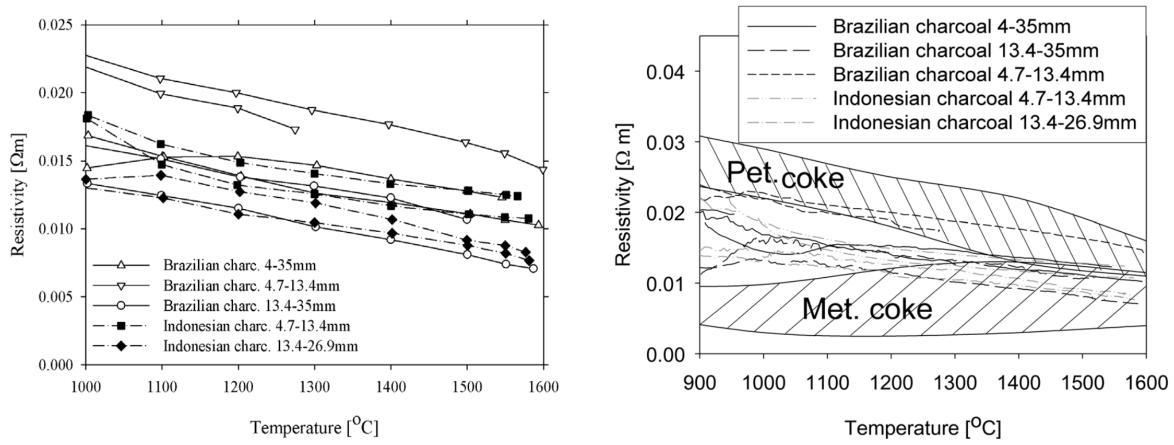

(a) (b)

Figure 2.3: The electrical resistivity of different charcoals with different grain sizes in the high temperature area [5]. Figure (b) compares the electrical resistivity for different carbon materials.

The final step in the reduction reactions for the manganese alloy production is reduction of MnO, Reaction 1.5. In this reaction MnO reacts with solid carbon and produces Mn and CO. The MnO is mixed with the slag, and therefore it is important that the carbon material reacts with the slag to produce the desired amount of manganese. It is found that coke shows a higher reactivity for Mn reduction than chars and charcoal, but the difference between them is not so great that it is a determining factor for which materials to use [13].

2.2 CO_2 reactivity

The Boudouard reaction, Reaction 1.4, gives the rate of the CO_2 reactivity of the carbon materials. In Table 2.3 it can be seen that coke with CO_2 reactivity around 0.002 %FixC/s has a lower reactivity than charcoal with CO_2 reactivity around 0.02 %FixC/s [10]. This difference between charcoal and coke is of a factor 10. The total consumption of carbon per ton of manganese will hence be higher using charcoal compared to coke.

$$CO_2 + C = 2CO \tag{1.4}$$

The Boudouard reaction, Equation 1.4, determines the equilibrium between CO and CO_2 partial pressures in the submerged arc furnace in coexistence with solid carbon if this equation is in equilibrium. In Figure 2.4 it is seen that with increasing temperature the reaction are shifted to the right and the partial CO pressure will increase. The increase of CO partial pressure increases the amount of carbon material that has reacted with the CO_2 gas inside the furnace, and this consumption of carbon material increases the amount of carbon material needed for the manganese alloy production and it increases the energy consumption of the process since the Boudouard reaction is endothermic with $\Delta H^0 = 172.4$ kJ/mol and therefore consumes heat [14]. According to Figure 2.4 it can be seen that a mixture of 50% CO and 50% CO_2 need temperatures around 1100 °C in order to react.

Given the case of using 50% CO and 50% CO_2 gas in a CO_2 reactivity test, with 35 g of carbon material in the furnace at a start temperature of 1100 °C. The temperature is assumed to fall since the Boudouard reaction is endothermic. HSC Chemistry 9 [33] was used to find the temperature balance during the CO_2 reactivity test considering the Boudouard reaction being the only aspect that affects the temperature. From this the temperature will drop from 1100 °C to 207 °C. The calculations are given in Appendix A.1. In reality the CO_2 test is performed in a furnace that might apply power to keep a high temperature through the test, so the temperature fall might not be as large as the calculations states.

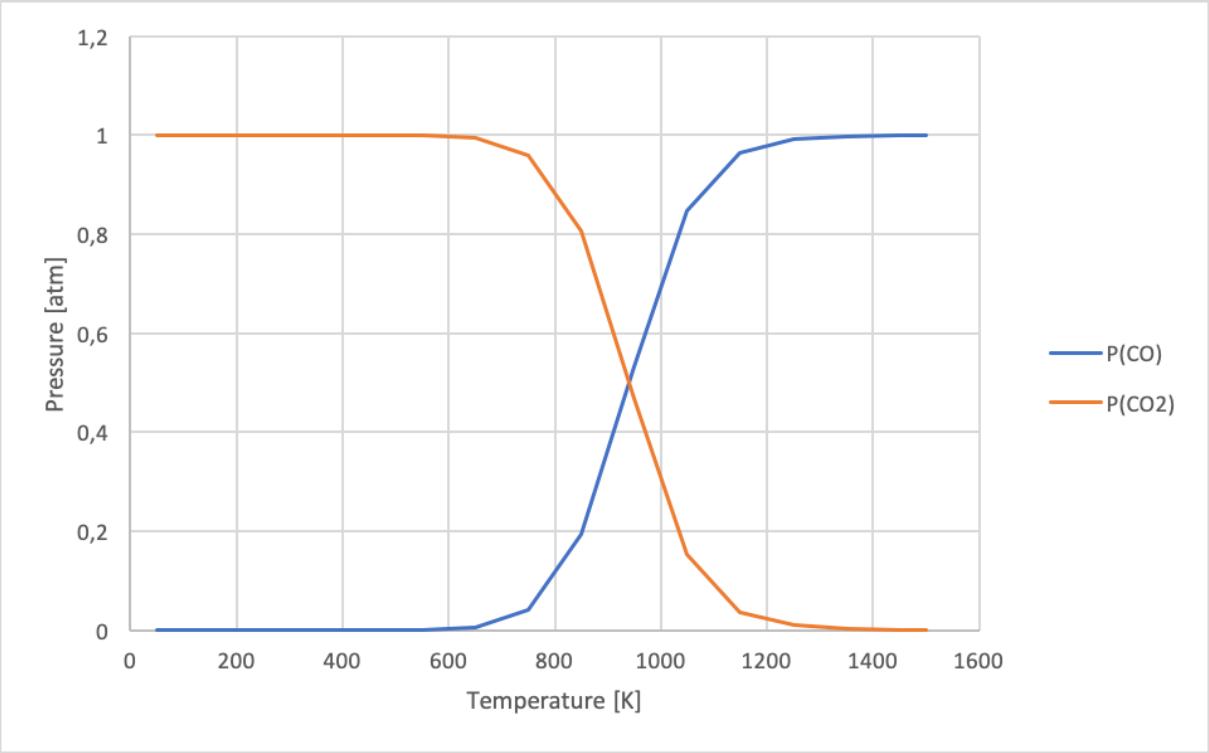

Figure 2.4: The figure shows the partial pressures of CO and CO_2 gas in the furnace according to the Boudouard reaction, Equation 1.4 and change in temperature. The figure is made in HSC Chemical 9 [33]

According to studies [5] a change from using coke as the main carbon reductant in Mn production to using charcoal, the off-gas composition will change and there will be required new routines for the furnace operations. The main reason for this is that there is a change in properties when using charcoal instead of coke. Table 2.3 shows the properties of industrial charcoal and metallurgical coke [5]. It is seen that the charcoal has a lower amount of fixed carbon, that results in an increased amount of carbon material needed to get the same amount of carbon in the furnace. A solution to increase the volume of the added carbon material is by densification of charcoal, either mechanically or thermochemical [6], [10], [25]. These methods will also reduce the CO_2 reactivity of charcoal, which solve the challenge with higher CO_2 reactivity for charcoal than for coke.

In earlier research it is found that a weight increase of the charcoal is an effect of cracking of methane at temperatures around 1100 °C [8]–[10], and decreases the CO_2 reactivity of the carbon material [6], [8], [9], [34]. In Figure 2.5 these effects can be seen where the raw material has a higher CO_2 reactivity, R, than the charcoal densified with a densification degree between 10-15%. From the figure it can also be seen that the charcoal with -2% densification degree (or weight loss) has a small increase in the CO_2 reactivity compared to the raw material.

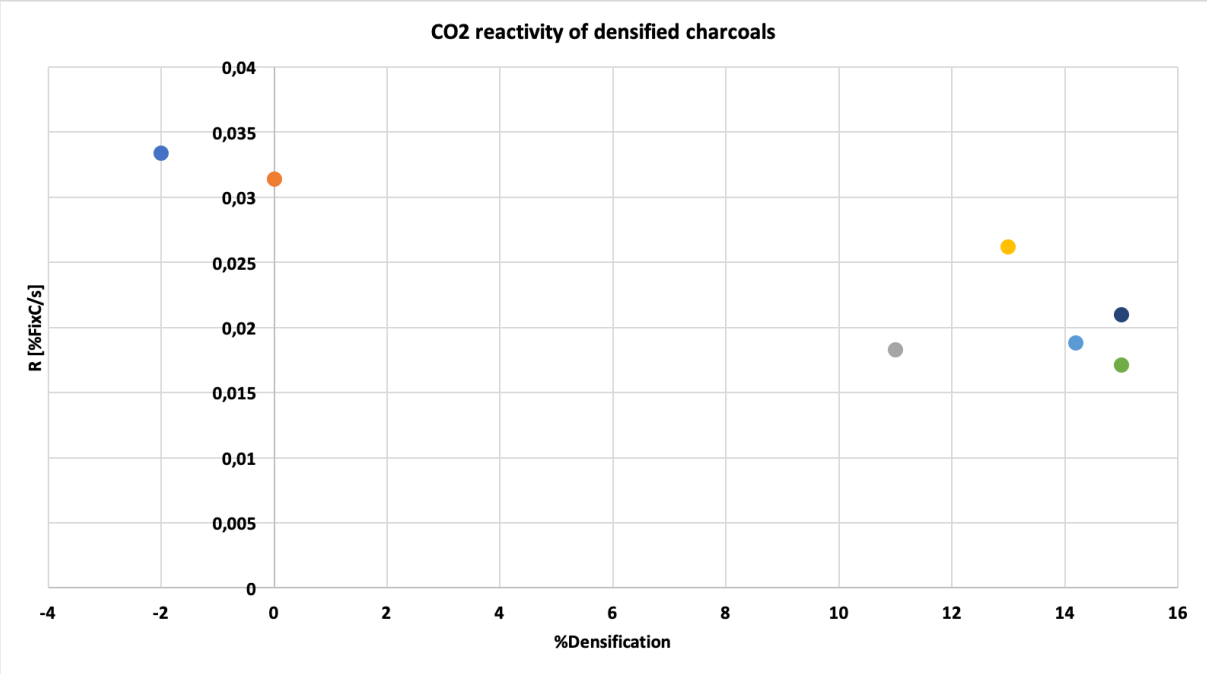

Figure 2.5: The CO_2 reactivity to different densification degrees after densification of charcoal using cracking of methane from earlier densification experiments [8], [9], [25].

The effect of alkalis

Potassium is present in the manganese production furnace, this because both the manganese ore and the to some extent the carbon materials contain potassium [35]. In the coke bed the potassium content is found to be 3.5% K_2O [36]. Since the coke bed is in the high temperature area, it can be assumed that alkalis have evaporated from the coke bed to the lower temperature areas. From this it can be assumed that there will be an alkali content higher than 3.5% K_2O for the carbon materials in the lower temperature zones. There are studies performed on how the potassium will affect the charcoal, and studies show that the CO_2 reactivity increases when the alkalis are present [37], [38]. The increased CO_2 reactivity comes from potassium acting like a catalyst for the Boudouard reaction, Reaction 1.4 [39].

Increasing the content of potassium using gas impregnation procedures is studied in several studies [34], [39]. The most used method for impregnation of carbon materials at the Norwegian University of Science and Technology is gas K-impregnation where potassium carbonate (K_2CO_3) is mixed with active carbon to react at temperatures above 1000 °C. From Reaction 2.2 the reaction to produce potassium is given.

$$K_2CO_3 + 2C = 2K(g) + 3CO(g) \tag{2.2}$$

A second method to impregnate the charcoal with alkalis is to use a wet impregnation method where a solution is used [40]. The solution used for the impregnation is a mixture of alkali and distilled water, where the carbon material will be K-impregnated while soaking in the solution with varying impregnation time and molarity of the solution.

When comparing composition and type of alkalis the reaction rate increased with alkali content in char for low temperatures up to an alkali content of 2200 mmol/kg char = 8.6 wt% [40], and after this level of alkalis, the reaction rate stayed constant with increasing potassium content.

The Boudouard reaction rate, Reaction 1.4 is strongly affected by factors like temperature, CO_2 partial pressure and potassium content [39]. If ranking the different alkali's effect on the reaction rate, there it is showed for temperatures higher than the melting point for potassium carbonate that K_2CO_3 has a higher catalytic effect than Na_2CO_3 and Li_2CO_3 [38]. Also, studying the pure alkali's there are shown that K and Na has the highest catalytic effect [40].

There are several aspects that can affect the CO_2 reactivity of carbon materials, but alkalis is definitely one of them. The effect of increased potassium on the CO_2 reactivity is showed in Figure 2.6, where the increase in potassium increases the CO_2 reactivity, R. In the figure, it can also be seen that for values up to around 4 $\%K_2O$, the CO_2 reactivity of charcoal is higher than for coke, above 4 $\%K_2O$ it is not possible to say according to the values found.

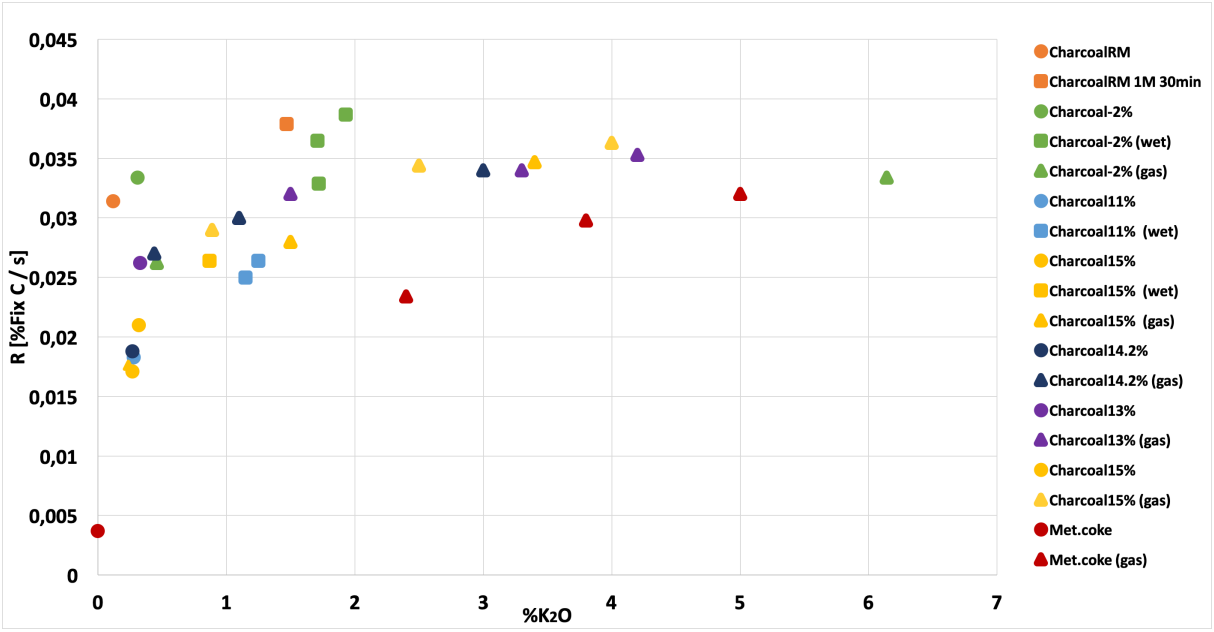

Figure 2.6: CO_2 reactivities measured versus potassium content from earlier research Different densification degrees from earlier densification experiments [8], [9], [25]. The values for all the data points in this figure is given in Table A.1.

Earlier research has found that both wet and gas K-impregnation can be used to increase the potassium content in the charcoal. It is found that by gas K-impregnation the potassium content in the charcoal increased more than for wet K-impregnation [9], this can also be seen in Figure 2.6. The figure shows that gas K-impregnation have gained values up to 6 $\%K_2O$ where the maximum for wet K-impregnation is up to 2 $\%K_2O$. From the CO_2 reactivity it can be seen that with potassium content above 3 $\%K_2O$ the effect of reducing the charcoal CO_2 reactivity with densification is removed and the CO_2 reactivity becomes similar to the raw material.

3 Method

A description of the raw materials, the experimental procedures and the apparatus for the experiments performed for this project will be given in this section. The main experiments in this report is gas and wet potassium impregnation of charcoal with the goal of understanding the effect of potassium on the carbon materials in the manganese furnace. After the charcoal is impregnated with potassium, the CO_2 reactivity of the samples is measured to compare the effects of the potassium levels achieved. Scanning Electron microscopy (SEM) and Computed Tomography (CT) analyses is used to see how the potassium attaches to the carbon materials using different potassium impregnation methods.

The nomenclature for the carbon materials in this thesis will be given as CharcoalXX%YY%K, where XX show the densification degree and YY show the percentage of K_2O in the charcoal after impregnation. If the samples are not densified or impregnated with potassium, then that part of the name will be excluded. The %K will have a subscript g or w, depending on which impregnation method is used, K_g for gas K-impregnation and K_w for wet K-impregnation. The raw material will be named CharcoalRM and heat treated charcoal will be named CharcoalHT.

3.1 Raw material

For the experiments in this thesis there is used three types of raw materials, they will be named CharcoalRM, CharcoalHT and Coke. The proximate analysis of the raw materials is given in Table 3.1. CharcoalRM is untreated charcoal, and is the same charcoal as received from the industry used as raw material in earlier research [8], [9]. CharcoalHT is produced in earlier work [9], and is made from a heat treatment of CharcoalRM. The heat treatment heated CharcoalRM up to 1100 °C in an argon atmosphere. The coke used is denoted CK-003 in the SINTEF storage system, which is a polish coke. The size of the carbon material particles is between 5-16 mm, for CharcoalRM the size distribution is showed in Figure 3.1. In Appendix A.4 the values for the composition of the raw material and the treated samples is given, with the composition of volatiles, ash and fixed carbon and potassium content.

Table 3.1: The composition of CharcoalRM, CharcoalHT and Coke from a proximate analysis performed by Sintef Norlab. K_2O is given as a percentage of the total amount of ash.

	CharcoalRM	**CharcoalHT**	**Coke**
Fix C	85.2 %	94.90 %	86.65 %
Volatiles	12.7 %	2.41 %	2.05 %
Ash	2.1 %	2.69 %	11.3 %
K_2O	5.6 %	14.63 %	1.42 %

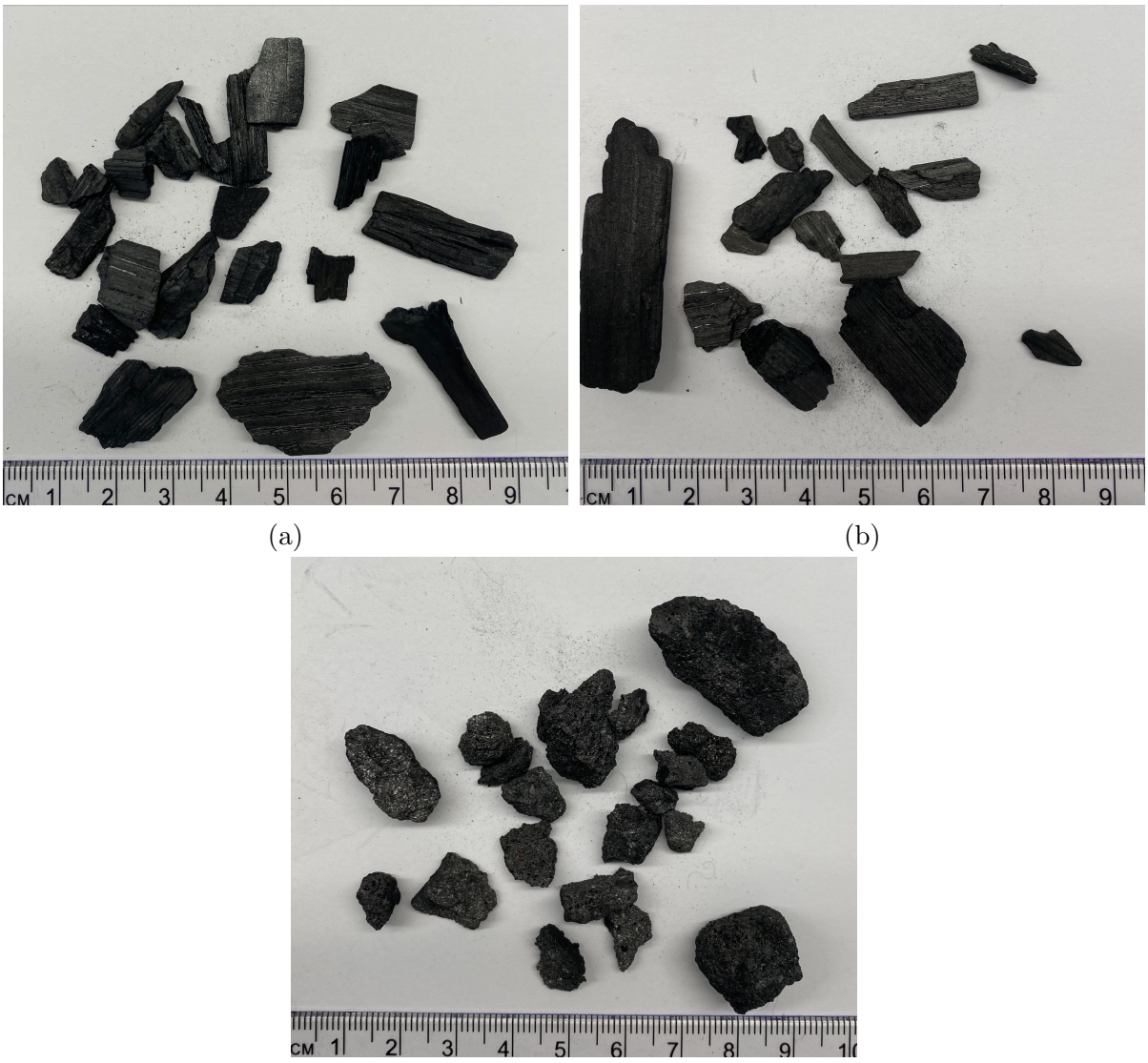

(a) (b)

(c)

Figure 3.1: The raw materials showed with size distribution of 5-16 mm. Figure (a) is CharcoalRM, Figure (b) is CharcoalHT and Figure (c) is Coke.

Several gases and chemicals is used for the experimental work, but the potassium is for both K-impregnations potassium carbonate K_2CO_3 from Alpha Aesar with 99.0% purity [41]. The gas K-impregnation also uses Ar(g) which was 99.999% pure and active carbon or charcoal fines. The CO_2 reactivity also used Ar (g), but used CO (g), CO_2 (g) and synthetic air also. The three last gases is all from Linde gas, but could not get information about the gases in time.

A total of 700 g of carbon material was divided into eight equal parts. The material was first sieved to a size distribution of 5-16 mm, before the charcoal was again divided into two groups; 5-9 mm and 9-16 mm. Each of the 5-9 mm groups were mixed with a 9-16 mm group, ensuring that the size distribution was the same for every experiment. This to minimize the effect size has on the CO_2 reactivity of the samples.

3.2 Gas K-impregnation of charcoal

The gas K-impregnation of the carbon materials were performed in an induction furnace using an inert atmosphere with argon gas. In the furnace the experiment is carried out in a crucible with in- and outlet of gas on the bottom and top of the furnace, as showed in Figure 3.2. The raw materials in gas K-impregnation was a mixture potassium carbonate and active carbon or charcoal fines. The potassium source was crushed and placed in three smaller crucibles in the bottom of the main crucible in the furnace. These smaller crucibles were placed around the gas distributor. On top of the smaller crucibles a holder made of grid is placed with the thermocouple placed in the middle with the charcoal distributed around.

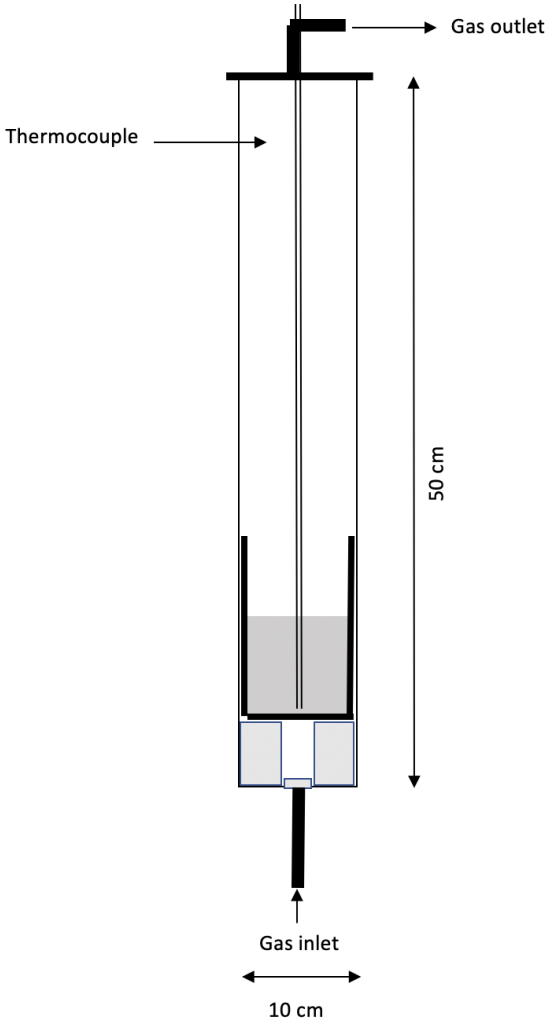

Figure 3.2: The experimental set up for gas K-impregnation of charcoal.

There are three experiments performed using gas K-impregnation of carbon materials, two using charcoal and one using coke as the carbon material to be impregnated. For all of the experiments, 75 g K_2CO_3 and 15 g active C is used as a potassium source together with 200 g of charcoal. The experimental parameters for the three experiments performed for this thesis is given in Table 3.2. After the gas impregnation the charcoal is divided into three layers in order to see how the potassium content varies with increasing distance from

the potassium source, the layers showed in Figure 3.3. The layers are divided separating the layers by removing carbon material by hand.

Table 3.2: The experimental procedures for the gas K-impregnation experiments performed. Here showing which materials used and the measured weight of the different components.

Carbon Material	**Weight carbon material**	**Weight K_2CO_3**	**Weight active C or charcoal fines**	**Holding time at 1100 °C**
CharcoalRM	200 g	75 g	15 g charcoal fines	1.5 h
CharcoalHT	200 g	75 g	15 g active C	2 h
Coke	200 g	75 g	15 g active C	2 h

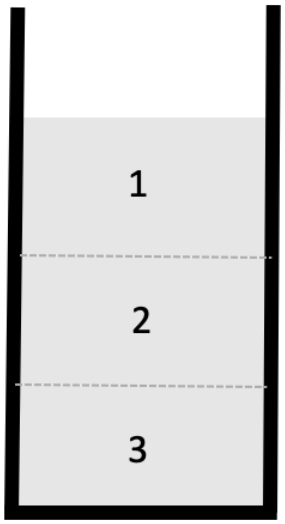

Figure 3.3: The three layers in the grid holder after gas K-impregnation of 200 g charcoal.

The actual temperature program for the three gas K-impregnations in this thesis is shown in Figure 3.4, 3.5 and 3.6. During the gas K-impregnation there was a constant flow of argon gas of 2 L/min. The temperature in the crucible will be increased to 1000 °C and held at this temperature for 1.5 or 2 hours. After this the sample will be cooled down to room temperature before the sample is taken out of the crucible.

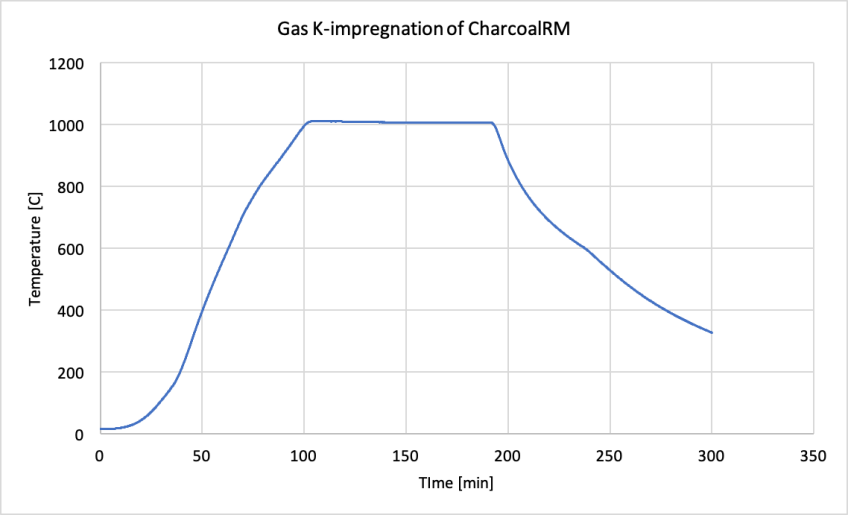

Figure 3.4: Temperature versus time in the gas impregnation of CharcoalRM.

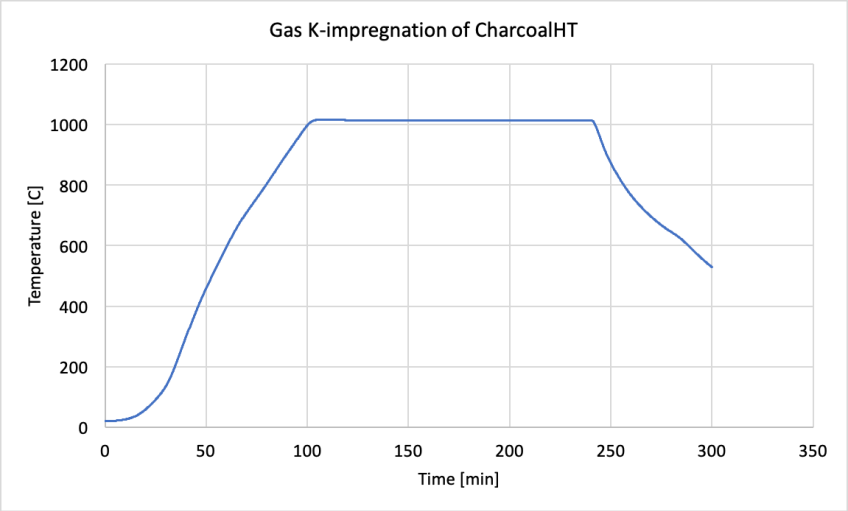

Figure 3.5: Temperature versus time in the gas impregnation of CharcoalHT.

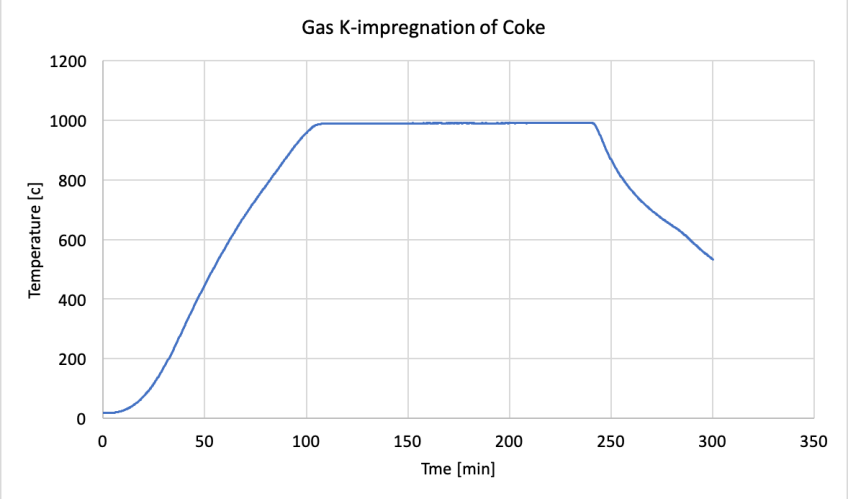

Figure 3.6: Temperature versus time in the gas impregnation of Coke.

There have been two incidents with self-ignition of the charcoal during this project, one of them while the author was handling the samples. The self-ignition after gas potassium impregnation is possible since charcoal can auto ignite at temperatures above 349 °C, given in Table 3.3. The gas K-impregnation gives a charcoal with elevated potassium content, and alkalis is known to react exothermic with water and the same with moisture in air. According to Reaction 2.2 there can be metallic potassium produced from gas K-impregnation. The potassium and its risk of increasing temperature after taking the charcoal out of the inert atmosphere during the experiment is a matter that needs to be taken into consideration. There was an incident with the charcoal almost taking fire after one gas K-impregnation when taken out of the crucible. This was due to the reaction between potassium impregnated charcoal and air.

Table 3.3: Autoigniton temperatures for different carbon materials [42]

Fuel	**Autoignition temperature [°C]**
Carbon	700
Carbon monoxide	609
Charcoal	349
Coke	700

$$K_2CO_3 + 2C = 2K(g) + 3CO(g) \tag{2.2}$$

Due to this incident, the samples were analyzed in an XRD to see if there were pure potassium on the charcoal or if it had oxidized or something similar. This was done by Nicholas Smith at SINTEF [43]. There were two samples that was analyzed: one that had been kept in inert atmosphere and one that was stored in air after the impregnation experiment. For the last sample, the charcoal surface was clearly changing color during the two hours in an oxidizing atmosphere, shown in Figure 3.7. It is showed from XRD analysis that the potassium on the charcoal after K-impregnation is oxidized to oxides stable at room temperature after two hours. It can also be seen in Figure 3.7, where the bottom layer becomes lighter after the oxidation.

(a) (b)

Figure 3.7: Photo of the charcoal right after the sample is unloaded and divided by layers (a) after the K-impregnation, and the charcoal after the unloading where the K-impregnated sample have been able to oxidize in air for 2h (b).

The results from the XRD analysis of the sample without exposure to an oxygen rich atmosphere is given in Figure 3.8. Here it can be seen from the elevations in the curve that the XRD analysis found tops matching the different oxides KO_2 and KOH. It was found that the charcoal right after the experiment has a noticeable amount of KO_2 super oxide and not metallic K. This super oxide is not stable and can react exothermic in room temperature. The potassium superoxide is a product of hot potassium reacting with oxygen, which in this case comes from the CO_2 (g). From the XRD analysis, there is also some KOH which is a product of KO_2 reacting with water or moisture. For the sample oxidized in air for 2 hours, no KO_2 could be found.

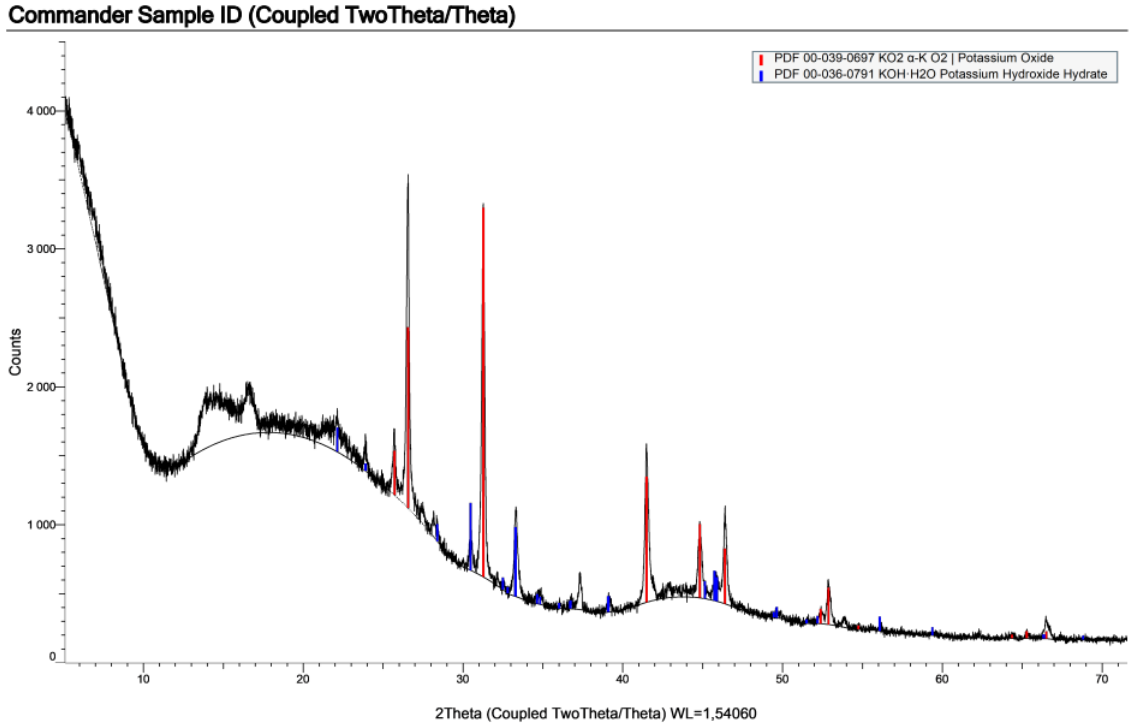

Figure 3.8: The analysis from XRD of the charcoal without exposure to an oxygen rich atmosphere after the Gas K-impregnation [43].

The danger with the KO_2 oxide is that it reacts with moisture, following Reaction 3.1. This reaction is exothermic and will produce heat as the reaction goes. Since the charcoal has an auto ignition temperature at 349 °C, the charcoal would be able to fire if the KO_2 reacts enough to increase the temperature above 349 °C. Equation 3.2 and 3.3 gives the calculations performed to prove that the reduction of KO_2 to KOH is exothermic. First the equilibrium constant K_{25^0C}, Equation 3.2 is much larger than 1. This implies that the reaction will go to the right. Also since the enthalpy in Equation 3.3 is negative, this means that the reaction is exothermic and will produce heat. The calculations using the data program HSC is given in Figure A.4. It can be assumed that P_{O2}=0.21 and P_{H2O}=0.03 due to content in air at 25 °C.

$$2KO_2 + H_2O(g) = 2KOH + \frac{3}{2}O_2(g) \tag{3.1}$$

$$K_{25^0C} = \frac{p_{O_2}^{3/2} a_{KOH}^2}{p_{H_2O} a_{KO_2}^2} = 4.27E + 008 \tag{3.2}$$

$$\Delta H^0 = -40,1kJ \tag{3.3}$$

To avoid other incidents with self-ignition of charcoal, the charcoal is after gas K-impregnation divided into three trays where the sample is evenly distributed into thin layers to be able to get the charcoal to oxidize without increasing the temperature enough for self-ignition.

Figure 3.7 shows an example of one of these boxes where the bottom layer, layer 3, from one of the impregnation experiments were left to oxidize.

3.3 Wet K-impregnation of charcoal

The wet K-impregnation of charcoal is performed in a beaker with a solution of distilled water and potassium carbonate (K_2CO_3). A magnetic stirrer is used for the whole experiment with a stirring rate of 700 rpm at 80 °C, see Figure 3.9. When the solution is at 80 °C the charcoal is added to the solution and then stirred for 60 minutes. After the charcoal has stayed in the solution for 60 minutes, the solution is poured out of the beaker and the charcoal is dried at 100 °C for 24h in a muffel furnace in an oxidizing atmosphere (air).

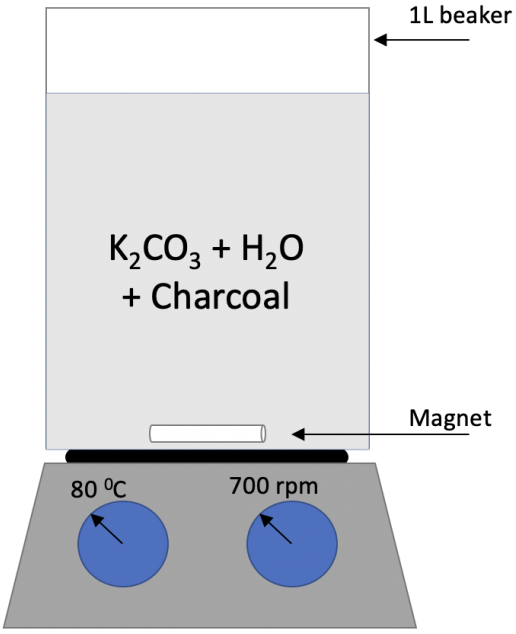

Figure 3.9: The experimental setup for the wet K-impregnation experiment. Showing the used temperature and stirring rate.

In this thesis there is performed 6 wet K-impregnations, and the experimental data for each experiment is given in Table 3.4. The only difference between the wet K-impregnations is which carbon material is used as raw material and the molarity of the solution. There is performed experiments with three different molarities used; 1, 2.5 and 5 for both CharcoalRM and CharcoalHT.

Table 3.4: Overview of the wet K-impregnation experiments. The variables for these experiments is which carbon material that has been impregnated, the amount of charcoal impregnated and temperature, time and stirring rate for the experiment.

	Carbon material	**Weight charcoal [g]**	**rpm**	**Temperature [°C]**	**Time [min]**	**Volume distilled water [mL]**	**Weight K_2CO_3 [g]**
1	CharcoalRM	62.50	700	80	60	1000	69.1
2	CharcoalRM	62.50	700	80	60	1000	172.75
3	CharcoalRM	62.50	700	80	60	1000	345.5
4	CharcoalHT	62.50	700	80	60	1000	69.1
5	CharcoalHT	62.50	700	80	60	1000	172.75
6	CharcoalHT	62.50	700	80	60	1000	345.5

3.4 CO_2 reactivity

To measure the CO_2 reactivity of the charcoal, the charcoal is analyzed using a thermogravimetric furnace. The set-up is showed in figure 3.10. Here the crucible is made of stainless steel and there is gas inlet and outlet at the top of the crucible. The gas goes from the inlet tube, through the double walls of the crucible, through a gas distributor on the bottom of the crucible and into the charcoal. The gas distributor is a ceramic perforated gas distributor. The thermocouple is placed on the middle of the distributor and the charcoal is placed around.

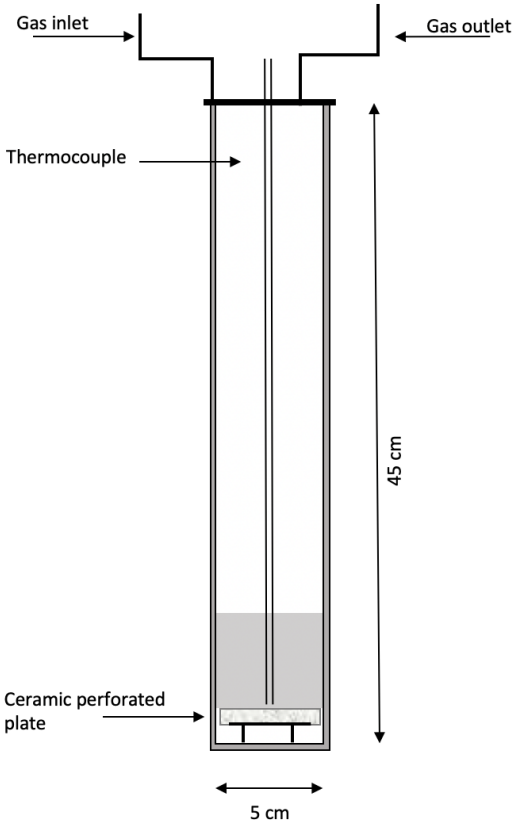

Figure 3.10: The experimental set up for CO_2 reactivity measurements of charcoal. The gray area shows the placement of the charcoal.

CO_2 reactivity is measured as the reaction rate until 20% of the fixed carbon has reacted. The charcoal is heated up to 1070 °C while purging argon gas at 2 L/min and 4 L/min for different time lengths, see Figure 3.12. Keeping the charcoal at 1070 °C, the gas flow through the crucible will be changed to 50% CO and 50% CO_2 gas. The carbon in the charcoal will react with the gases in the crucible according to the Boudouard reaction, Reaction 1.4, and the weight of the charcoal is measured to see when 20 % of the fixed carbon has reacted. After measuring the crucible temperature and weight of the charcoal throughout the experiment, the CO_2 reactivity is found by plotting the reduction of the weight per time. The slope of the plotted curve represents the CO_2 reactivity of the charcoal, example showed in Figure 3.11. Due to some weight increase in the beginning of CO and CO_2 purging, all of the slopes found in this thesis will be calculated 100 seconds

after the purging of CO and CO_2 gas starts.

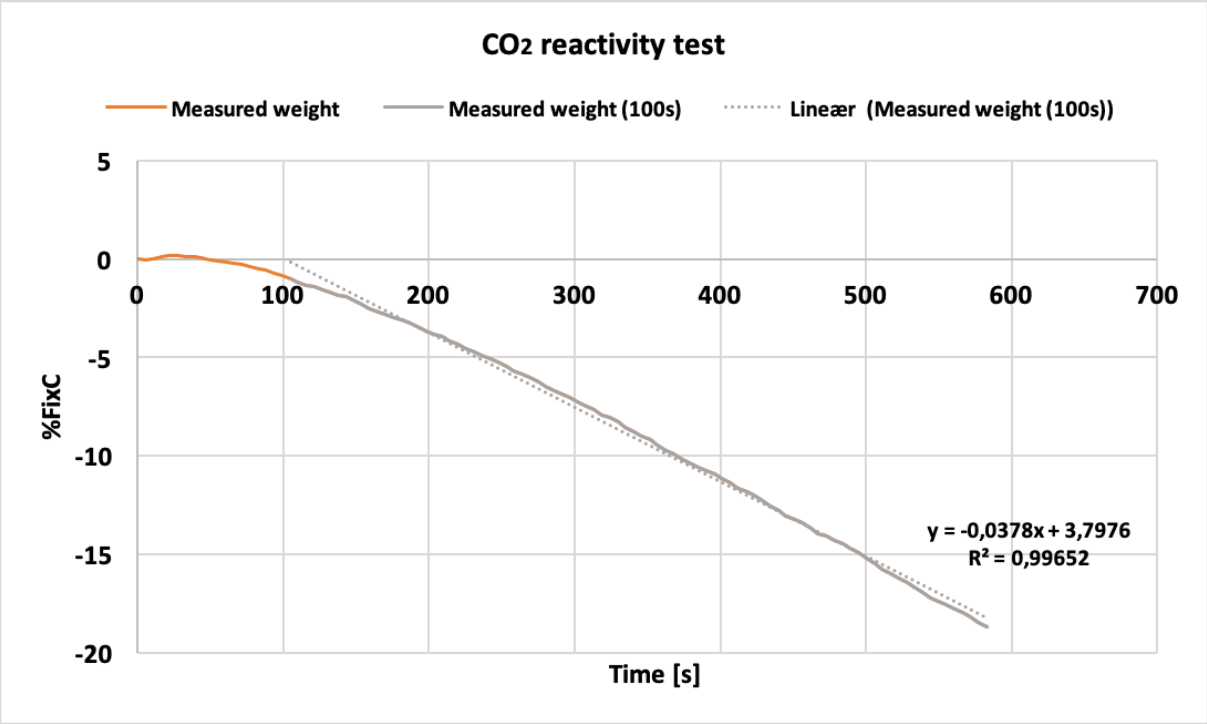

Figure 3.11: Example of one CO_2 reactivity test measuring the %FixC. The curve shows weight reduction during the experiment versus time. The gray curve is the measured reduction in %FixC after 100 seconds of purging CO and CO_2 gas. The gray dotted line, is is used to find the slope of the curve. In this example the curve, and the CO_2 reactivity, is 0.0378 %FixC/s.

Table 3.5: Overview over the temperature and gas program for the CO_2 reactivity tests. The time period where it says "??:??:??" is because the time for 20% of the fixed carbon has reacted is varying between the experiments.

Time Interval [hh:mm:ss]	**End Temperature [°C]**	**CO [L/min]**	**CO2 [L/min]**	**Ar [L/min]**
00:00:30	0	0	0	0
01:48:00	1070	0	0	2
00:30:00	1070	0	0	4
??:??:??	1070	2	2	0
01:00:00	20	0	0	2

Temperature and gas development through the CO_2 reactivity test is showed in Table 3.5. The carbon material will be heated up to 1070 °C with a flow of argon gas of 1 L/min purging through the crucible. The heating takes 108 minutes, and after this the flow of argon is increased to 4 L/min for 30 minutes. After this the atmosphere in the crucible is changed to CO and CO_2 gas, with a flow of 2 L/min of both gases. This gas composition is held until 20% of the fixed carbon in the carbon material has reacted. Then the atmosphere is changed to argon gas again for cooling.

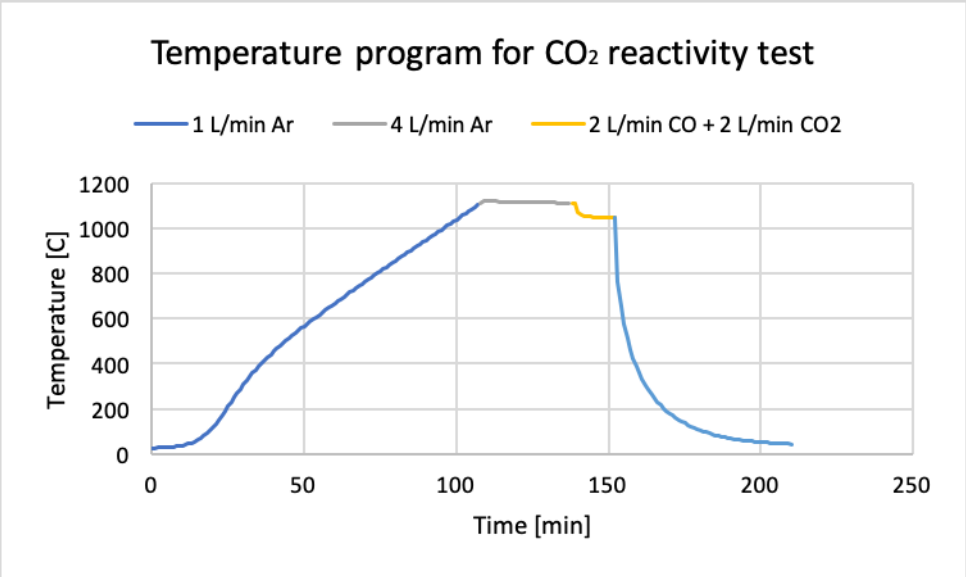

Figure 3.12: The gas and temperature program for the whole CO_2 reactivity test. The yellow curve where there is purging of CO and CO_2 gas will be where the CO_2 reactivity is measured.

When purging CO and CO_2 there will be a temperature drop due to the Boudouard reaction being endothermic. Figure 3.13 shows one example of a CO_2 reactivity test with the corresponding temperature drop. The weight measured in Figure 3.11 is measured at the same time.

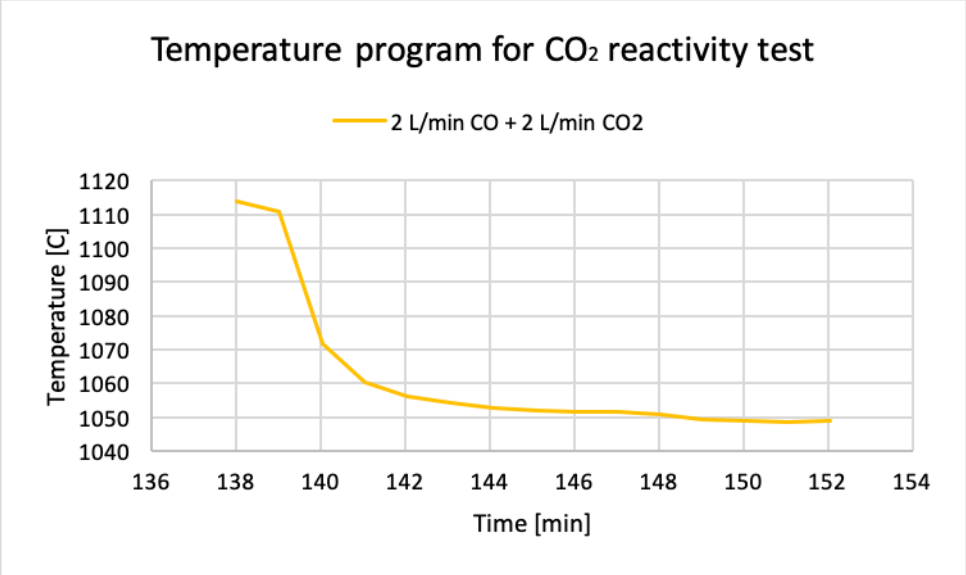

Figure 3.13: The gas and temperature program for CO_2 reactivity measurements of charcoal. This figure only shows the part where 50% CO and 50% CO_2 is purging. The temperature drop seen in this figure, is the temperature drop measured for the CO_2 reactivity test.

There has been performed 14 CO_2 reactivity experiments, and all the experimental data is given in Table 3.6.

Table 3.6: Overview over the different CO_2 reactivity measurements. The carbon material and treatment states which pre treatment and material used for the experiments. 1M, 2.5M and 5M is the molarity of the solution used for wet K-impregnation of the material. The CO_2 experiments on coke were performed by Vincent Canaguier from SINTEF.

Carbon material	**Treatment**	**Reaction temperature**	**Weight carbon material**
CharcoalRM	Wet K-imp 1M	1070 °C	30.41 g
CharcoalRM	Wet K-imp 2.5M	1070 °C	30.86 g
CharcoalRM	Wet K-imp 5M	1070 °C	35.65 g
CharcoalRM	Gas K-imp bottom layer	1070 °C	25.93 g
CharcoalRM´	Gas K-imp midle layer	1070 °C	34.74 g
CharcoalHT	None	1070 °C	32.53 g
CharcoalHT	Wet K-imp 1M	1070 °C	33.88 g
CharcoalHT	Wet K-imp 2.5M	1070 °C	32.04 g
CharcoalHT	Wet K-imp 5M	1070 °C	34.18 g
CharcoalHT	Gas K-imp top layer	1070 °C	30.86 g
CharcoalHT	Gas K-imp midle layer	1070 °C	32.86 g
Coke	None	1070 °C	30.94 g
Coke	Gas K-imp bottom layer	1070 °C	23.00 g
Coke	Gas K-imp midle layer	1070 °C	31.01 g

After one of the CO_2 reactivity tests, one of the charcoal samples began to self-ignite. This comes from the reaction equation 2.2 where potassium oxides react to pure potassium. Since the CO_2 reactivity test is performed in an inert atmosphere, the same problem as after the gas K-impregnation will occur here. The pure potassium will when exposed to air react to form KO_2 and KOH which is exothermic. This will again make the temperature increase, and if the temperature reaches 349 °C or anything else with lower auto ignition temperature get next to the sample, there might be fire. Because of this the end of the experiment was changed to include 30 minutes with air to let the potassium react inside the crucible so the charcoal would be stable at room temperature.

3.5 Scanning Electron Microscopy

The samples were studied using visual inspection in a Scanning Electron Microscope (SEM), used to understand the morphology and structure of the surface and the middle of the samples. From this method, the geometry and distribution of potassium after gas- and wet K-impregnation were studied. This was also used to see if there were differences between which particles the potassium impregnated more than others.

The SEM works by sending a thin beam of primary electrons against the surface of the sample to be studied, by studying the different reflections from the primary electron beam multiple signals can be used to understand the sample [44]. Examples on different signals that will give information about the sample is secondary electrons, back scattered electrons and x-ray radiation, and these signals will be used to study the samples in this thesis. Secondary Electron (SE) beam is used to get an image of the material surface morphology.

The Back Scattered Electrons (BSE) is used to find out which materials is of the same atomic number or not. How this signal can separate between the different atomic numbers is due to the increase in atomic number increases the signal, and makes the higher atomic number seem brighter in the pictures. For this project, it is the difference between the carbon with atomic number 6 and potassium with atomic number 19 that will be important, where in pictures the potassium will appear as bright particles/areas.

X-ray radiation is the last signal used, and by the method for Energy Dispersive X-ray Spectroscopy (EDS) the wavelengths of the x-rays is measured. Different materials will have different intensity of the wavelengths, and that makes it possible to get an overview of the present materials and phase composition of the sample.

3.6 Computed tomography

Computed tomography (CT) is in this thesis used as a method to analyze which elements is present in the carbon materials using x-rays. The x-rays analyses the samples from three directions; x-, y- and z-direction. When the x-rays reaches the elements in the sample, different elements will reflect different intensity of the wavelengths of the returning x-rays. Detectors detect the x-rays when returning from the particles and is transmitted to a computer which analyses the data. This data show a image of the sample with different shades of gray. The different tones will represent different elements, potassium would appear lighter than carbon.

Stein Rørvik from SINTEF performed the CT analysis for this thesis, on both gas and wet K-impregnated samples.

4 Results

The possibility to replace coke with charcoal in the ferromanganese alloy production is studied further in this chapter. The carbon materials are impregnated with alkalis using gas K-impregnation and wet K-impregnation. The potassium impregnated samples are analyzed using CT and SEM before the CO_2 reactivity is measured. The composition of the carbon materials is also found through proximate and ash analysis. Finally, the CO2 reactivity for the various materials are tested. In this section, the results from this study will be presented.

Notice that for each material made in this thesis, the sample is divided into batches for each analysis. This means that there might be differences between the batches used for chemical analysis, CO_2 reactivity and surface inspection, despite that care is taken to equalize the batches.

Remember that the nomenclature for the carbon materials in this thesis will be given as CharcoalXX%YY%K, where XX is the densification degree of the charcoal and YY is the percentage of K_2O in the charcoal after impregnation. The K at the end of the name will have a g or a w as a subscript, depending on which impregnation method is used, K_g for gas K-impregnation and K_w for wet K-impregnation.

4.1 Gas K-impregnation of carbon materials

Three gas K-impregnations of untreated charcoal (CharcoalRM), heat treated charcoal (CharcoalHT) and coke were executed for this thesis to increase the alkali content in the carbon materials. After the gas K-impregnation the samples were analyzed with proximate and ash analysis, but also visual inspection using SEM and CT.

4.1.1 Chemical analysis

Volatile, ash and fixed carbon content is measured through a proximate analysis, which for this thesis is performed by SINTEF Norlab. The results from the proximate analysis is given in Table 4.1. In this table, there is also given the % of K_2O, which is from the ash analysis. The K_2O is given as a percentage of the ash, and is used to calculate the total potassium content in the samples after K-impregnation. This will apply for all the proximate and ash analysis given in the rest of this thesis. The complete ash analyses is given in Appendix A.4.

Table 4.1: Volatiles, %FixC and ash from the proximate analysis of the gas K-impregnated materials. K_2O is from the ash analysis and is given as a percentage of the ash, where $\%K_2O$ is the total percentage of potassium in the sample. CharcoalRM is from earlier research, but given for comparison [8].

Sample name	**Volatiles**	**%FixC**	**Ash**	**K_2O**	**$\%K_2O$**
CharcoalRM	12.7	85.2	2.1	5.6	0.12
CharcoalRM2.95%K_g	5.65	80.87	13.48	21.9	2.95
CharcoalRM4.24%K_g	4.7	85.92	9.38	45.2	4.24
CharcoalRM1.77%K_g	2.00	94.65	3.35	52.7	1.77
CharcoalHT	2.41	94.90	4.75	14.63	0.39
CharcoalHT6.86%K_g	4.81	82.17	13.02	52.7	6.86
CharcoalHT1.11%K_g	2.13	94.72	3.15	35.1	1.11
CharcoalHT0.27%K_g	1.59	95.5	2.91	9.4	0.27
Coke	2.05	86.65	11.3	1.42	0.16
Coke2.86%K_g	2.62	78.58	18.8	15.2	2.86
Coke5.14%K_g	0.62	87.77	11.61	44.3	5.14
Coke0.38%K_g	1.17	88.90	9.93	3.85	0.38

After gas K-impregnation, the impregnated carbon material was divided into three layers, as described in the Method chapter. The achieved potassium content for each layer is given in Table 4.2. Comparing the potassium values in these layers, with the potassium content in the raw materials, all the layers have an increase in potassium content. For CharcoalRM the middle layer has the highest potassium content with 4.34%K_2O, where the bottom layer follows with 2.95%K_2O. Considering the values for CharcoalHT, the bottom layer has the highest potassium content with 6.68%K_2O followed by the middle layer 1.11%K_2O and lastly the top layer with 0.27%K_2O. For the gas K-impregnated coke, the middle layer is again the layer with the highest potassium content with 5.14%K_2O, followed by the bottom layer with 2.86%K_2O. For coke, as for the other gas K-impregnations, the top layer has the lowest potassium content. The highest potassium content is for CharcoalRM and coke the middle layer, where for CharcoalHT the highest potassium content is for the bottom layer. A higher K-deposition will be given by a higher K-vapor pressure, a lower temperature and a larger surface and porosity in the materials, and hence it is is believed that this will give the various K-contents in the bottom and lower layer. The average K deposition is however close for the three materials so we do not see that the properties of the materials have a large effect in this setup and with these materials. This will be further discussed in the next chapter.

Table 4.2: Overview over the potassium content in the three different layers after the Gas K-impregnation of CharcoalRM, CharcoalHT and Coke.

	CharcoalRM	**CharcoalHT**	**Coke**
Top layer	1.77 %K_2O	0.27 %K_2O	0.38 %K_2O
Middle layer	4.24 %K_2O	1.11 %K_2O	5.14 %K_2O
Bottom layer	2.95 %K_2O	6.86 %K_2O	2.86 %K_2O
Average values	2.99 %K_2O	2.75 %K_2O	2.79 %K_2O

4.1.2 CT of gas K-impregnated charcoal

In earlier research, there were performed gas K-impregnation of the heat-treated Charcoal-2% [9], and of the densified Charcoal15% [8]. The bottom layers from these gas K-impregnations were analyzed using CT to see how the potassium attaches to through the charcoal. The bottom layer from the gas K-impregnation of Charcoal-2% have a potassium content of 6.14%K_2O, where the bottom layer for Charcoal15% have 3.40%K_2O.

From the CT analysis, the charcoal was filmed from three directions, the x, y and z direction. Screenshots from each of these films for Charcoal-2%6.14%K_g is given in Figure 4.1, 4.2 and 4.3, representing respectively x-, y- and z-direction. For Charcoal15%3.40%K_g the CT pictures is given in Figure 4.4, 4.5 and 4.6. The potassium is shown as white or lighter areas, and the gray areas represents the carbon in the charcoal.

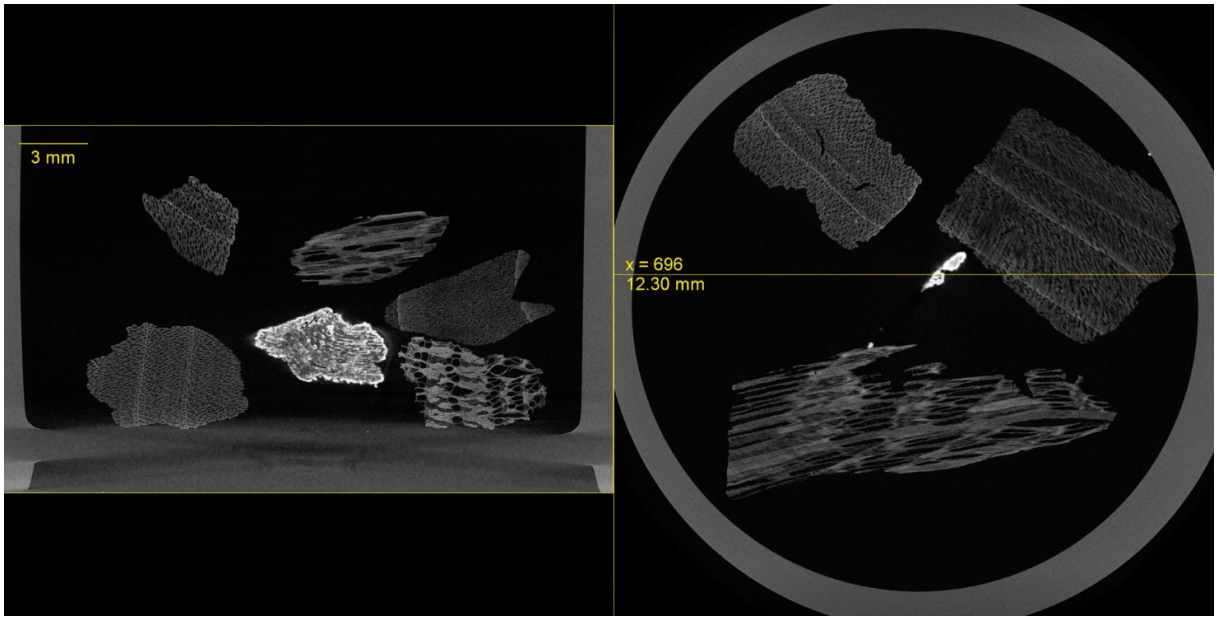

Figure 4.1: Screenshot from the CT analysis of the gas K-impregnated Charcoal-2%6.14%K_g filming through the charcoal sample following the x-axis.

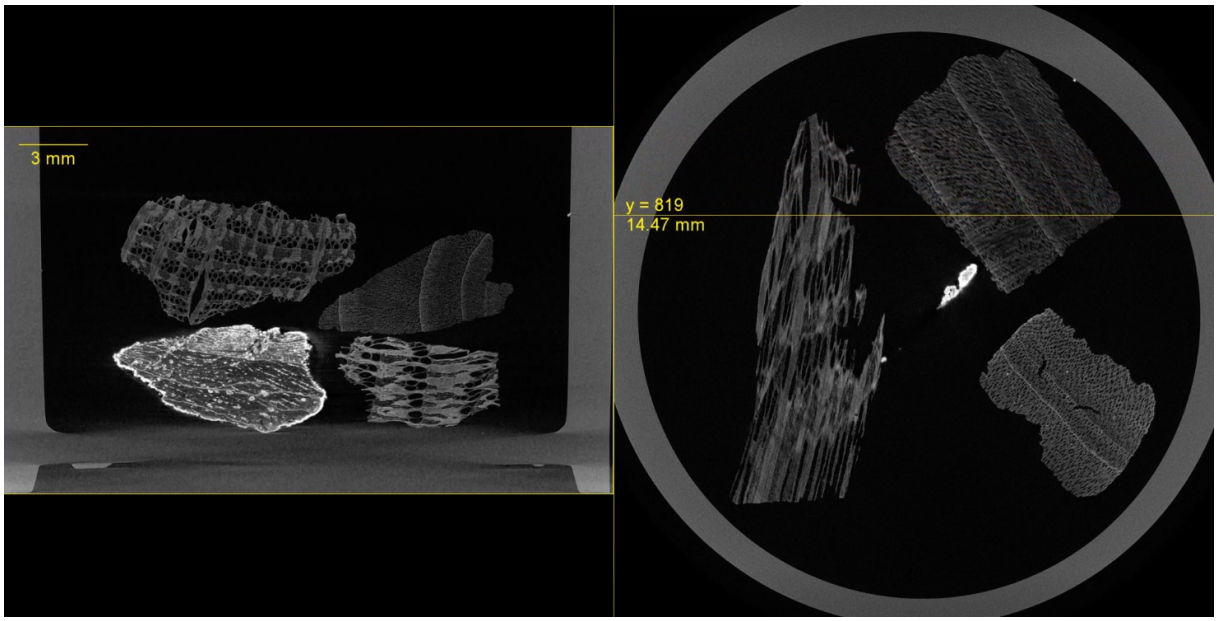

Figure 4.2: Screenshot from the CT analysis of the gas K-impregnated Charcoal-2%6.14%K_g filming through the charcoal sample following the y-axis.

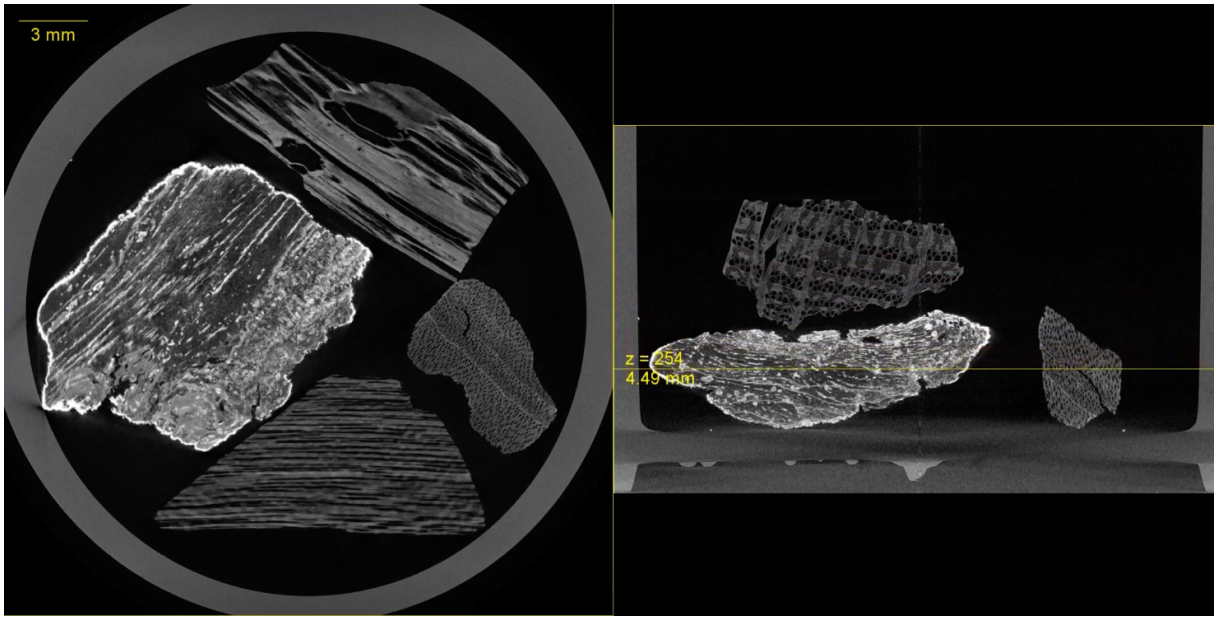

Figure 4.3: Screenshot from the CT analysis of the gas K-impregnated Charcoal-2%6.14%K_g filming through the charcoal sample following the z-axis.

Six particles are scanned in Figure 4.1, 4.2 and 4.3 and all of them with varying structure and different attachment of the potassium after the gas K-impregnation. First considering the lightest particle in all the images. Around this particle, it can be seen a thin white line of potassium around the edge of the particle, it can also be seen smaller lines and particles of potassium inside the charcoal particle. The potassium seems to be distributed evenly through the whole particle and it looks to be more potassium on this piece than on other particles. For the other particles, the potassium content and distribution seems to

be the same. All the particles are in darker gray, but with different shades of gray. There might be potassium in this particle, but from these pictures it is hard to state what is potassium and what is from density differences and pores in the particles.

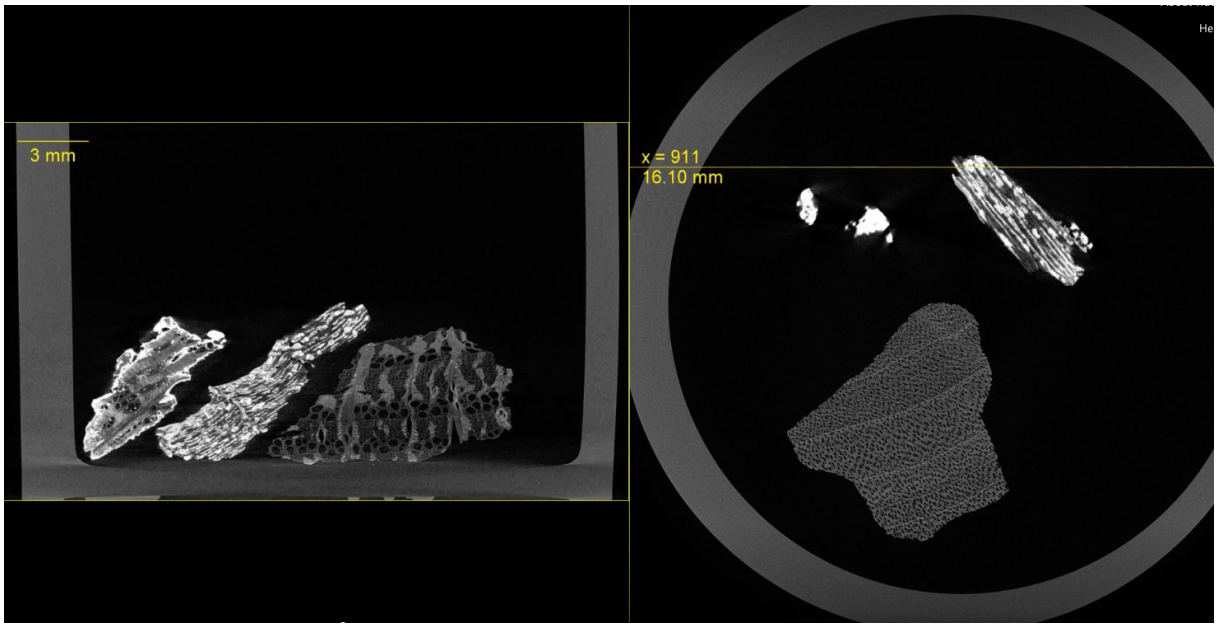

Figure 4.4: Screenshot from the CT analysis of the gas K-impregnated Charcoal15%3.40%K_g filming through the charcoal sample following the x-axis.

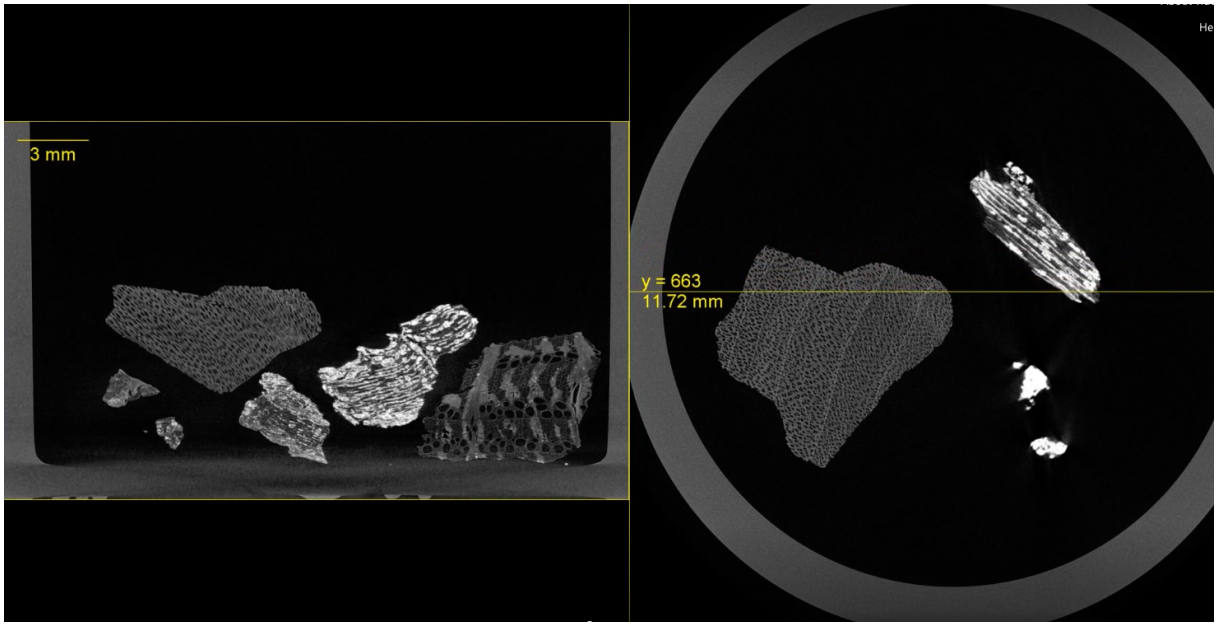

Figure 4.5: Screenshot from the CT analysis of the gas K-impregnated Charcoal15%3.40%K_g filming through the charcoal sample following the y-axis.

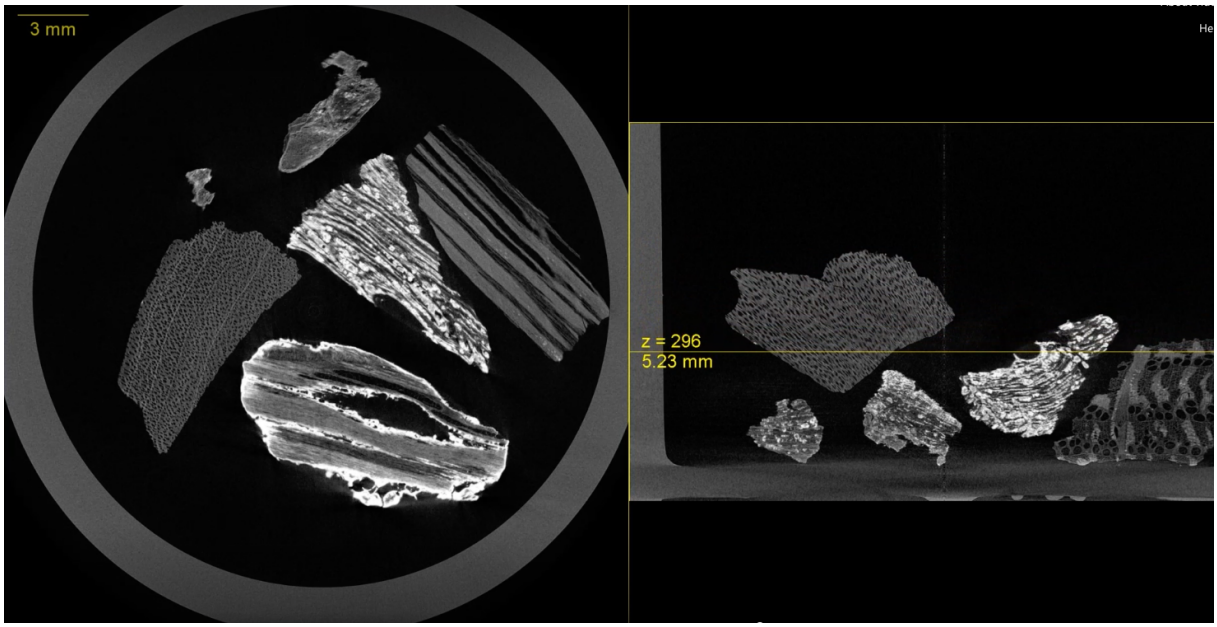

Figure 4.6: Screenshot from the CT analysis of the gas K-impregnated Charcoal15%3.40%K_g filming through the charcoal sample following the z-axis.

For Charcoal15%3.40%K_g two lighter particles can be seen in Figure 4.4, 4.5 and 4.6. These particles have potassium particles present throughout the particle, and a thin, white line around the edge of the particle. There can also be found lines of potassium where potassium has filled some of the capillary pores from the wooden structure of the charcoal. For the rest of the charcoal particles the tendency seems to be the same as for Charcoal-2%6.14%K_g, where the particles is all in a darker tone of gray, and most likely consisting of carbon.

To summarize, the particles is either completely impregnated with potassium or there is no clear potassium impregnation in the particles. For the completely impregnated particles there is found potassium as particles, as a thin line around the particle and inside pores. For Charcoal-2%6.14%K_g there were one completely impregnated particle, while there were two for Charcoal15%3.40%K_g. How the particle distribution is for the rest of the charcoal is hard to state when only some particles is studied using CT.

4.1.3 Surface analysis of gas K-impregnated charcoal using SEM

After CharcoalRM and CharcoalHT were gas K-impregnated, the bottom layers from both materials were analyzed with SEM. To understand how the potassium attaches to the charcoal during the Gas K-impregnation, the material surface and center is analyzed to see the placement of potassium on the charcoal. The SE picture shows the morphology of the surface, while the BSE picture shows the different elements with dark gray for carbon and lighter gray for potassium. To be able to show the center, the materials is cut in half. Confirming that the different colors or shades of gray in the BSE figures to be potassium or carbon, the samples is analyzed using EDS.

The surface of CharcoalRM2.95%K_2O_g is displayed in Figure 4.7 and 4.8. In these pictures, the surface is relatively flat, but have particles almost covering the whole particle. Figure 4.7a and 4.8a show the morphology of the particle. In these pictures, there are areas that are whiter. This comes from the accumulation of charge in the charcoal particle. This phenomenon can happen when there are particles on the surface, not connected good enough to the surface, so the charge can't escape. From the BSE pictures, Figure 4.7b and 4.8b, most of the surface is light gray, but some darker areas are visible in some places on the surface. This shows that the surface of this particle is covered with smaller potassium particles, but there are some places where the carbon from the charcoal is visible. Comparing the BSE pictures with the EDS pictures in Figure 4.9, the lighter areas in the BSE figures is the same as the red (potassium) areas in the EDS pictures. Where the darker areas in the BSE pictures is the same as the green (carbon) areas in the EDS picture.

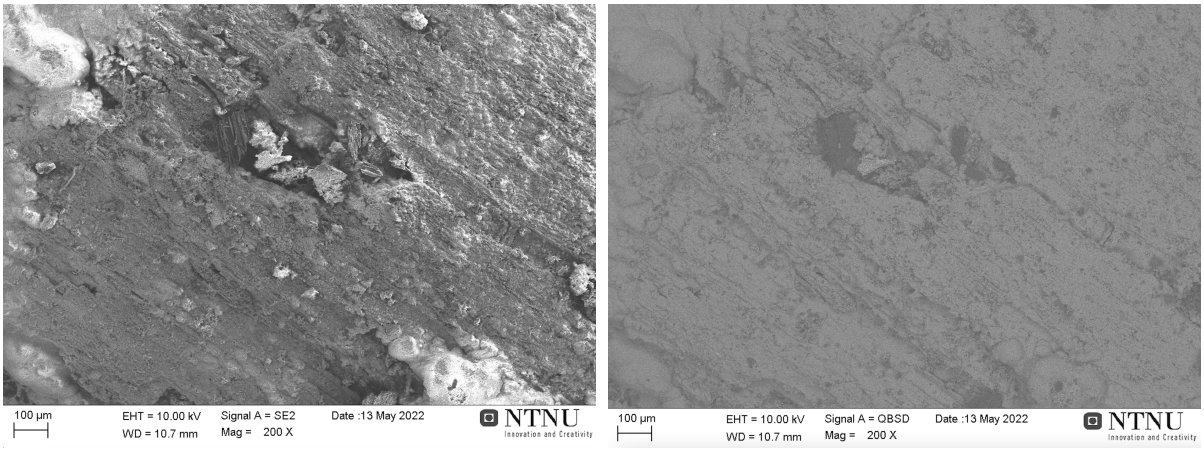

(a) (b)

Figure 4.7: The surface of one CharcoalRM2.95%K_g particle from SEM using SE to show the morphology on the surface (a) and BSE picture to show the different elements on the surface (b). Pictures taken with a magnification of 200MAG.

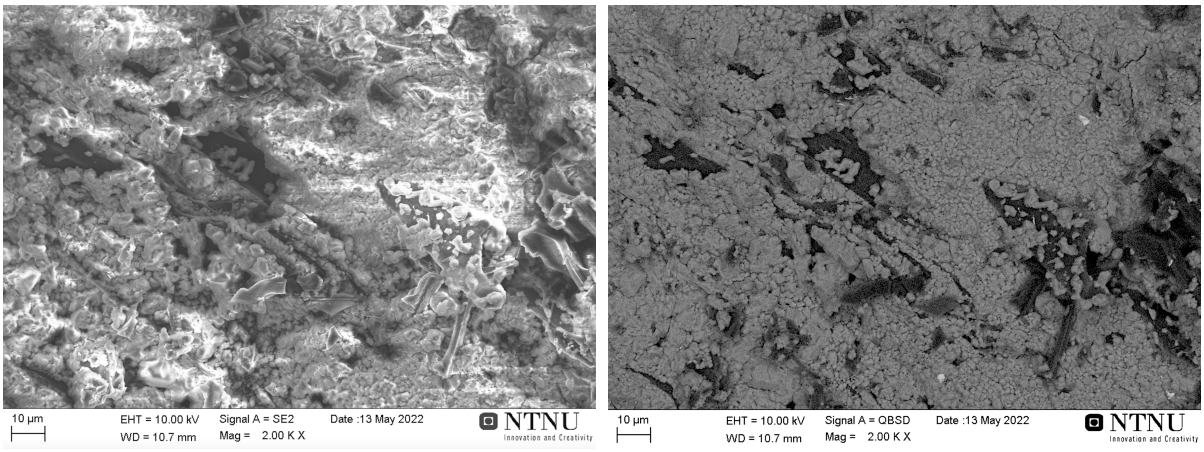

(a) (b)

Figure 4.8: The surface of one CharcoalRM2.95%K_g particle from SEM using SE to show the morphology on the surface (a) and BSE picture to show the different elements on the surface (b). Pictures taken with a magnification of 2000 MAG.

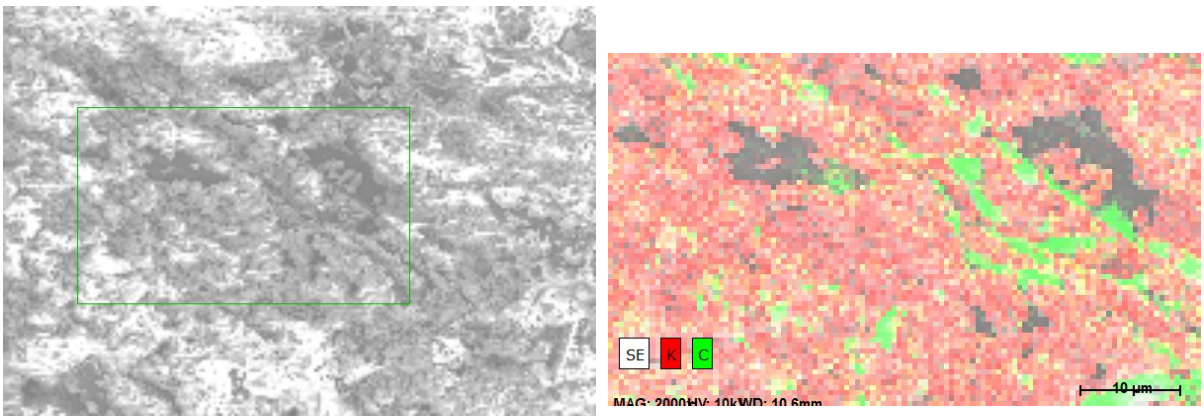

(a) (b)

Figure 4.9: The surface of one CharcoalRM2.95%K_g particle from SEM using SE to show the morphology on the surface (a) and EDS picture to show the different elements on the surface (b). Pictures taken with a magnification of 2000 MAG.

The center of one particle from CharcoalRM2.95%K_g is showed in Figure 4.10 and 4.11, where the particle is divided in half before studied in SEM. In these pictures, the particle has many pores of different sizes, and in the SE pictures, Figure 4.10a and 4.11a, the morphology of the center of the charcoal with all its pores can be seen. In the pores, there can be seen particles attached to the pore walls. The pictures of the inside of the particle, taken with BSE is displayed in Figure 4.10b and 4.11b. Carbon is found as darker gray areas which mainly makes the pore structure in the charcoal particle, where the potassium is the lighter gray particles, most of which found on the pore walls. The potassium is seen to be particles with size up to 5 μm. Comparing the BSE pictures with the EDS pictures in Figure 4.12, the lighter areas inside the pores in the BSE figures is the same as the red (potassium) areas in the EDS pictures. Where the darker pore structure in the BSE pictures is the same as the green (carbon) areas in the EDS picture.

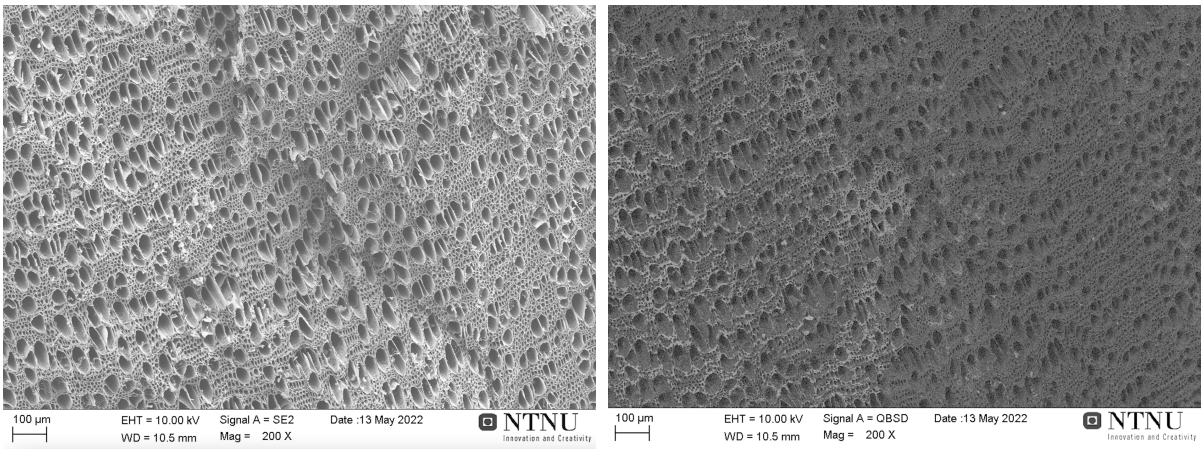

(a) (b)

Figure 4.10: The middle of one CharcoalRM2.95%K_g particle from SEM using SE to show the morphology on the surface (a) and BSE picture to show the different elements on the surface (b). Pictures taken with a magnification of 200 MAG.

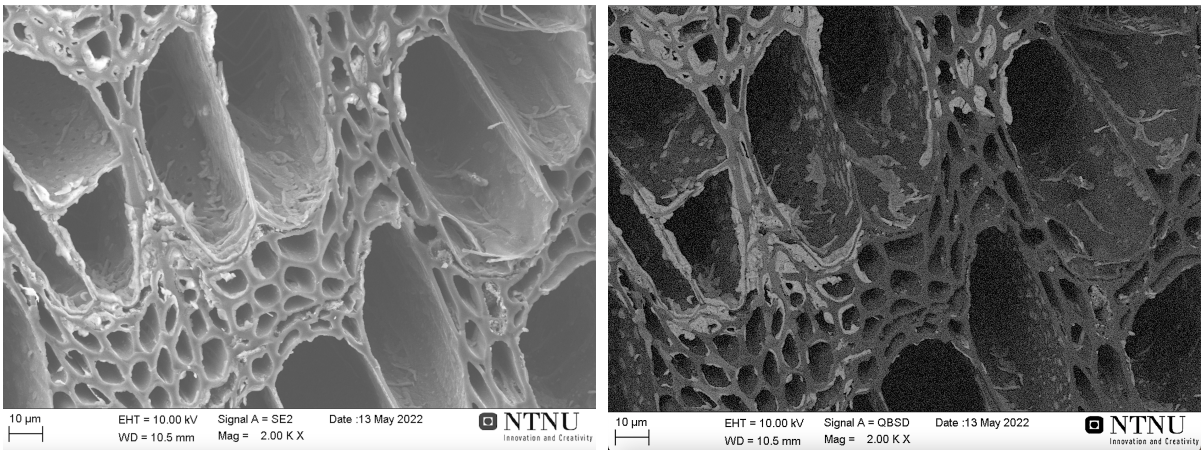

(a) (b)

Figure 4.11: The middle of one CharcoalRM2.95%K_g particle from SEM using SE to show the morphology on the surface (a) and BSE picture to show the different elements on the surface (b). Pictures taken with a magnification of 2000 MAG.

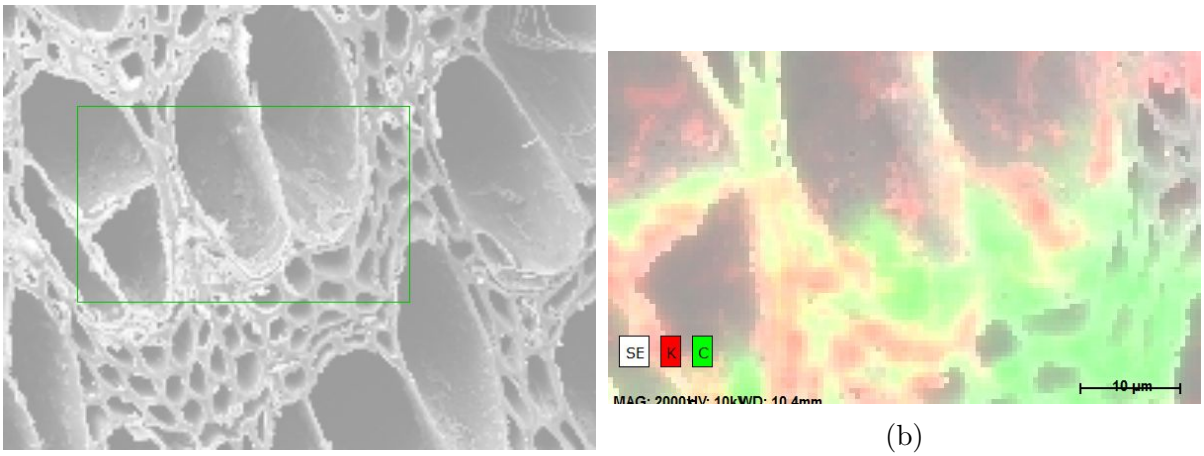

(a) (b)

Figure 4.12: The middle of one CharcoalRM2.95%K_g particle from SEM using SE to show the morphology on the surface (a) and EDS picture to show the different elements on the surface (b). Pictures taken with a magnification of 2000 MAG.

CharcoalHT6.68%K_g, which is the bottom layer from the gas K-impregnation of CharcoalHT, is also studied using SEM. The surface of one of the charcoal particles is showed in Figure 4.13 and 4.14, in both figures there is one picture using SE and one using BSE. From the pictures using SE, the surface is relatively flat with several particles on top of the surface. The surface particles are small, around 2-5 μm. When analyzing the same surface using BSE, there are several small particles on the surface in a white color (potassium) and some of the particles is gray as the charcoal particle (carbon). The potassium particles are distributed on the surface, but not covering the surface as found for other impregnated charcoal samples. Comparing the BSE pictures with the EDS pictures in Figure 4.15, the lighter particles in the BSE figures are the same as the green (potassium) particles in the EDS pictures. Where the darker particle surface in the BSE pictures are the same as the red (carbon) areas in the EDS picture.

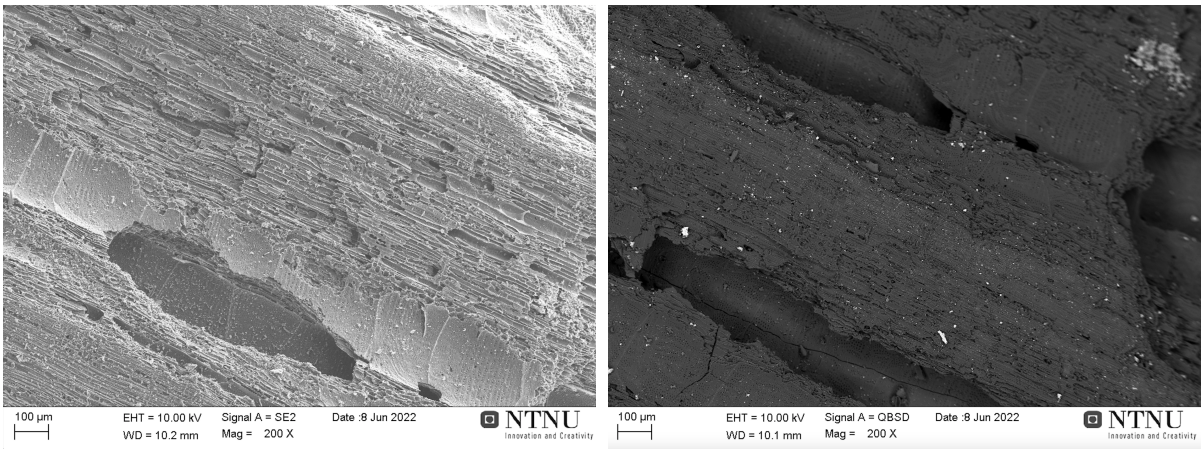

(a) (b)

Figure 4.13: The surface of one CharcoalHT6.86%K_g particle from SEM using SE to show the morphology on the surface (a) and BSE picture to show the different elements on the surface (b). Pictures taken with a magnification of 200 MAG.

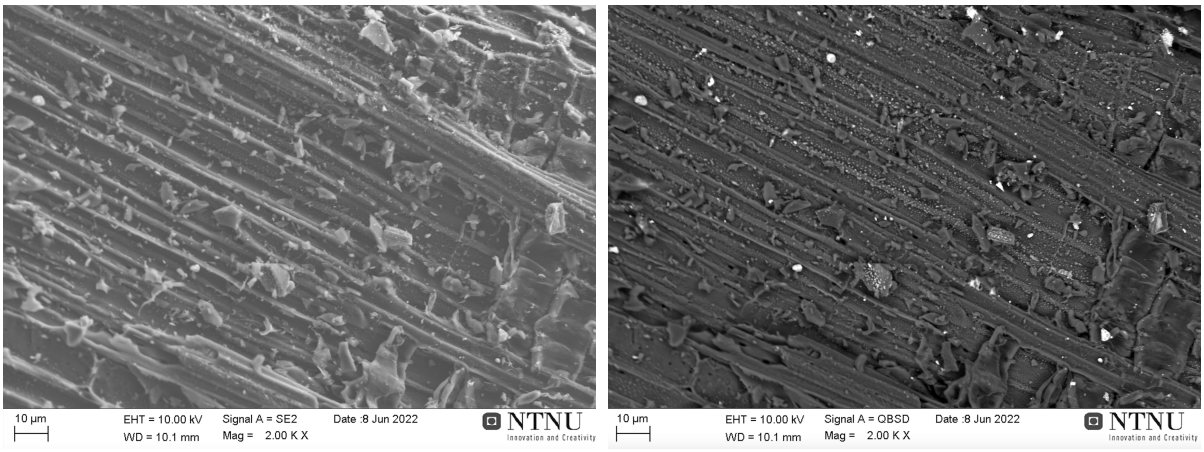

(a) (b)

Figure 4.14: The surface of one CharcoalHT6.86%K_g particle from SEM using SE to show the morphology on the surface (a) and BSE picture to show the different elements on the surface (b). Pictures taken with a magnification of 2000 MAG.

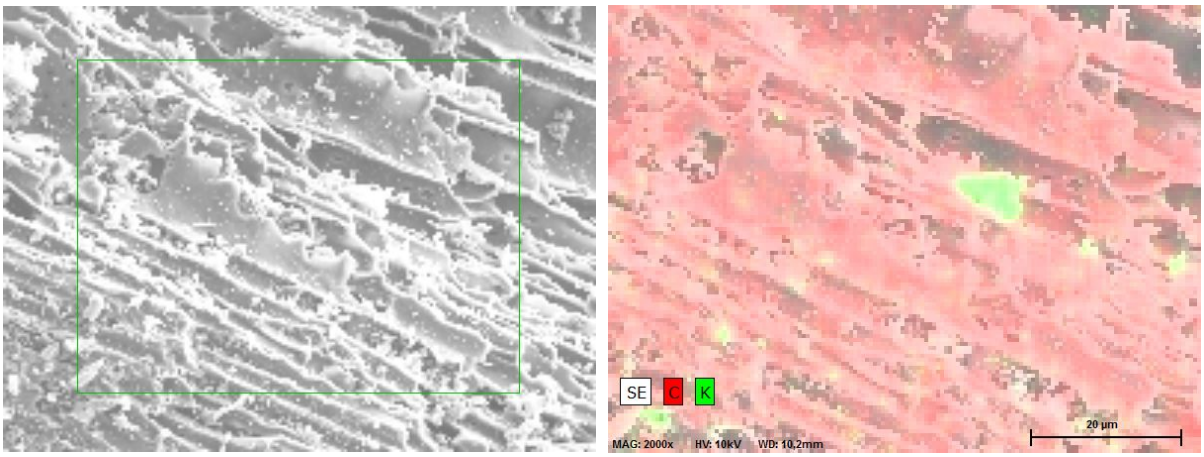

(a) (b)

Figure 4.15: The surface of one CharcoalHT6.86%K_g particle from SEM using SE to show the morphology on the surface (a) and EDS picture to show the different elements on the surface (b). Pictures taken with a magnification of 2000 MAG.

The middle of CharcoalHT6.68%K_g is studied in SEM, showed in Figure 4.16 and 4.17. Through SE the morphology of the middle of this particle is showed, 4.16a and 4.17a. From these figures the capillary pores of the wooden structure is showed in the charcoal particle. It can also be seen in Figure 4.16a that in the middle of the surface there is an area which do not have many particles, where the surrounding pore structure are more covered in particles. Studying this using BSE the particles on the surroundings is lighter than the pore structure. Increasing the magnification from 200 MAG to 2000 MAG it can be seen in Figure 4.17b that the particles covering parts of the surface is small and around 1 μm, and are attached to the pore walls making the pores smaller. Comparing the BSE pictures with the EDS pictures in Figure 4.18, the lighter areas formed by the small particles in the BSE figures is the same as the green (potassium) areas in the EDS

pictures. Where the darker areas in the BSE pictures is the same as the red (carbon) areas in the EDS picture.

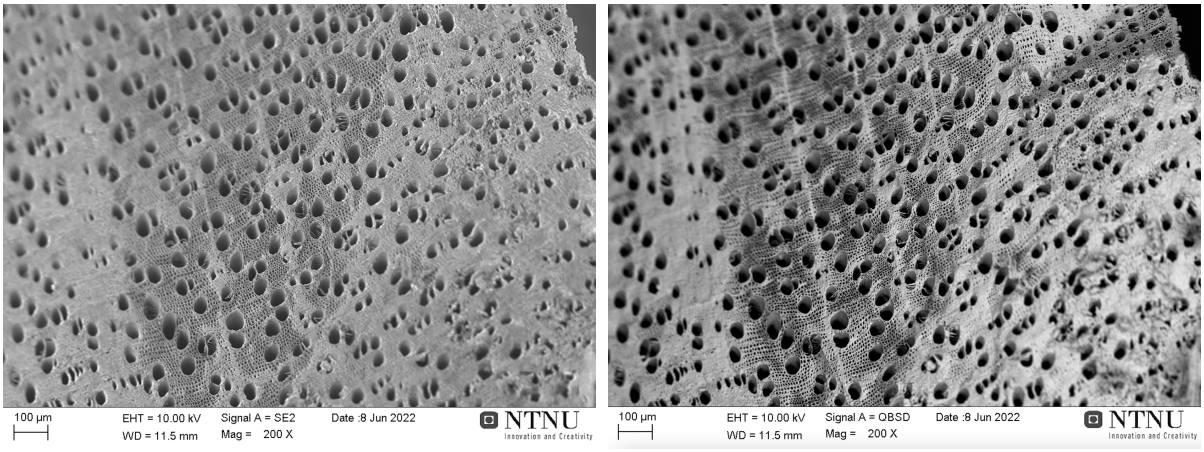

(a) (b)

Figure 4.16: The middle of one CharcoalHT6.86%K_g particle from SEM using SE to show the morphology on the surface (a) and BSE picture to show the different elements on the surface (b). Pictures taken with a magnification of 200 MAG.

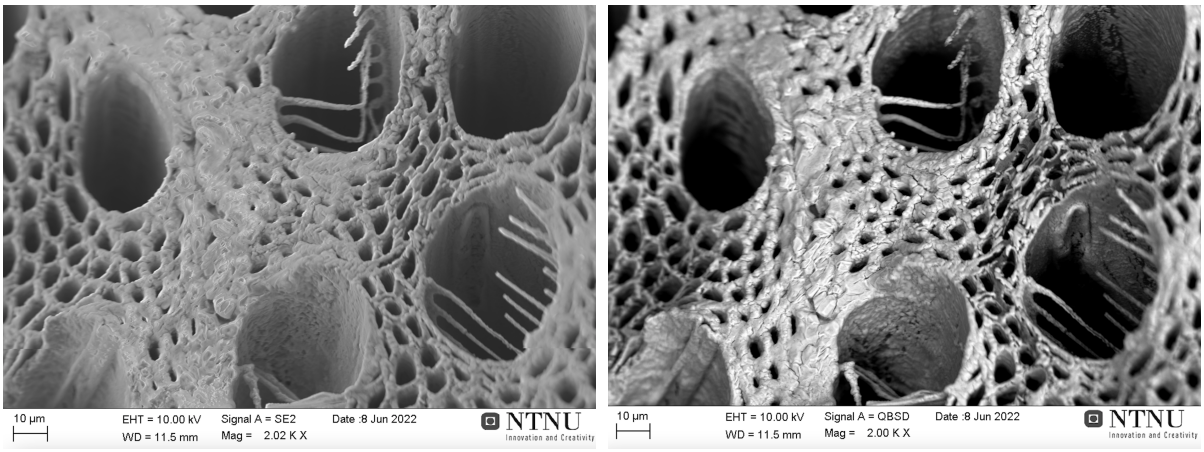

(a) (b)

Figure 4.17: The middle of one CharcoalHT6.86%K_g particle from SEM using SE to show the morphology on the surface (a) and BSE picture to show the different elements on the surface (b). Pictures taken with a magnification of 2000 MAG.

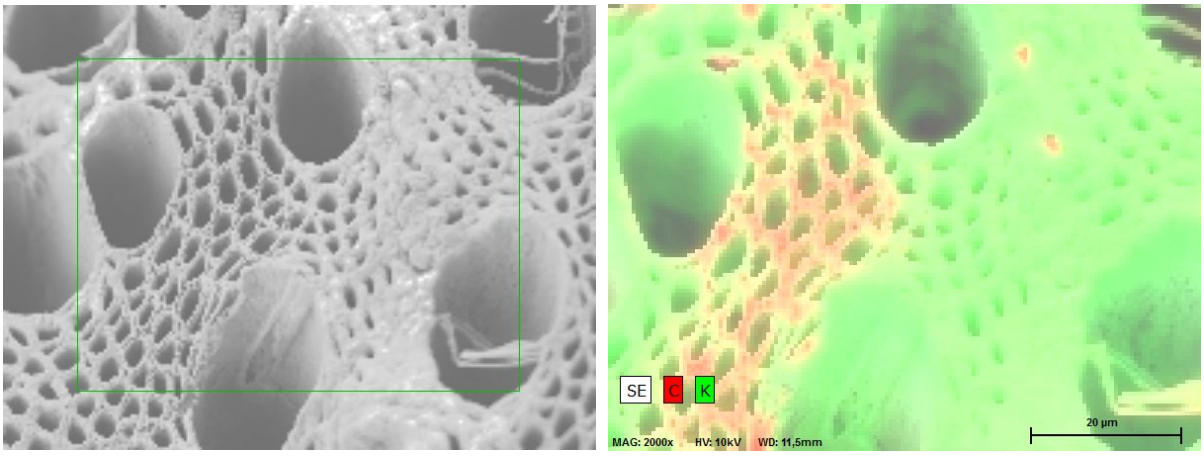

(a) (b)

Figure 4.18: The middle of one CharcoalHT6.86%K_g particle from SEM using SE to show the morphology on the surface (a) and EDS picture to show the different elements on the surface (b). Pictures taken with a magnification of 2000 MAG.

For most of the particles studied in SEM, the potassium particles from the gas K-impregnation either attaches to the surface of the capillary pores in the charcoal, or cover the surface with a varying amount of potassium particles. It also seems that there is a variation of the amount potassium attached to the charcoal particles, since some of the particles is almost covered, while other only have a few potassium particles on the surface.

4.2 Wet K-impregnation of charcoal

Six wet K-impregnations is done for this thesis, three on the untreated charcoal (CharcoalRM) and three on heat treated charcoal (CharcoalHT). On each of the carbon materials there were used solutions with 1M, 2.5M and 5M of potassium. After the wet K-impregnation the samples were analyzed with proximate and ash analysis to find the chemical composition, but also visual inspection of the surface using SEM and CT.

4.2.1 Chemical analysis

The chemical composition of the samples is found through proximate and ash analysis, both performed by SINTEF Norlab, as for the gas K-impregnated samples. For the complete analysis of the wet K-impregnates samples, see Appendix A.4. Table 4.3 shows the proximate analysis of the samples, with K_2O from the ash analysis. The last element in the table is $\%K_2O$, which is calculated to find the total amount of potassium in the impregnated carbon materials.

Table 4.3: Volatiles, %FixC and ash from the proximate analysis of the wet K-impregnated materials. K_2O is from the ash analysis and is given as a percentage of the ash, where $\%K_2O$ is the total percentage of potassium in the sample. CharcoalRM is from earlier research, but given for comparison [8].

Sample name	**Volatiles**	**%FixC**	**Ash**	**K2O**	**%K_2O**
CharcoalRM	12.7	85.2	2.1	5.6	0.12
CharcoalRM1.45K_w	16.12	79.13	4.75	30.48	1.45
CharcoalRM5.23K_w	15.80	71.80	12.40	42.20	5.23
CharcoalRM8.71K_w	16.72	65.03	18.25	47.71	8.71
CharcoalHT	2.41	94.9	2.69	14.63	0.39
CharcoalHT3.21K_w	5.07	87.77	7.16	44.8	3.21
CharcoalHT3.43K_w	6.54	82.75	10.71	32.0	3.43
CharcoalHT10.53K_w	8.63	71.32	20.05	52.5	10.53

The goal with impregnation of the samples is to change the alkali content of the carbon materials. In Table 4.4 the achieved potassium contents for the different wet K-impregnations is separated for which carbon material is used as raw material and molarity of the solution used for the wet K-impregnation. The table shows the achieved $\%K_2O$ for the different carbon materials, and the $\%K_2O$ increases with increasing molarity. The 5 molar solution gives the highest potassium contents with 8.71%K_2O and 10.53%K_2O. 1 molar solution gives the lowest $\%K_2O$ of 1.45 and 3.21.

Table 4.4: Overview over the gained potassium content from different molarities after wet K-impregnation of CharcoalRM and CharcoalHT.

	CharcoalRM	**CharcoalHT**
1M	1.45 $\%K_2O$	3.21 $\%K_2O$
2.5M	5.23 $\%K_2O$	3.43 $\%K_2O$
5M	8.71 $\%K_2O$	10.53 $\%K_2O$

4.2.2 CT of wet K-impregnated charcoal

In earlier research, there were performed a wet K-impregnation of Charcoal-2% and Charcoal11% [9], where Charcoal-2% was a charcoal after heat treatment of CharcoalRM and Charcoal11% was densified resulting in 11% densification. The samples were analyzed using CT to see how the potassium attaches to the charcoal. The wet K-impregnated samples used have potassium content of 1.93%K_2O for Charcoal-2% and 1.25%K_2O for Charcoal11%.

CT analysis of the charcoal was filmed from three directions, the x, y and z direction. Screenshots from each of these films for Charcoal-2%1.93%K_w is given in Figure 4.19, 4.20 and 4.21, representing respectively x-, y- and z-direction. For Charcoal11%1.25%K_w the different directions is showed in the Figures 4.22, 4.23 and 4.24. The potassium is shown as white or lighter areas on the gray areas which represents the carbon from the charcoal. Four particles were analyzed for the wet K-impregnated samples as well, and there is a variation of the structure of the charcoal particles and how the capillary pores from the three goes through the charcoal particles.

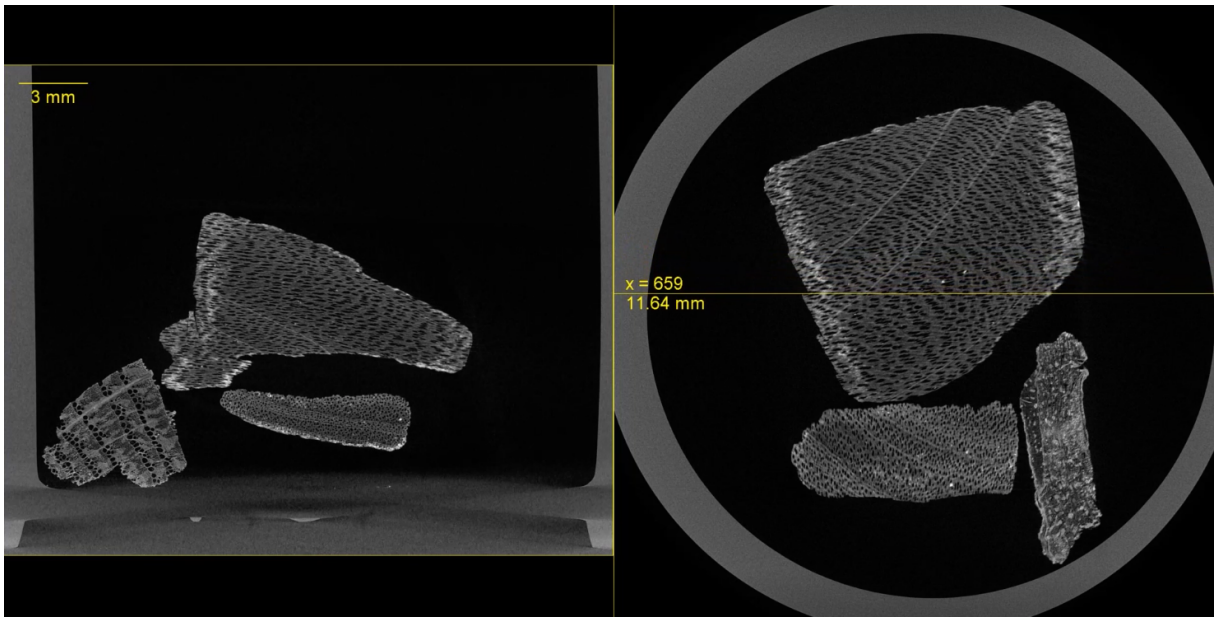

Figure 4.19: A screenshot from the CT analysis of the wet K-impregnated Charcoal-2%1.93%K_w filming through the charcoal sample following the x-axis.

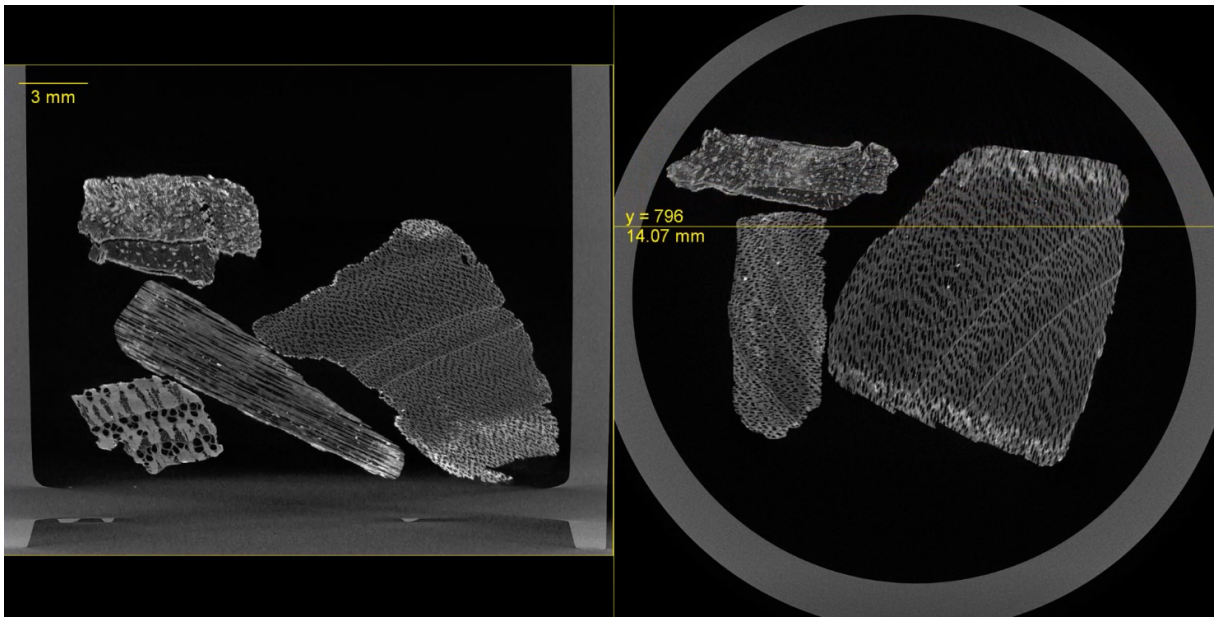

Figure 4.20: A screenshot from the CT analysis of the wet K-impregnated Charcoal-2%1.93%K_w filming through the charcoal sample following the y-axis.

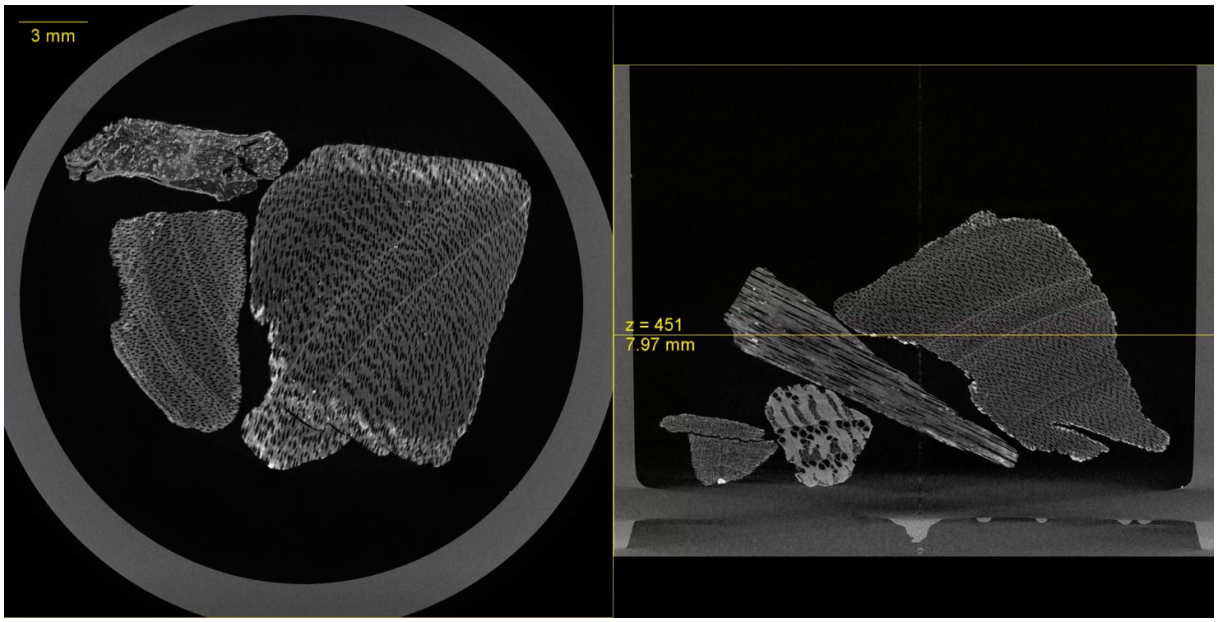

Figure 4.21: A screenshot from the CT analysis of the wet K-impregnated Charcoal-2%1.93%K_w filming through the charcoal sample following the z-axis.

One similarity for the wet K-impregnated particles in the Figures 4.19, 4.20 and 4.21 is that all the particles have an edge which are in a lighter tone of gray than the rest of the particle. This white edge goes almost 1 mm into the particles. Any other distribution of potassium is hard to see; however, it seems that there are some white particles in more central parts of the particles. One of the charcoal particles also seem to have potassium particles through the charcoal in a larger degree than the other.

Charcoal11%1.25%K_w and the distribution of potassium in these wet K-impregnated par-

ticles is as mentioned showed in Figure 4.22, 4.23 and 4.24. For most of the particles in these pictures, there is a white or lighter gray edge to the particles. The white edge is for these particles thinner than for the particles from Charcoal-2%1.93%K_w. It can be seen one particle where the potassium is placed as particles through the whole charcoal particle.

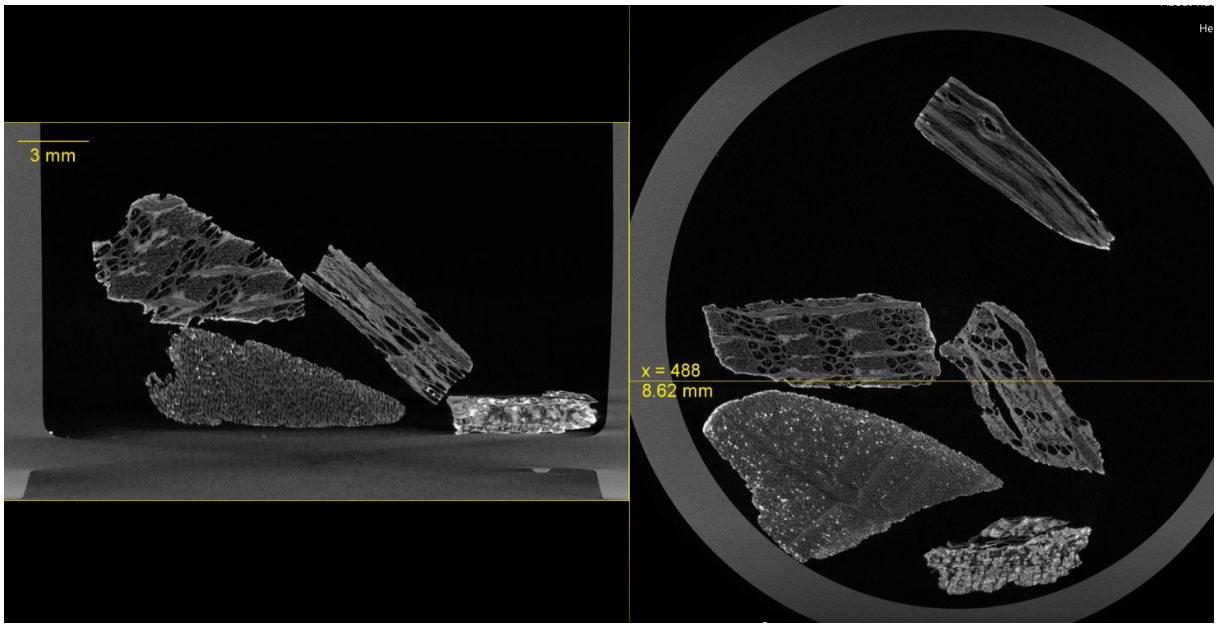

Figure 4.22: A screenshot from the CT analysis of the wet K-impregnated Charcoal11%1.25%K_w filming through the charcoal sample following the x-axis.

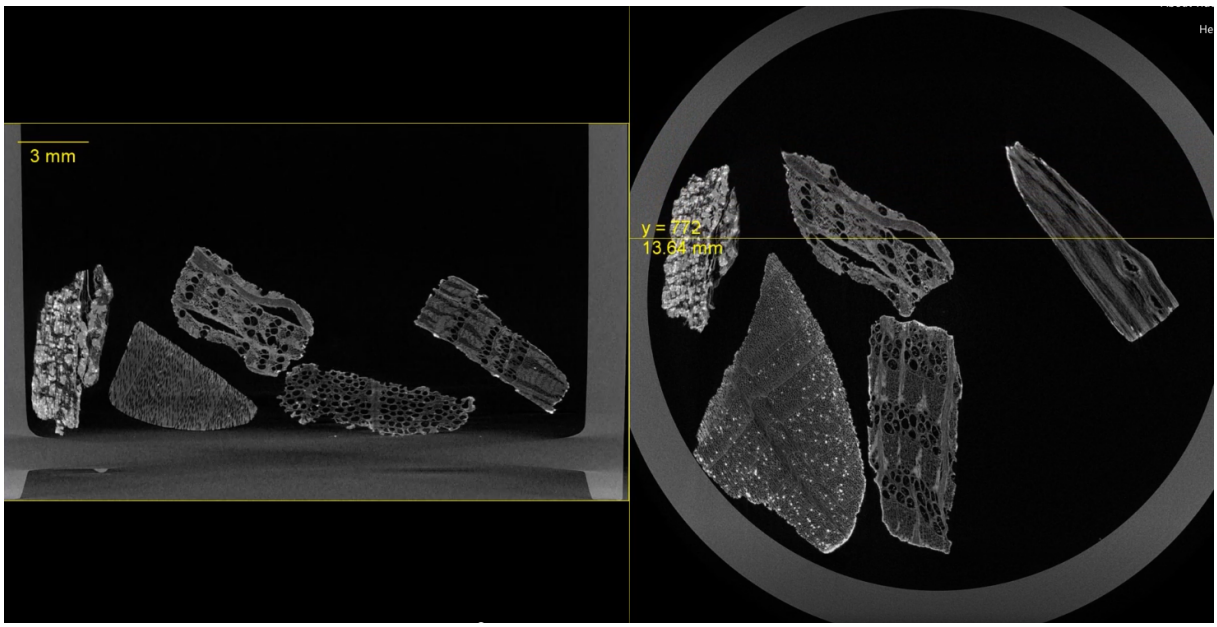

Figure 4.23: A screenshot from the CT analysis of the wet K-impregnated Charcoal11%1.25%K_w filming through the charcoal sample following the y-axis.

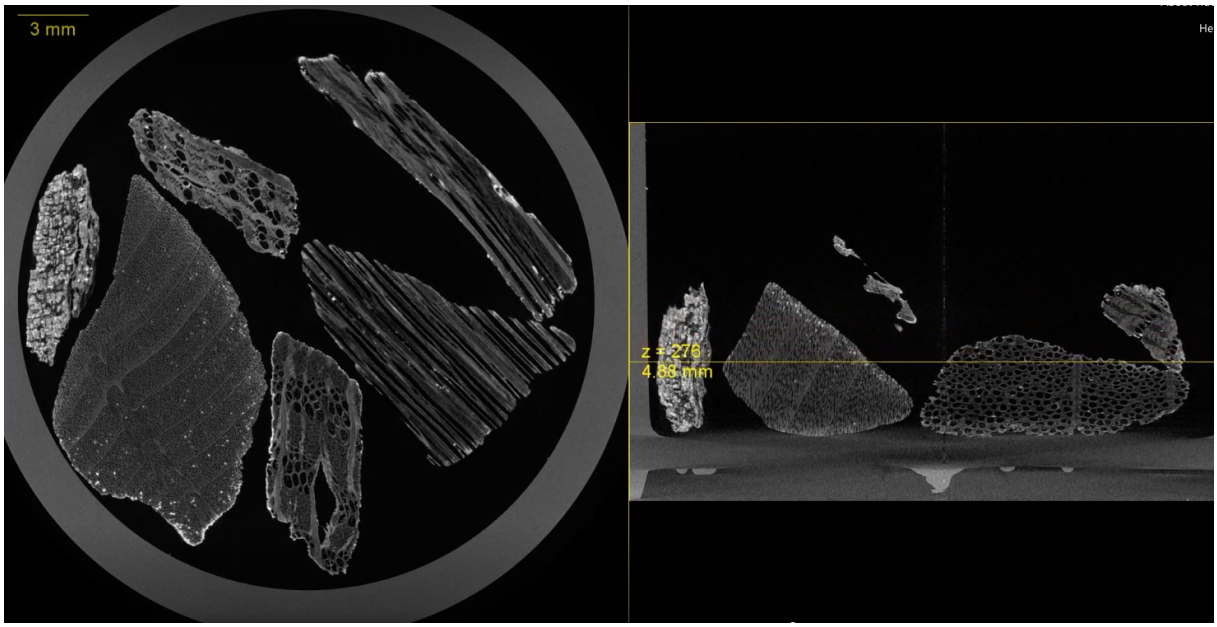

Figure 4.24: A screenshot from the CT analysis of the wet K-impregnated Charcoal11%1.25%K_w filming through the charcoal sample following the z-axis.

For the wet K-impregnated charcoal there is a white edge around most of the particles with a thickness around 1 mm. For both of the charcoals there is found one particle with potassium particles throughout. The rest of the charcoal particle is either found with a few potassium particles and/or with a white line of potassium around the edges.

4.2.3 Surface analysis of wet K-impregnated charcoal using SEM

The wet K-impregnated charcoal is analyzed using SEM. For the impregnated CharcoalRM, one particle from the impregnation using 5 molar solution, CharcoalRM8.71%K_w, is studied to see one example of how the particles attach to the surface. Figure 4.25 and 4.26 shows the surface of one particle with magnification of respectively 200 and 2000 MAG. The particle surface is relatively flat, and without visible pore structure. Particles of different sizes are covering the surface of the wet K-impregnated particle, but comparing the SE pictures with the BSE pictures, most of the particles on the surface is displayed as white particles, see Figure 4.25b and 4.26b. The white particles are potassium particles, and the particles that remain gray is of carbon. The potassium lays as particles on top of the charcoal, but also filling in small voids/pores on the surface. Comparing the BSE pictures with the EDS pictures in Figure 4.27, it can be seen that the white particles in the BSE figures is the same as the green (potassium) particles in the EDS pictures. Where the darker areas in the BSE pictures is the same as the red (carbon) surface in the EDS picture.

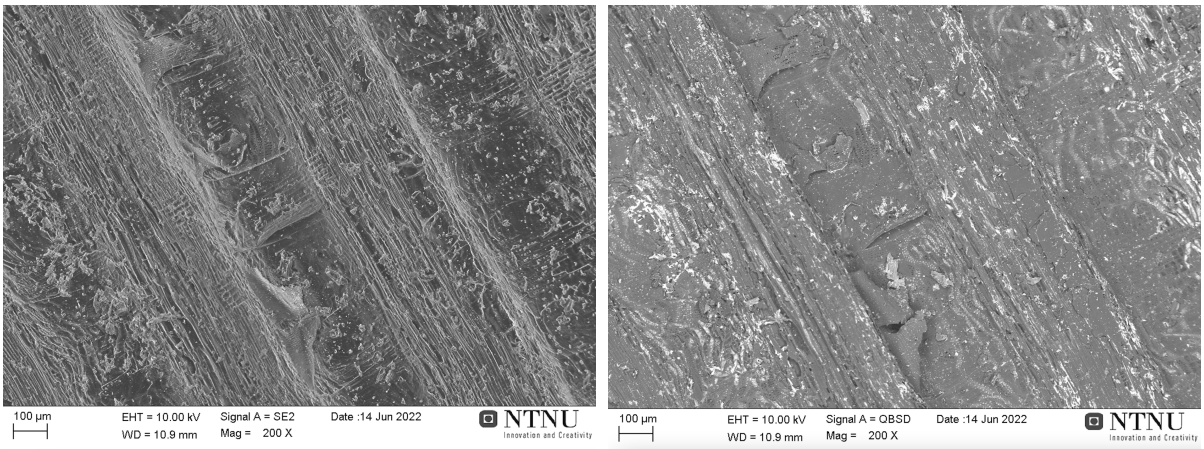

(a) (b)

Figure 4.25: The surface of one CharcoalRM8.71%K_w particle from SEM using SE to show the morphology on the surface (a) and BSE picture to show the different elements on the surface (b). Pictures taken with a magnification of 200 MAG.

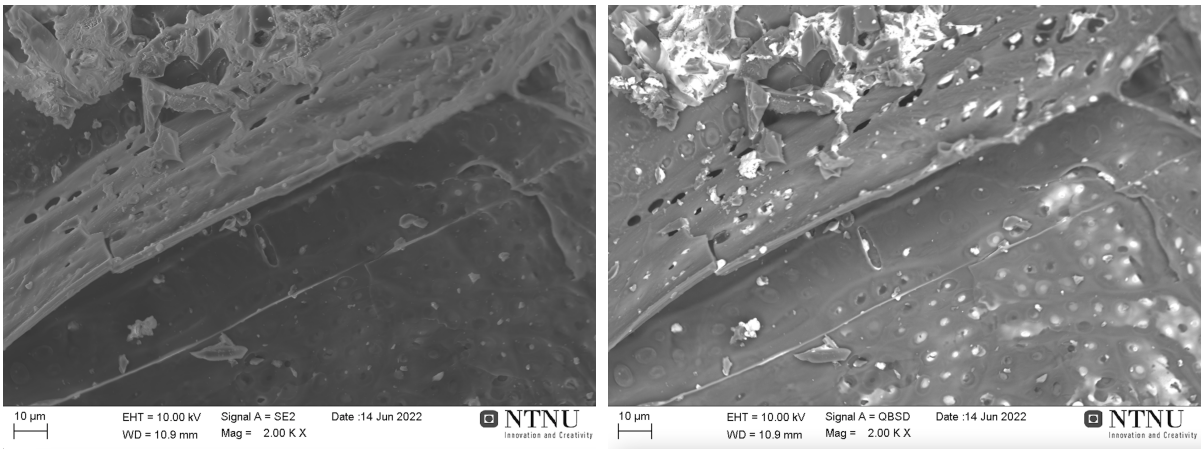

(a) (b)

Figure 4.26: The surface of one CharcoalRM8.71%K_w particle from SEM using SE to show the morphology on the surface (a) and BSE picture to show the different elements on the surface (b). Pictures taken with a magnification of 2000 MAG.

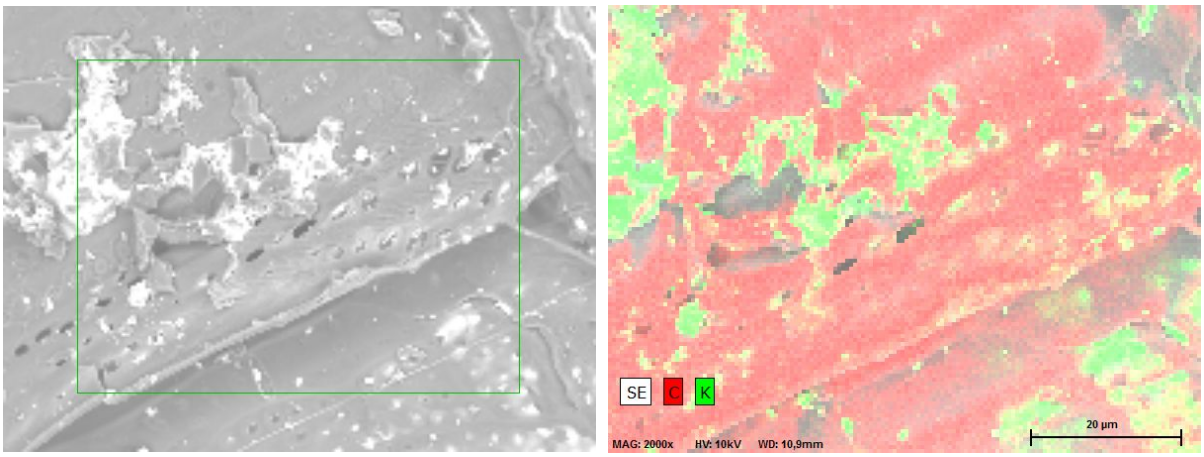

(a) (b)

Figure 4.27: The surface of one CharcoalRM8.71%K_w particle from SEM using SE to show the morphology on the surface (a) and EDS picture to show the different elements on the surface (b). Pictures taken with a magnification of 2000 MAG.

Another particle of CharcoalRM8.71%K_w was divided to display the structures in the middle of the particle, showed in Figure 4.28 and 4.29. In this particle, the charcoal structure consist of pores in mainly two sizes: smaller with around 10 μm diameter, and larger pores around 50 μm diameter. Some of the pores is filled with particles, and around half of the larger pores is filled with potassium particles. The potassium particles in the pores can be seen in the BSE pictures, Figure 4.28b and 4.29b, as white particles. Comparing the BSE pictures with the EDS pictures in Figure 4.30, the white particles in the BSE figures is the same as the green (potassium) particles in the EDS pictures. Where the darker areas in the BSE pictures is the same as the red (carbon) pore structure in the EDS picture.

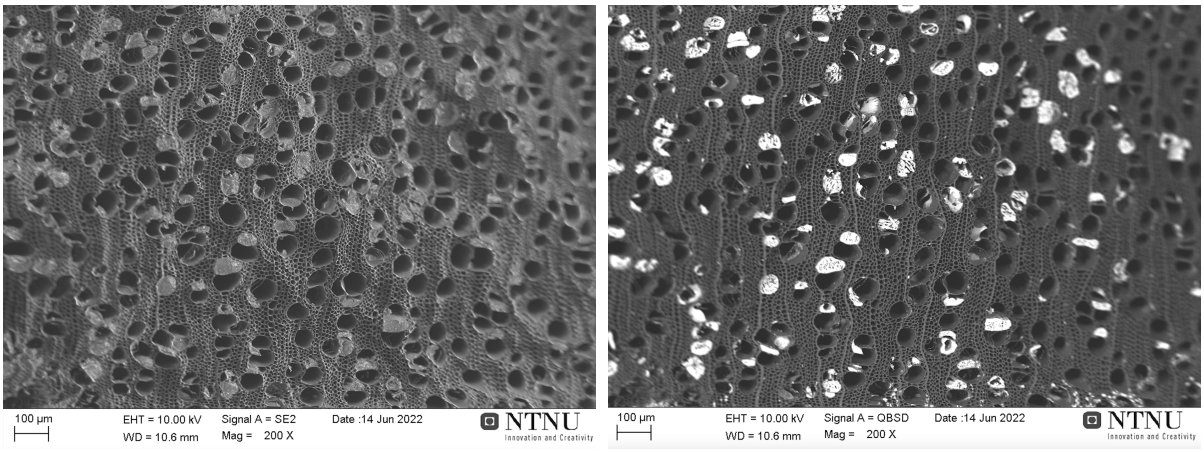

(a) (b)

Figure 4.28: The middle of one CharcoalRM8.71%K_w particle from SEM using SE to show the morphology on the surface (a) and BSE picture to show the different elements on the surface (b). Pictures taken with a magnification of 200 MAG.

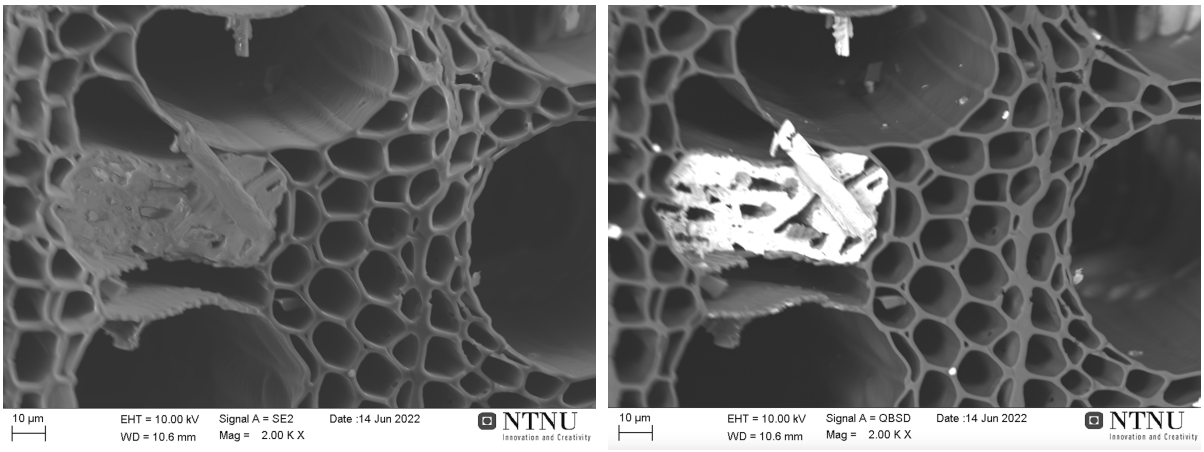

(a) (b)

Figure 4.29: The middle of one CharcoalRM8.71%K_w particle from SEM using SE to show the morphology on the surface (a) and BSE picture to show the different elements on the surface (b). Pictures taken with a magnification of 2000 MAG.

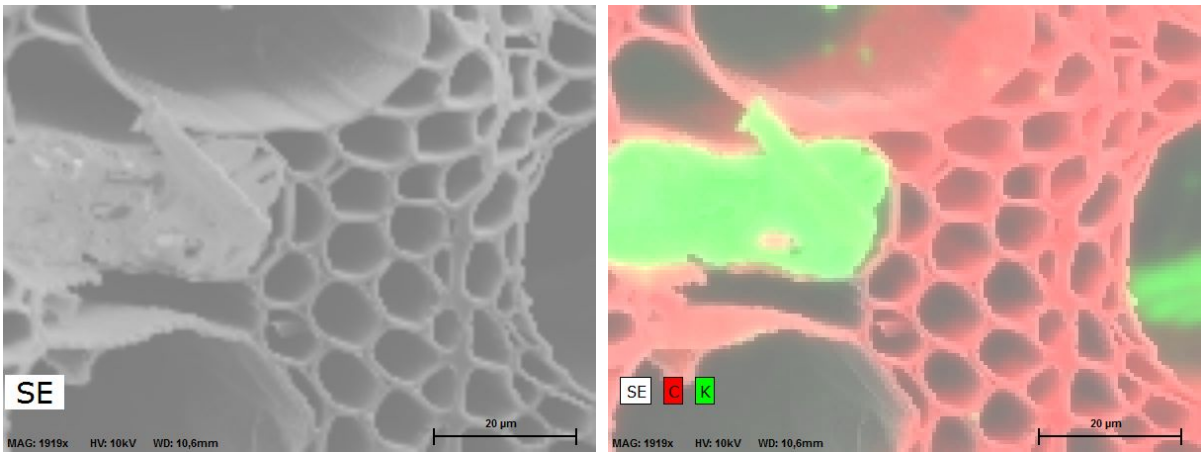

(a) (b)

Figure 4.30: The middle of one CharcoalRM8.71%K_w particle from SEM using SE to show the morphology on the surface (a) and EDS picture to show the different elements on the surface (b). Pictures taken with a magnification of 2000 MAG.

CharcoalHT10.53%K_w was also analyzed in SEM, results showed in Figure 4.31 and 4.32. Studying the pictures from SE analysis, Figure 4.31a and 4.32a, the surface is relatively flat for this particle as well, but there are particles of different sizes on the charcoal surface. The particles are in this case placed in clusters on elevations on the charcoal surface. Most of these particles is from BSE analysis showed as white particles, which implies that the particles are potassium. Some of the larger particles is in the same gray tone as the carbon in the charcoal, and is therefore assumed to be of carbon. Comparing the BSE pictures with the EDS pictures in Figure 4.33, the white and light gray particles in the BSE figures is the same as the green (potassium) particles in the EDS pictures. Where the darker areas in the BSE pictures is the same as the red (carbon) surface in the EDS picture.

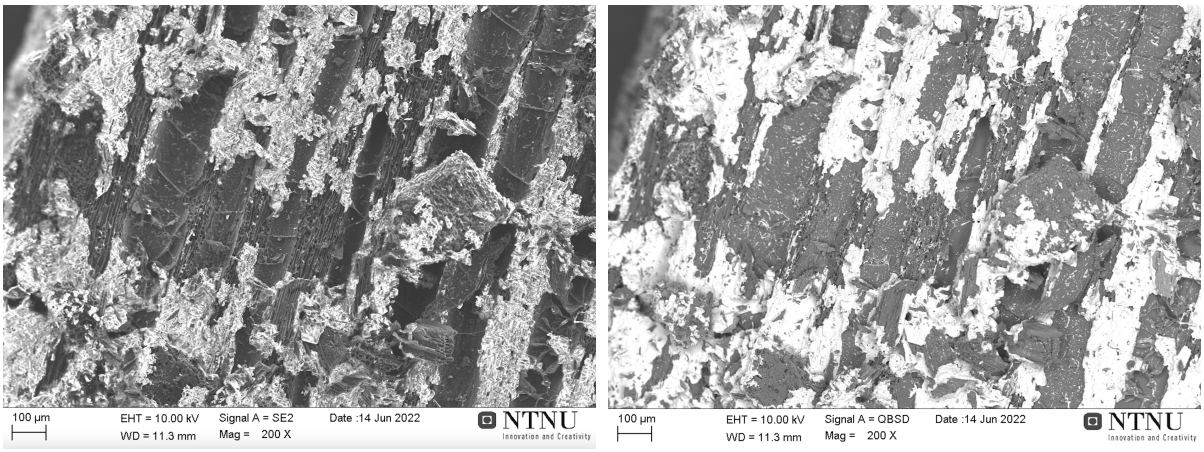

(a) (b)

Figure 4.31: The surface of one CharcoalHT10.53%K_w particle from SEM using SE to show the morphology on the surface (a) and BSE picture to show the different elements on the surface (b). Pictures taken with a magnification of 200 MAG.

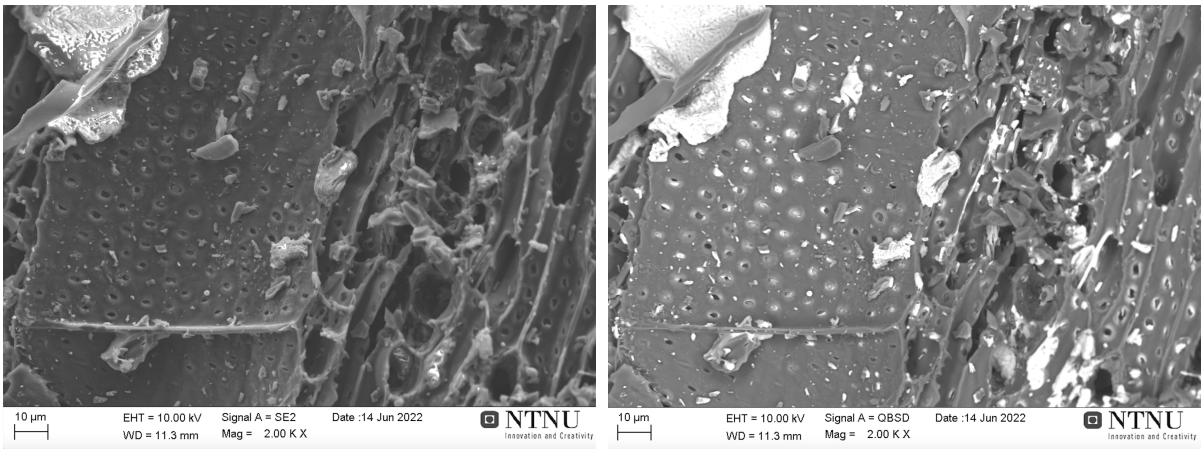

(a) (b)

Figure 4.32: The surface of one CharcoalHT10.53%K_w particle from SEM using SE to show the morphology on the surface (a) and BSE picture to show the different elements on the surface (b). Pictures taken with a magnification of 2000 MAG.

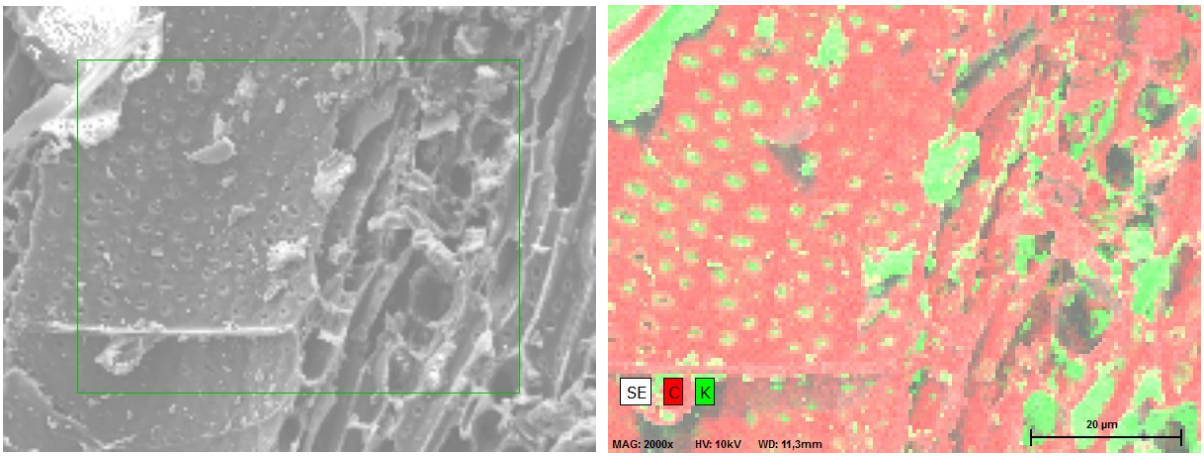

(a) (b)

Figure 4.33: The surface of one CharcoalHT10.53%K_w particle from SEM using SE to show the morphology on the surface (a) and EDS picture to show the different elements on the surface (b). Pictures taken with a magnification of 2000 MAG.

A particle from CharcoalHT10.53%K_w is also divided to be able to see how the potassium attaches to the center of the charcoal, the middle of one particle from CharcoalHT10.53%K_w is showed in Figure 4.34 and 4.35. It is possible to see some pores, but the pores are distributed over the surface and varying in size. If studying the BSE pictures 4.34b and 4.35b, the white particles, potassium particles, fills some of the pores. Some potassium particles are also attached to the pore walls, filling only parts of the pore. Comparing the BSE pictures with the EDS pictures in Figure 4.36, the white particles filling in some of the pores in the BSE figures is the same as the green (potassium) particles in the EDS pictures. Where the darker areas in the BSE pictures is the same as the red (carbon) surface in the EDS picture.

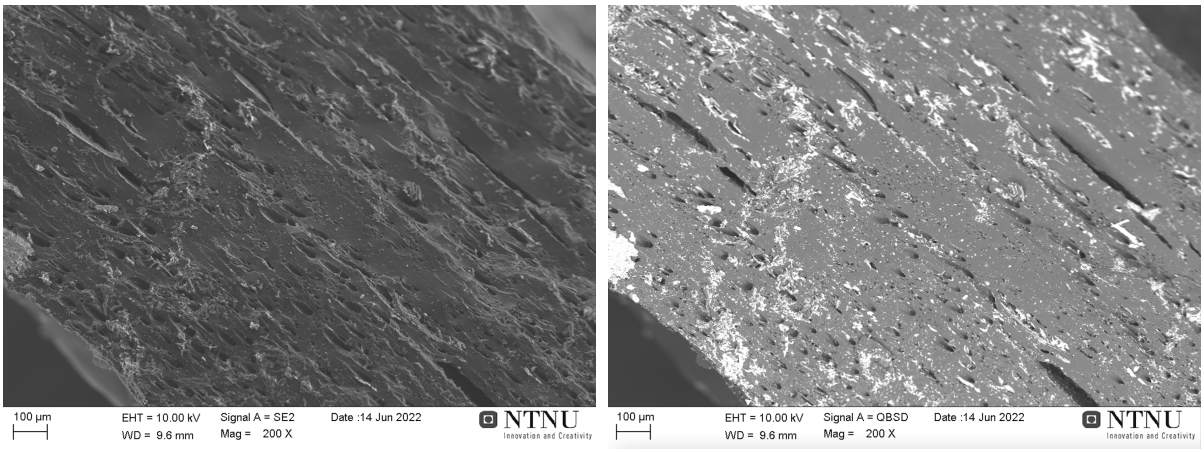

(a) (b)

Figure 4.34: The middle of one CharcoalHT10.53%K_w particle from SEM using SE to show the morphology on the surface (a) and BSE picture to show the different elements on the surface (b). Pictures taken with a magnification of 200 MAG.

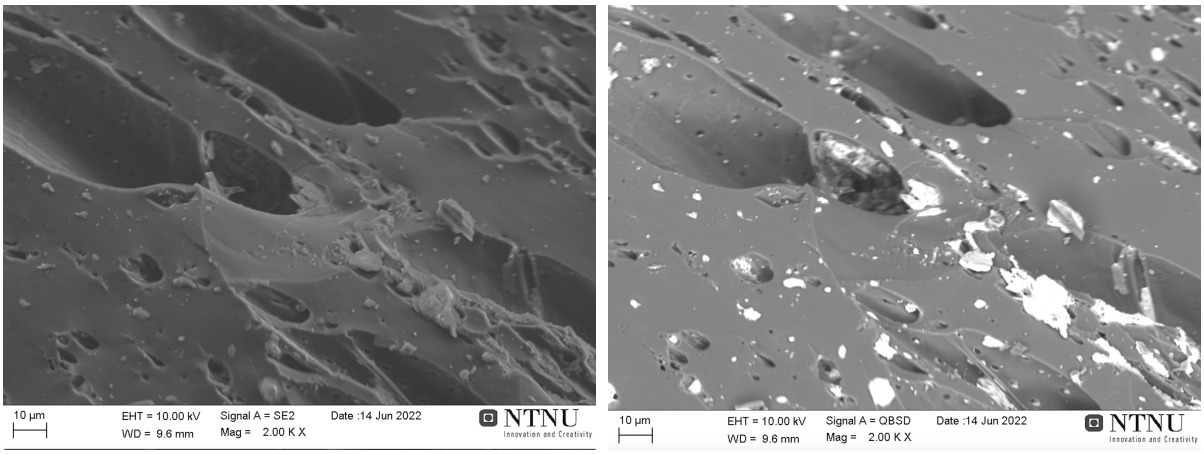

(a) (b)

Figure 4.35: The middle of one CharcoalHT10.53%K_w particle from SEM using SE to show the morphology on the surface (a) and BSE picture to show the different elements on the surface (b). Pictures taken with a magnification of 2000 MAG.

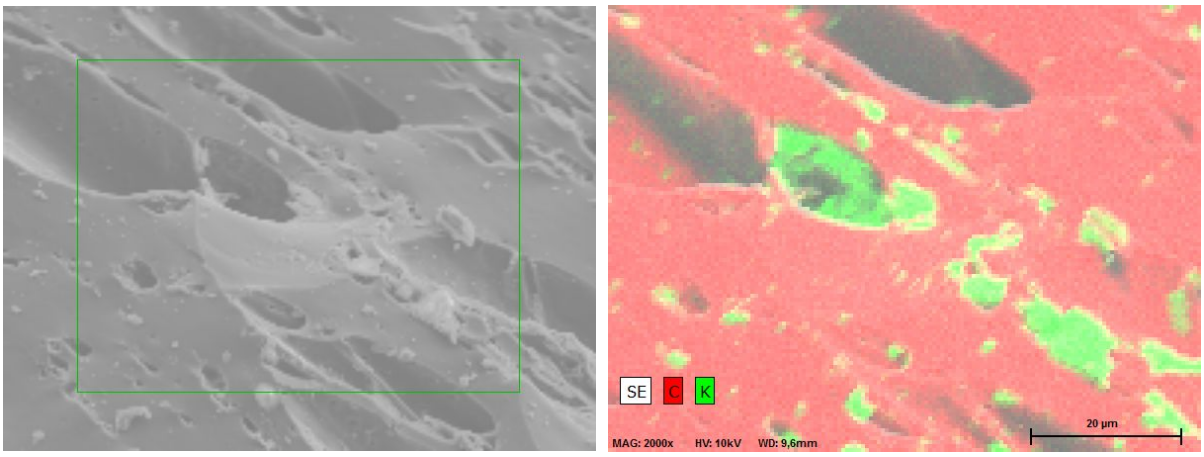

(a) (b)

Figure 4.36: The middle of one CharcoalHT10.53%K_w particle from SEM using SE to show the morphology on the surface (a) and EDS picture to show the different elements on the surface (b). Pictures taken with a magnification of 2000 MAG.

For the wet K-impregnated particles studied in SEM, all the particles have many particles of potassium on the surface and/or filling pores inside the particle. In some of the charcoal particles, the potassium is attached in clusters filling up pores in the charcoal, while other charcoal particles have potassium separated in large particles over the surface or inside the charcoal. Most of the potassium is for the wet K-impregnated samples placed in pores, smaller voids or elevations on the charcoal.

4.3 CO_2 reactivity

4.3.1 Gas K-impregnation and CO_2 reactivity

CO_2 reactivity of all the gas K-impregnated samples were measured, and all the curves made of the data from the analysis is given as plots in Appendix A.3. In Figure 4.37, 4.38 and 4.39, the curves from the CO_2 reactivity is displayed showing the time period with purging of CO and CO_2 gas. The curves are divided by their raw materials, that means Figure 4.37 shows the curves for the gas K-impregnated CharcoalRM, Figure 4.38 shows the curves for the gas K-impregnated CharcoalHT and Figure 4.39 shows the curves for gas K-impregnated coke. The curves show how fast 20% of the fixed carbon reacts while CO and CO_2 is purged through the carbon material at temperatures around 1100 °C. The slope of these curves is the CO_2 reactivity, which means that the curve with the steepest slope is the material with the highest CO_2 reactivity.

For the gas K-impregnated samples of CharcoalRM, Figure 4.37 shows the curves for the CO_2 reactivity of the two impregnated layers with the highest percentage of potassium. In this figure, raw material with a potassium content of 0.12% is the material with the lowest CO_2 reactivity, where the two curves with increased potassium content to 2.95% and 4.24% have steeper slopes, and therefore higher CO_2 reactivity.

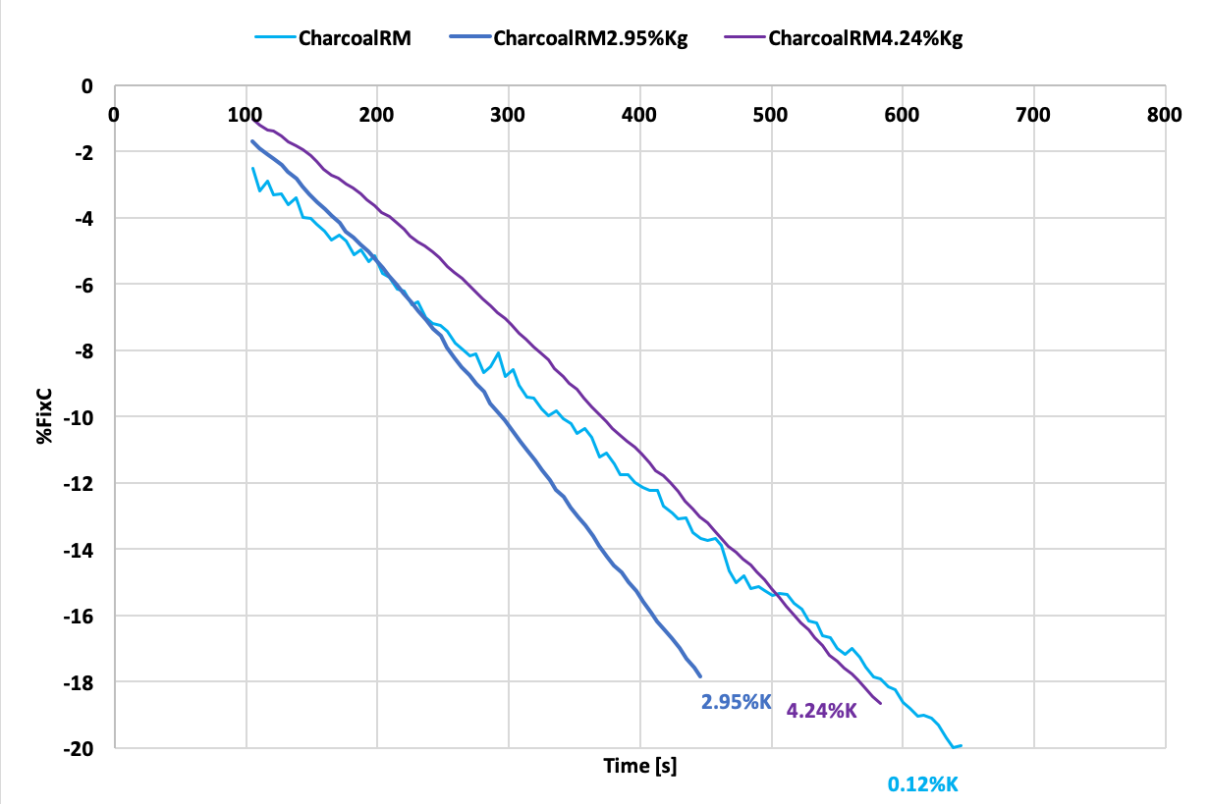

Figure 4.37: The figure shows the CO_2 reactivity of the gas K-impregnated charcoalRM. CharcoalRM is added for comparison, but is from earlier research [8]. %K represents $\%K_2O$.

The gas K-impregnated samples of CharcoalHT is showed in Figure 4.38. In this figure the lowest potassium content of 0.39%K_2O is also the curve with the least steep slope and therefore the lowest CO_2 reactivity. Where the curves get steeper for increasing potassium content for the rest of the curves. Resulting in that the bottom layer from the gas K-impregnation of CharcoalHT with 6.68%K_2O have the highest CO_2 reactivity due to the steepest slope.

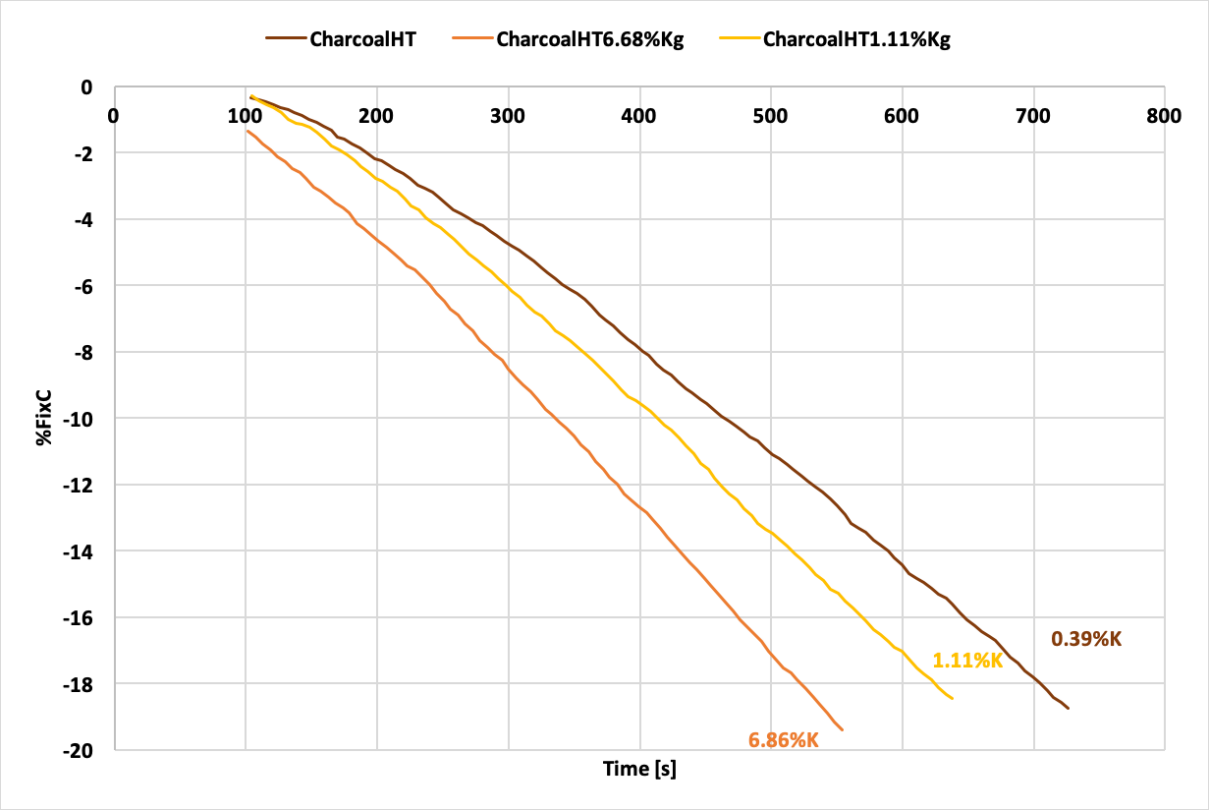

Figure 4.38: The figure shows the CO_2 reactivity of the gas K-impregnated charcoalHT. %K represents %K_2O

After gas K-impregnation of coke, the results from the CO_2 reactivity is showed in Figure 4.39. From the curves in this figure it can be seen that the raw material, the slope with 0.16%K_2O is the least steep slope, and will be the curve with lowest CO_2 reactivity. The two other curves have a significantly steeper slope, and therefore a CO_2 reactivity that is much higher. The slope with 2.86%K_2O is the curve with the steepest slope, and highest CO_2 reactivity, where the slope with the highest potassium content of 5.14%K_2O is slightly less steep.

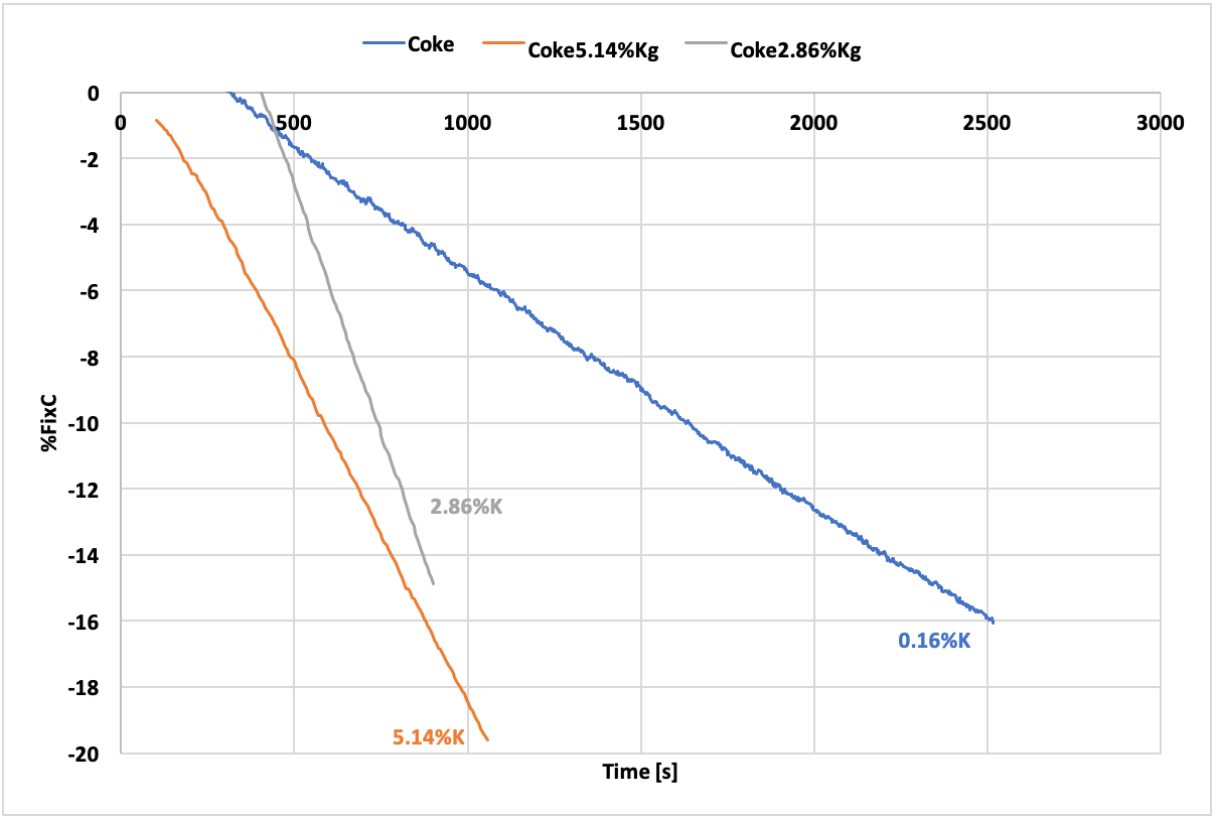

Figure 4.39: The figure shows the CO_2 reactivity of the gas K-impregnated coke. %K represents $\%K_2O$

As a summary of the CO_2 reactivity of the gas K-impregnated samples, Figure 4.40 shows the CO_2 reactivity versus potassium content for all the samples. The values can be found in Table 4.5. Compared to the raw materials, all the layers have an increase in potassium content as well as an increase in CO_2 reactivity. For the gas K-impregnation of CharcoalRM with bottom layer with $2.24\%K_2O$ and middle layer with $4.24\%K_2O$, the highest potassium content gives a smaller increase in the CO_2 reactivity than the increase in CO_2 reactivity for the bottom layer with lower potassium content. CharcoalHT on the other hand will have the highest potassium content for the bottom layer with $6.68\%K_2O$ and middle layer with $1.11\%K_2O$. For these samples the bottom layer with the highest potassium content, also have the highest increase in CO_2 reactivity, where the middle layer has a smaller increase in CO_2 reactivity. Lastly for coke, the raw material has clearly the lowest CO_2 reactivity, but it increases for the gas K-impregnated layers. For coke the middle layer have the highest CO_2 reactivity, but the bottom layer has the highest potassium content of $5.14\%K_2O$. The increase in the CO_2 reactivity for coke from the raw material to the coke with $2.86\%K_2O$, is the highest increase in CO_2 reactivity for all of the gas K-impregnated samples with similar potassium content.

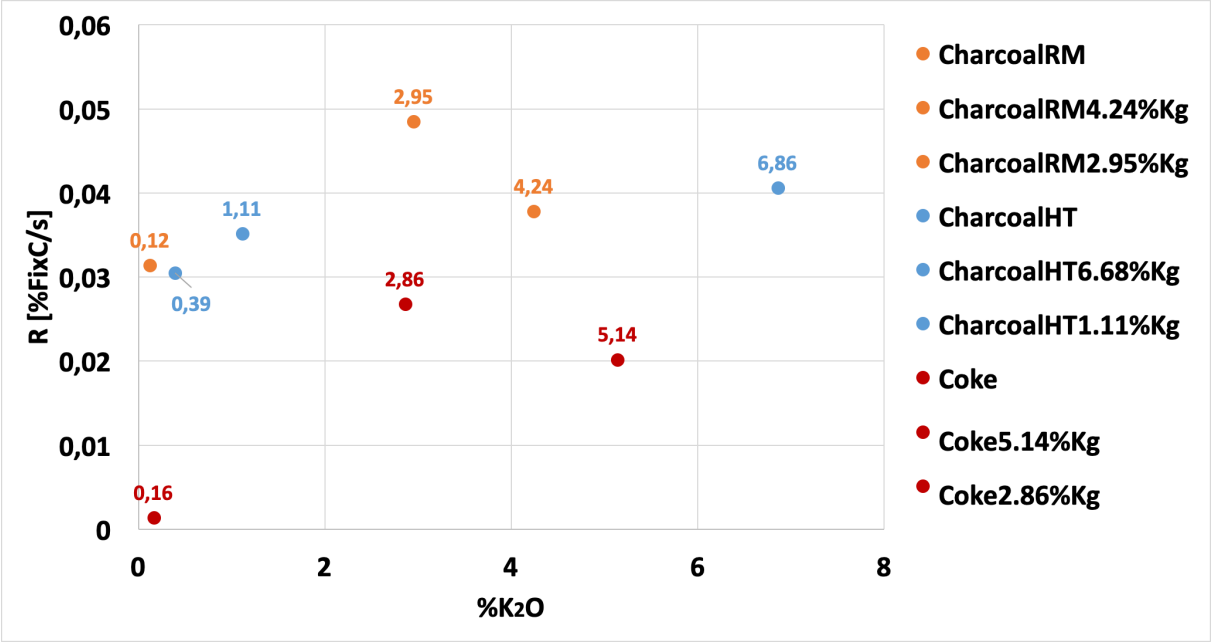

Figure 4.40: The figure shows the CO_2 reactivity of the gas K-impregnated CharcoalRM, CharcoalHT and Coke. The numbers attached to each point signifies the $\%K_2O$

Table 4.5: Shows an overview over the reaction parameters for the CO_2 reactivity tests and the potassium content for gas K-impregnated samples. CharcoalRM is added for comparison, but is from earlier research [8].

Sample	**%FixC**	**%K_2O**	**Reaction rate, R (%FixC/s)**	**R^2**
CharcoalRM	85.2	0.12	0.0314	0.999
CharcoalRM4.24K_g	85.92	4.24	0.0378	0.996
CharcoalRM2.95K_g	80.87	2.95	0.0485	0.997
CharcoalHT	94.6	0.39	0.0305	0.996
CharcoalHT1.11K_g	94.72	1.11	0.0352	0.998
CharcoalHT6.86K_g	82.17	6.86	0.0406	0.998
Coke	86.65	0.16	0.0014	0.995
Coke5.14K_g	87.77	5.14	0.0202	0.999
Coke2.86K_g	78.58	2.68	0.0268	0.984

4.3.2 Wet K-impregnation and CO_2 reactivity

All the wet K-impregnated samples were used for CO_2 reactivity measurements. The results are given as plots which is presented in Appendix A.3. The curves from the CO_2 reactivity for the wet K-impregnated samples is given in Figure 4.41 and 4.42, which represent the time period where there was purging of CO and CO_2 gas. The curves show how fast 20% of the fixed carbon reacts showing the loss of %FixC versus time. Since both CharcoalRM and CharcoalHT were wet K-impregnated, the CO_2 reactivity curves are divided into Figure 4.41 for CharcoalRM and Figure 4.42 for CharcoalHT.

CO_2 reactivity of CharcoalRM is showed in Figure 4.41, where the charcoal impregnated with 1M solution is showed as 1.45%K_2O, using 2.5M solution is showed as 5.23%K_2O and 5M solution as 8.71%K_2O. The last curve is the untreated CharcoalRM with 0.12%K_2O used for comparison [8]. CharcoalRM have both the lowest %K_2O and the least steep slope, which means the lowest CO_2 reactivity. For the 1M and 2.5M solution with respectively 1.45%K_2O and 5.23%K_2O, the difference between the CO_2 reactivity is small due to the almost similar slope of the curves. Studying the charcoal with 8.71%K_2O the slope is somewhat steeper than the other curves, resulting in the CO_2 reactivity being a bit higher.

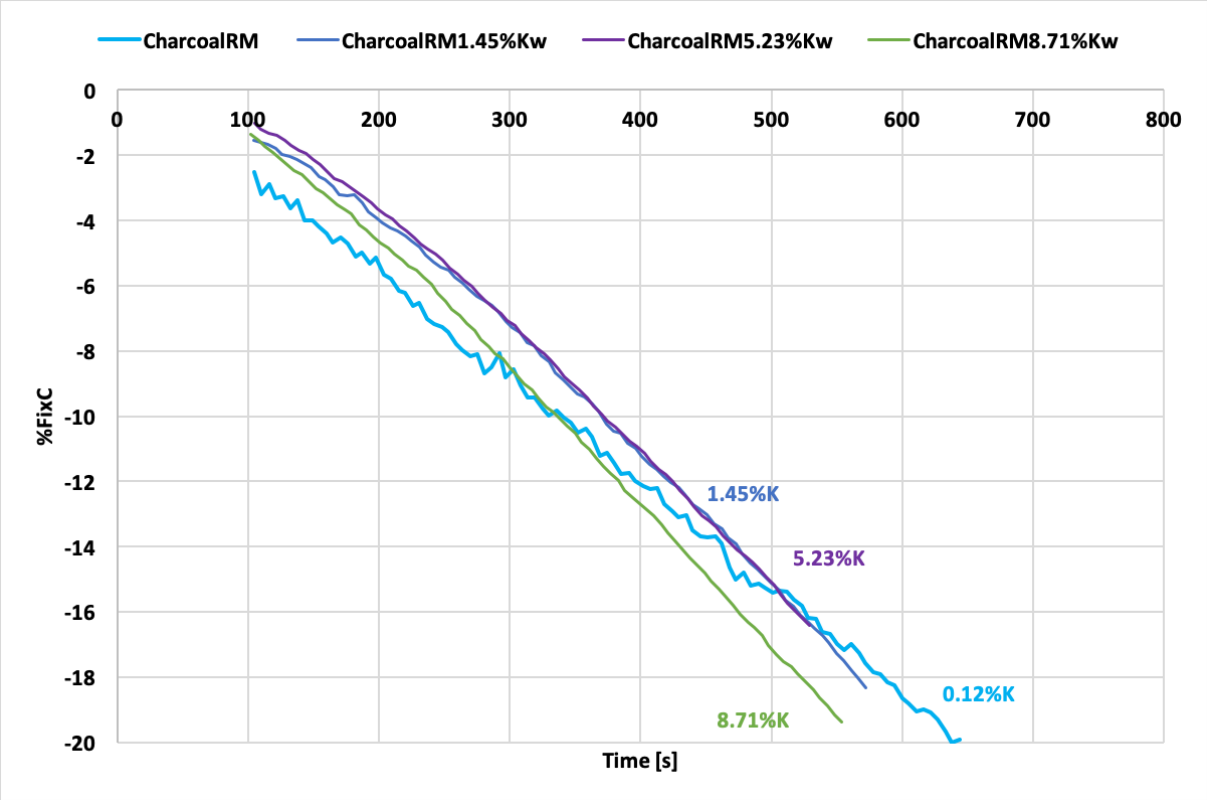

Figure 4.41: The figure shows the CO_2 reactivity of the wet K-impregnated CharcoalRM. CharcoalRM is added for comparison, but is from earlier research [8]. %K represents %K_2O.

The wet K-impregnated samples of CharcoalHT is presented in Figure 4.42, where the charcoal impregnated with 1M solution is showed as 3.21%K_2O, with 2.5M solution as 3.41%K_2O and 5M solution as 10.53%K_2O. The curves is marked with the potassium content achieved after the wet K-impregnation. CharcoalHT with 0.39%K_2O have the lowest CO_2 reactivity, since the curve is the least steep. For the charcoal impregnated with 1M and 2.5M solution there is a small difference in the %K_2O achieved, and a small difference between the CO_2 reactivity since the slope of the curves is almost the same. Looking at the last curve with the highest percentage of potassium, the potassium content is significantly higher than for the other samples, but the CO_2 reactivity is almost the same as for the other K-impregnated samples. This resulted in almost the same CO_2 reactivity for all the wet K-impregnated samples of CharcoalHT.

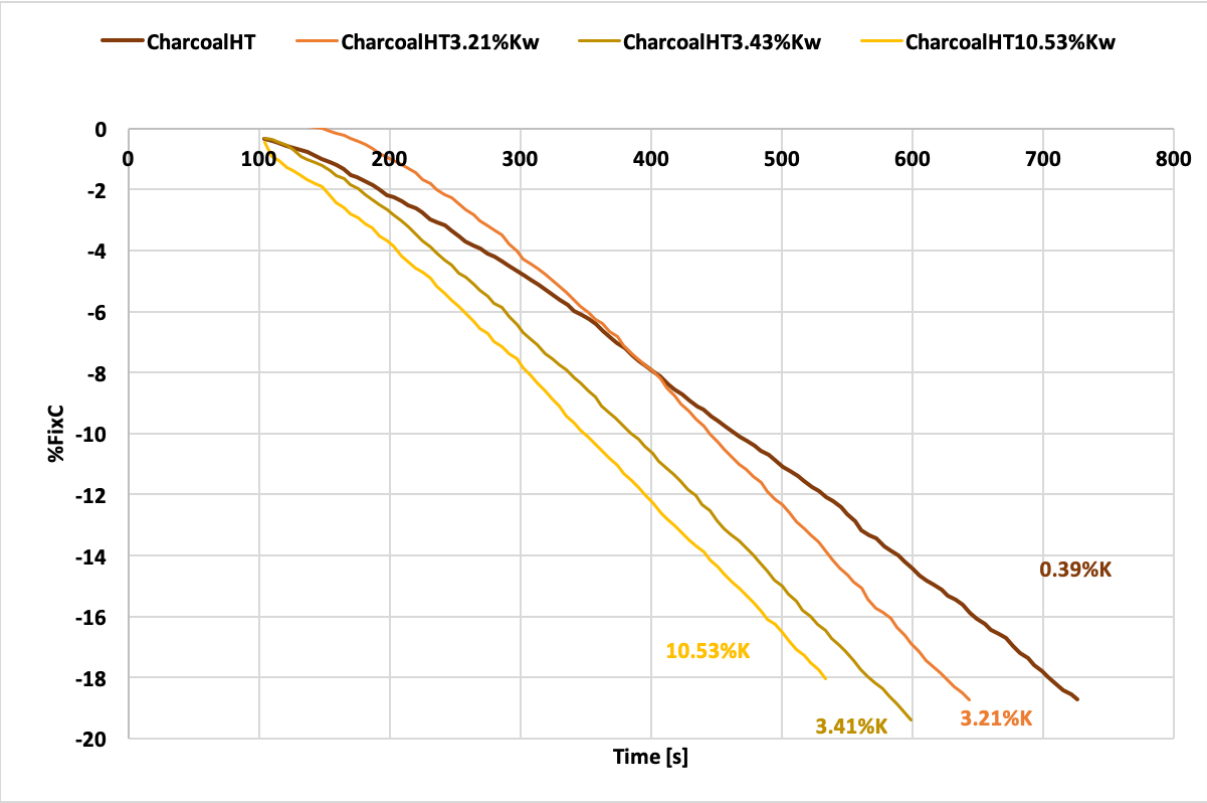

Figure 4.42: The figure shows the CO_2 reactivity of the wet K-impregnated CharcoalHT. %K represents %K_2O.

A summary of the wet K-impregnated samples CO_2 reactivities is showed in Figure 4.43 and the values in Table 4.6. From the figure, comparing the raw materials with the K-impregnated samples, there is an increase in the CO_2 reactivity with increasing the potassium content in the wet K-impregnation. After around 3%K_2O it looks to have stabilized to a CO_2 reactivity around 0.04 %FixC/s. Due to the stabilization, there is almost no change in CO_2 reactivity with increasing potassium content between 3%K_2O to 10%K_2O. There is some variety between the samples, but they all are small and within the uncertainty area for the experiments.

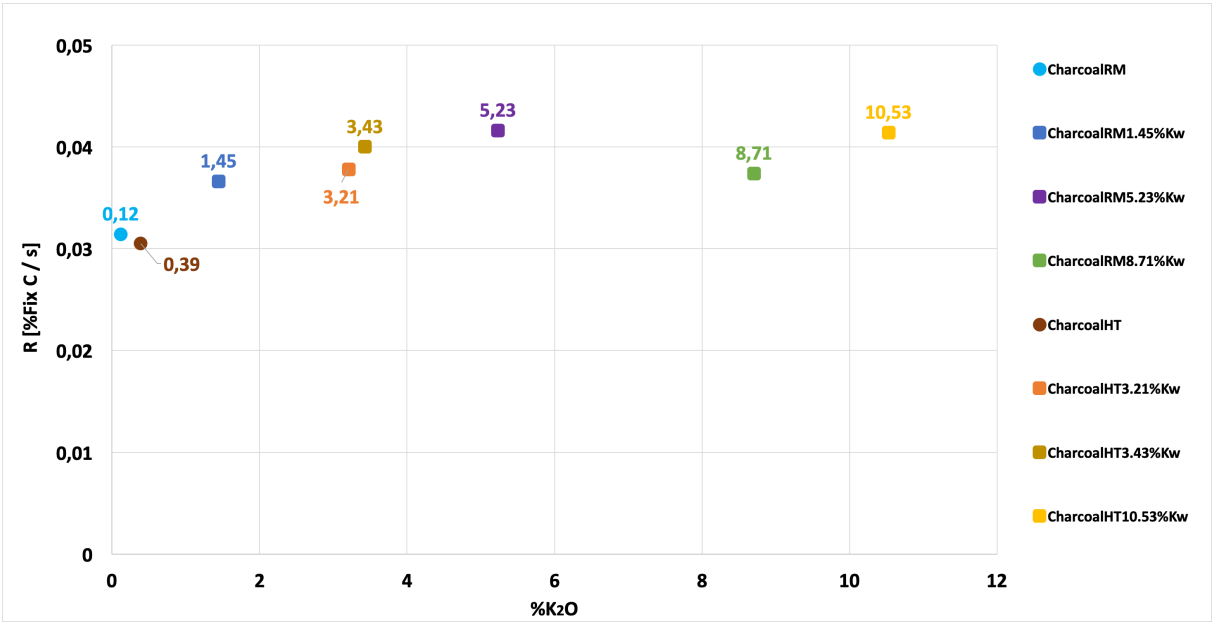

Figure 4.43: The figure shows the CO_2 reactivity of the wet K-impregnated CharcoalRM and CharcoalHT.

Table 4.6: Shows an overview over the reaction parameters for the CO_2 reactivity tests and the potassium content for wet K-impregnated samples. CharcoalRM is added for comparison, but is from earlier research [8].

Sample	**%FixC**	**%K_2O**	**Reaction rate, R (%FixC/s)**	**R^2**
CharcoalRM	85.2	0.12	0.0314	0.999
CharcoalRM1.45K_w	79.1	1.45	0.0366	0.995
CharcoalRM5.23K_w	71.8	5.23	0.0416	0.999
CharcoalRM8.71K_w	65.0	8.71	0.0374	0.997
CharcoalHT	94.6	0.39	0.0305	0.996
CharcoalHT3.21K_w	87.77	3.21	0.0378	0.985
CharcoalHT3.43K_w	82.75	3.43	0.0400	0.996
CharcoalHT10.53K_w	71.32	10.53	0.0414	0.998

4.3.3 Summary CO_2 reactivity

The CO_2 reactivity measured in this thesis is plotted in Figure 4.44 and Table 4.7, together with the values for CharcoalRM [8] and CharcoalHT. In Figure 4.44 the colors represent which material that were used as raw material and the shape of the points represents which impregnation method is used. The figure show the CO_2 reactivity versus $\%K_2O$, and shows together how the CO_2 reactivity changes with increasing potassium content. From the figure, the CO_2 reactivity for the charcoals increases with increasing potassium content compared to the raw materials. However, the increase in CO_2 reactivity seems to be stabilizing the charcoal after $3\%K_2O$ to a value around 0.04%FixC/s.

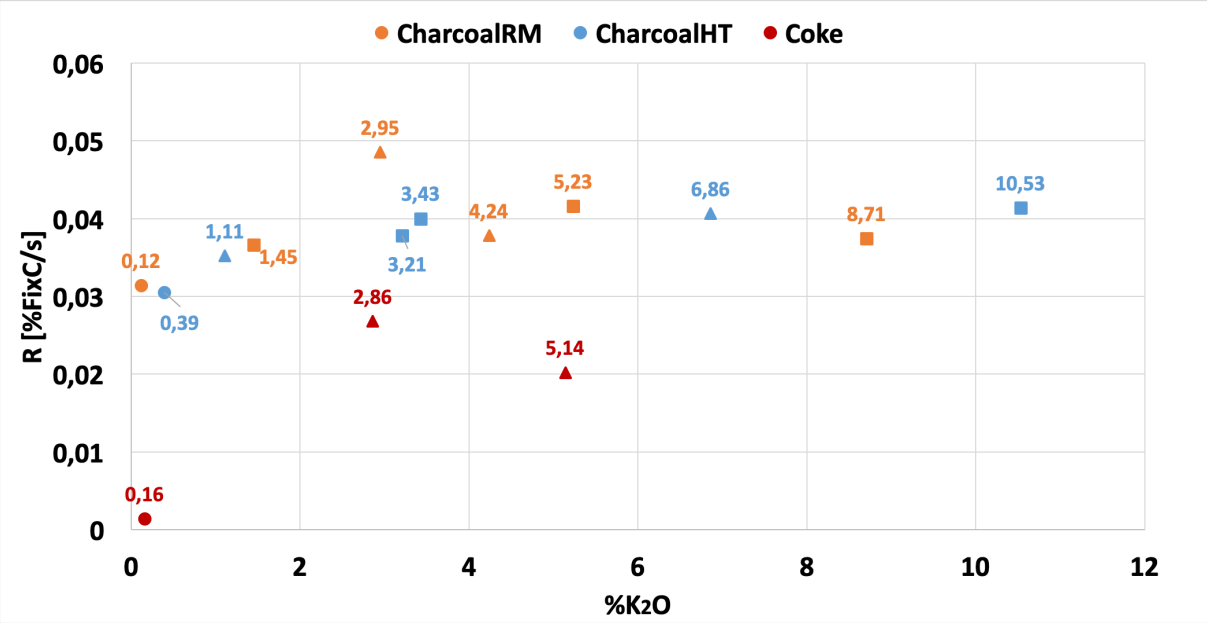

Figure 4.44: The figure shows the CO_2 reactivity of the gas and wet K-impregnated CharcoalRM, CharcoalHT and coke. The circular points represents the raw materials, the squares is the wet K-impregnated samples and the triangles is the gas K-impregnated samples.

Table 4.7: Shows an overview over the reaction parameters for the CO_2 reactivity tests and the potassium content for gas K-impregnated samples. CharcoalRM is added for comparison, but is from earlier research [8]

Sample	**%FixC**	**%K_2O**	**Reaction rate, R (%FixC/s)**	**R^2**
CharcoalRM	85.20	0.12	0.0314	0.999
CharcoalRM4.24K_g	85.92	4.24	0.0378	0.996
CharcoalRM2.95K_g	80.87	2.95	0.0485	0.997
CharcoalRM1.45K_w	79.1	1.45	0.0366	0.995
CharcoalRM5.23K_w	71.8	5.23	0.0416	0.999
CharcoalRM8.71K_w	65.0	8.71	0.0374	0.997
CharcoalHT	94.6	0.39	0.0305	0.996
CharcoalHT1.11K_g	94.72	1.11	0.0352	0.998
CharcoalHT6.86K_g	82.17	6.86	0.0406	0.998
CharcoalHT3.21K_w	87.77	3.21	0.0378	0.985
CharcoalHT3.43K_w	82.75	3.43	0.0400	0.996
CharcoalHT10.53K_w	71.32	10.53	0.0414	0.998
Coke	86.65	0.16	0.0014	0.995
Coke5.14K_g	87.77	5.14	0.0202	0.999
Coke2.86K_g	78.58	2.68	0.0268	0.984

4.3.4 Temperature drop during CO_2 reactivity test

The Boudouard reaction is an endothermic reaction, and when purging CO and CO_2 through the crucible at 1100 °C, the Boudouard reaction is supposed to take place. An endothermic reaction will consume heat, and in this part of the results the temperature drop during the CO_2 reactivity test is measured. The temperature drop is measured from the purging of CO and CO_2 begins, and after 300 seconds with purging of the gases. The measured temperature drop for all the CO_2 reactivity measurements performed in this thesis is given in Table 4.8. In Figure 4.45 and 4.46 the values for respectively wet K-impregnated and gas K-impregnated samples is plotted.

Table 4.8: Temperature drop during CO_2 reactivity measurement for all of the wet and gas K-impregnated charcoal samples.

	Temperature (0 sek)	Temperature (300 sek)	Temperature drop
CharcoalRM1.45%K_w	1110.6	995	115.6
CharcoalRM5.23%K_w	1107.9	919.9	188
CharcoalRM8.71%K_w	1111.6	935.1	176.5
CharcoalRM2.95%K_g	1111.4	903.8	207.6
CharcoalRM4.24%K_g	1110.9	977.4	133.5
CharcoalHT	1111.3	1038.2	73.1
CharcoalHT3.21%K_w	1096.7	997.2	99.5
CharcoalHT3.43%K_w	1109.5	977.4	132.1
CharcoalHT10.53%K_w	1109.1	960.2	148.9
CharcoalHT6.86%K_g	1109.8	945.9	163.9
CharcoalHT1.11%K_g	1095.5	1039.6	55.9

In Figure 4.45 the temperature drop for all the wet K-impregnated samples is given versus the measured potassium content of the samples. The temperature drop during the CO_2 reactivity increases when the K-content increases. However, it seems that there might be a decrease in the temperature drop after 6 %K_2O, since the values for these points are lower than the increase for the lower values would imply.

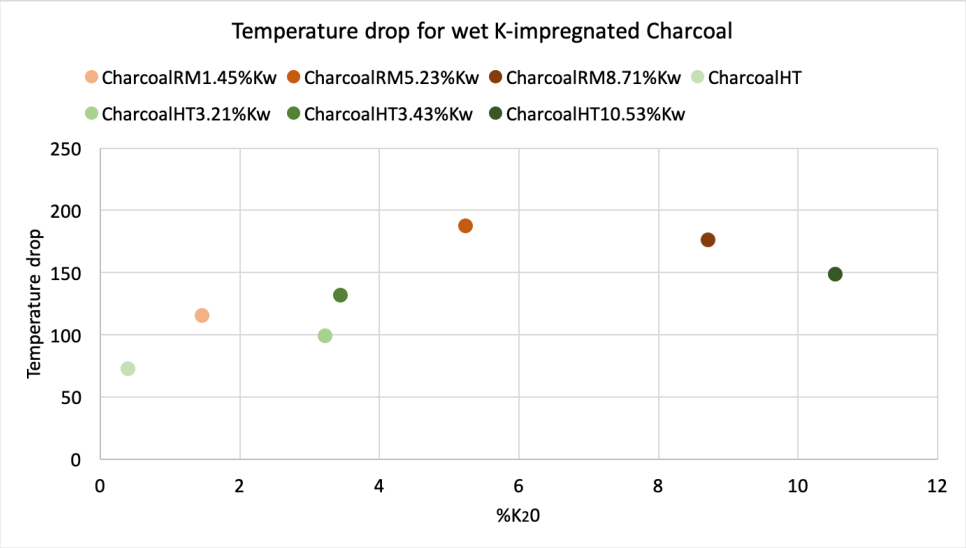

Figure 4.45: Temperature drop for the wet K-impregnated charcoal samples versus the measured $\%K_2O$ for each sample.

Temperature drop for the gas K-impregnated charcoal is presented in Figure 4.46 versus the K_2O of the samples. In this case, there is not as clear tendencies as for the wet K-impregnated samples. There is a decrease in the temperature drop for CharcoalRM when going from $2.95\%K_2O$ to $4.24\%K_2O$. The temperature drop for the raw material is in this figure not given. For CharcoalHT it will first be a decrease in the temperature with an increase in $\%K_2O$ from $0.39\%K_2O$ to $1.11\%K_2O$. When increasing the potassium content to $6.86\%K_2O$ it is an increase in the temperature drop again.

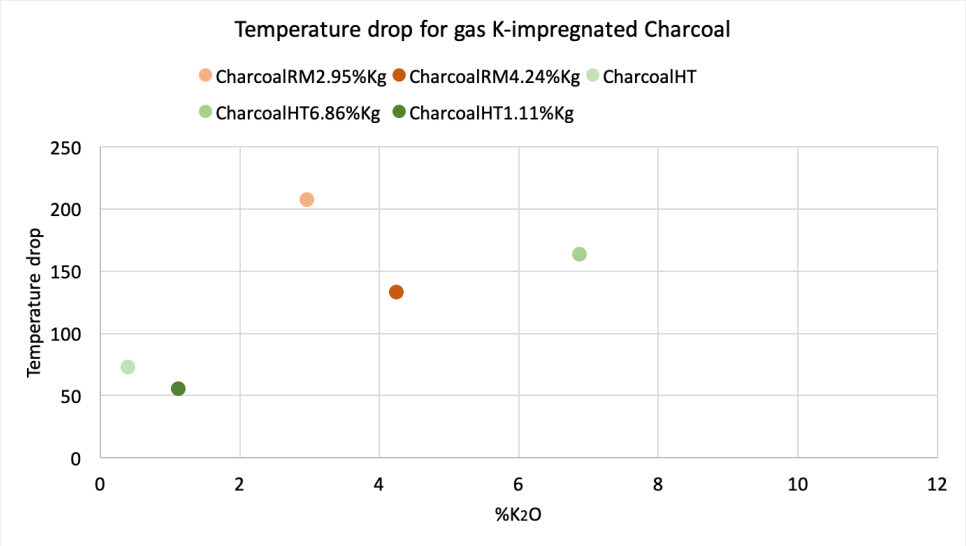

Figure 4.46: Temperature drop for the gas K-impregnated charcoal samples versus $\%K_2O$.

For all the CO_2 reactivity experiments the highest measured temperature drop is 207.6 °C for CharcoalRM2.95%K_g. Most of the other measured temperature drops is between 100 to 150 °C. There is no significant difference between the gas and wet K-impregnation, increased $\%K_2O$ however increases the temperature drop for most of the charcoals.

5 Discussion

The following chapter will discuss the results displayed and pointed out in the results, and comparing them with earlier research and theory. The impregnation methods will first be discussed separately while discussing the chemical analysis and the visual inspection of the samples, before the methods will be compared with each other. Lastly the CO_2 reactivity of the different materials will be discussed comparing the CO_2 reactivity to the other parameters separating the different samples.

As mentioned earlier the nomenclature for the carbon materials in this thesis will be given as CharcoalXX%YY%K, where XX show the densification degree of the charcoal and YY show the percentage of K_2O in the charcoal after impregnation.

5.1 K-content of samples with various impregnation techniques

All the gas and wet K-impregnated carbon materials were analyzed with proximate and ash analysis to find the out how the K content changed with deposition condition. The trends found for the impregnated samples from this thesis will be compared to what earlier research have achieved.

5.1.1 Chemical analysis of the Gas K-impregnated carbon material

The chemical analysis of the gas K-impregnated carbon materials showed that there was an increase in potassium content for all layers compared to the raw materials. Literature states that potassium carbonate will react with carbon and produce potassium at elevated temperatures, Reaction 2.2, and for the gas K-impregnation this is the case. A mixture of K_2CO_3 and C is mixed and placed in the bottom of the crucible with charcoal before the temperature were increased to 1000 °C. Since the potassium content in the charcoal increases for all the gas K-impregnations there can be assumed that Reaction 2.2 takes place and the produced potassium attaches to the carbon material during the gas K-impregnation.

$$K_2CO_3 + 2C = 2K(g) + 3CO(g) \tag{2.2}$$

There are three layers of carbon material in the crucible after the gas K-impregnation, and each of these layers is taken out of the crucible by hand. Table 4.2 shows that CharcoalHT have the highest $\%K_2O$ in the bottom layer with $6.68\%K_2O$, with decreasing potassium content for the middle and top layer with respectively $1.11\%K_2O$ and $0.27\%K_2O$. However, the gas K-impregnated CharcoalRM and coke have the highest potassium content in the middle layer. For CharcoalRM the middle layer with the highest potassium content of $4.24\%K_2O$ and for coke $5.14\%K_2O$. Table 5.1 shows that in all the earlier performed gas K-impregnation the bottom layer has been the layer with the highest potassium content, and the bottom layer is also the layer closest to the potassium source during the gas K-impregnation. This makes the gas K-impregnation of CharcoalRM and coke to stand out from the rest of the gas K-impregnated samples.

Table 5.1: Overview over the potassium content in the three different layers after the Gas K-impregnation of CharcoalRM, CharcoalHT and Coke, and results from earlier research from Table A.1.

	Top Layer ($\%K_2O$)	**Middle Layer** ($\%K_2O$)	**Bottom Layer** ($\%K_2O$)	**Source**
CharcoalRM	1.77	4.24	2.95	-
CharcoalHT	0.27	1.11	6.68	-
Coke	0.38	5.14	2.86	-
Charcoal15%	0.24	1.50	3.40	[8]
Charcoal-2%	0.40	0.46	6.14	[9]
CharcoalA	0.44	1.10	3.00	[10]
CharcoalB	1.50	3.30	4.20	[10]
CharcoalC	0.89	2.50	4.00	[10]
Met.Coke	2.40	3.80	5.00	[10]

One reason for the middle layer to have higher potassium content than the bottom layer might be that when separating the layers by hand, there have been some mixing between the layers so that some of the bottom layer particles becomes a part of the middle layer, and opposite. If this is the case some particles with high potassium content might been included as the middle layer increasing the potassium content in that layer, and low potassium particles decreases the $\%K_2O$ in the bottom layer. Another reason is when dividing charcoal into batches for the different experiments, particles with higher or lower potassium content were used for the different experiments, resulting in a varying potassium content in the samples used for the different analyses.

There might be that the middle layer had a higher potassium content. This could happen if the potassium gas is not distributed evenly during the impregnation, formation of gas channels or that the pore structure of the charcoal particles is different. Another method for the middle layer to have higher potassium content is that the potassium might attach to the bottom layer, but the temperature during the gas K-impregnation were high over a longer time so the potassium reacts with gas or loosens from the charcoal. This might able the potassium to move from the bottom layer to the middle layer. High and low K-content will be discussed further when discussing the CT and SEM results.

The particles are showed in the SEM and CT pictures to have different amounts of potassium, the average values for the different gas K-impregnated samples is quite similar with values 2.99%, 2.75% and 2.79% K_2O. Even if there is variation in which layer that achieves the highest potassium content for the different gas K-impregnation experiments, there is still a total average amount of potassium from the different impregnation experiments that have almost the same potassium content. Showing that the amount of potassium attached to the raw materials is the same, but there is a variation on where in the crucible the potassium attaches to the carbon materials.

5.1.2 Chemical analysis of the Wet K-impregnated charcoal

Both CharcoalRM and CharcoalHT were impregnated with potassium through wet K-impregnation with a solution varying between 1 molar, 2.5 molar and 5 molar. Increased potassium content is a result of wet K-impregnation of charcoal according to the values given in Table 4.3. It can also be seen that the potassium content is higher for higher molarity of the solution used for the impregnation. Using a 1 molar solution results in the lowest $\%K_2O$ values of $1.45\%K_2O$ for CharcoalRM and $3.21\%K_2O$ for CharcoalHT. By increasing the molarity to a 2.5 molar solution the potassium content in the impregnated charcoal increases to $5.23\%K_2O$ for CharcoalRM and $3.43\%K_2O$ for CharcoalHT. Increasing the molarity further, to a 5 molar solution the potassium content in the impregnated charcoal gives values of $8.71\%K_2O$ for CharcoalRM and $10.53\%K_2O$ for CharcoalHT.

Earlier it is found that the wet K-impregnation increases the potassium content [8], [9], but the maximum published values is up to $2\%K_2O$. The same research tried to study the change in potassium content if varying the time used for charcoal in the 1 molar potassium rich solution during the impregnation. When using impregnation times 30, 60 and 90 minutes, the achieved potassium content varied between 1-$2\%K_2O$. If comparing these results with the potassium content achieved in this thesis with higher molarity of the solution, there is a tendency that increasing the molarity increases the potassium content more than increasing the time, see Figure 5.1.

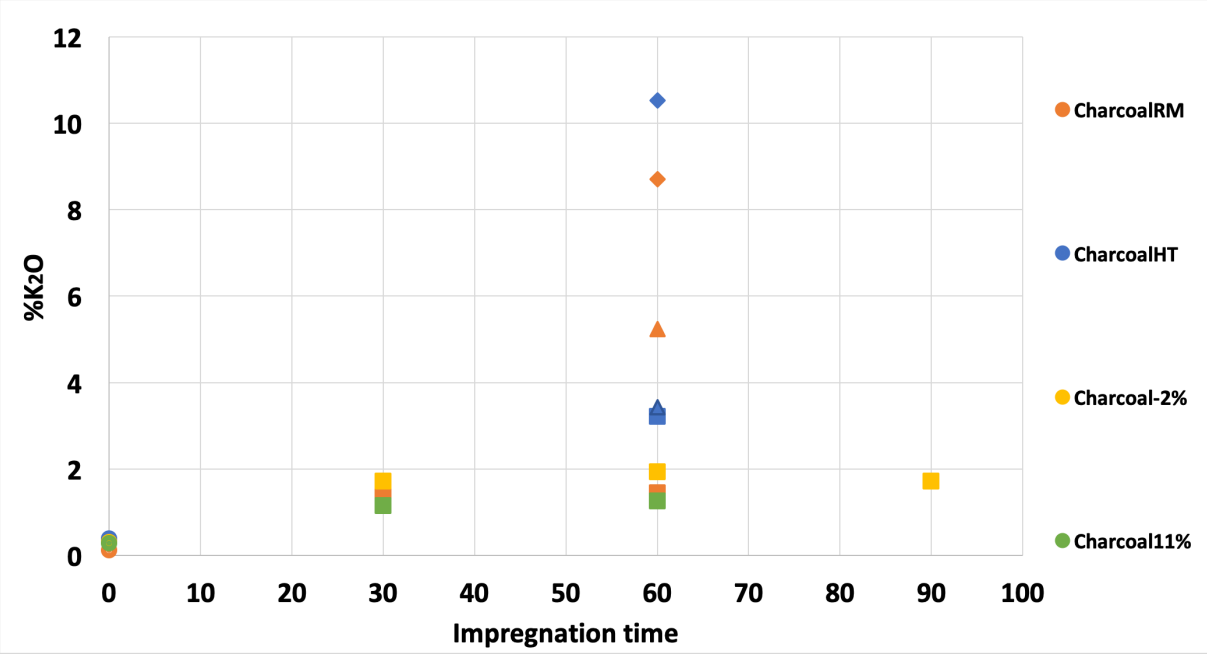

Figure 5.1: Achieved potassium content with different impregnation times with wet K-impregnation of different charcoals. Circular points is the raw material as reference, where squares is wet K-impregnation with 1M solution, triangles with 2.5M solution and the diamond with 5M solution.

Why the molarity of the solution increases the potassium content more than increased impregnation time, might be because the charcoal takes in a constant amount of solution, independent of the molarity of the solution. For the time periods chosen in this thesis, the

charcoal might be saturated with solution. When increasing the molarity of the solution the charcoal might be able to take in more potassium through the same amount of solution and therefore increase the total potassium content in the charcoal. To support this theory, it can be noticed that changing the molarity of the solution from 1 to 2.5 molar solution seems to double the potassium content in the wet K-impregnated charcoal. A 5 molar solution gives almost 5 times higher potassium content in the charcoal. If the increase in $\%K_2O$ will continue with an increase in the molarity of the solution can't be stated from the results so far.

5.1.3 Comparing methods

Potassium content in the different impregnated samples is varying for both methods. Considering the gas K-impregnated samples, the top layer has a quite low potassium content which is almost the same as for the raw material used for the gas K-impregnation. For the bottom and middle layer there is an increase of the potassium content to the highest achieved potassium content 6.68%K_2O, but most of the samples have values between 2.5-5%K_2O. For the wet K-impregnated samples there is also a variation in the potassium values, but if considering the values with 2.5 and 5 molar solution, all the samples have values higher than 3.43%K_2O and the maximum value achieved is 10.53%K_2O.

This report gives the potassium values as %K_2O, and if transforming the values to %K, then the values would be reduced to 83% of the original value. For the two highest potassium contents measured in this thesis, the values would be changed from 10.53 %K_2O to 8.74 %K and 8.71 %K_2O to 7.22 %K. Due to this, all the measured points in this report could be shifted to 17% lower values when considering pure potassium content. No matter which value used, the tendencies and conclusions found in this report will still be the same.

In the manganese alloy furnace, it was found that there were about 3.5%K_2O in the coke bed [36], and higher values are believed to be in the carbon materials in the lower temperature areas. Both gas and wet K-impregnation can achieve values above 3.5%K_2O, making both methods possible to use to study the effect of potassium on charcoal and coke. For gas K-impregnation, the bottom and middle layers is the only layers that have achieved potassium levels above 3.5%K_2O. Where the wet K-impregnated samples have the whole batch with the same potassium content. Four of the nine gas K-impregnation experiments in Table 5.1 have values above 3.5%K_2O in the bottom layer. For the wet K-impregnated samples, none of the charcoals impregnated with 1 molar solution achieved a potassium content above 3.5%K_2O. Increasing the potassium content to 2.5 molar solution, the values is higher, but only one of two samples have a high enough potassium content. The 5 molar solution have a significantly higher potassium content, with 8.71%K_2O and 10.53%K_2O. Both methods can increase the potassium content to levels that can be used to analyze the effect of potassium on the carbon materials inside the manganese alloy furnace.

The gas K-impregnated samples have a great variation of the potassium content through the batch, which results with carbon material that have lower potassium content than what the furnace holds. It is assumed in this thesis that the potassium content after the wet K-impregnation is constant, and therefore all the wet K-impregnated charcoal with potassium content above 3.5%K_2O can be used. This results in a more efficient method where all the impregnated material can be used for further analysis.

Another aspect with the two impregnation methods is the energy use when impregnating charcoal. The gas K-impregnation requires higher amounts of energy due to the high temperature during the experiment, and only parts of the carbon material can be used to understand the carbon materials in the manganese furnace. The wet K-impregnation only heats the solution up to 80 °C and will therefore require less energy, and since assuming a constant potassium content in the charcoal, all the carbon material can be used if the batch achieves high enough potassium content.

5.2 Visual inspection of K in carbon materials with SEM and CT

Both gas and wet K-impregnated samples were analyzed in SEM and CT. For this part, it is important to state that there are different charcoals used for SEM and CT, which might bring some uncertainties to the results. However, the gas and wet K-impregnation of all the samples is performed in the same manner, so the only difference is the pre-treatment of the charcoal used for the impregnation.

After the SEM analysis, the potassium particles after the gas K-impregnation is found attached to the surface of the capillary pores of the charcoal or covering the charcoal particle with a varying amount of potassium particles. From CT analysis, many of the same tendencies can be found, the potassium is either found as charcoal particles completely impregnated with potassium, or as charcoal particles where there can not be seen any potassium.

For the wet K-impregnated charcoal, most of the particles examined in SEM showed that their surface was partly covered with potassium particles. Some of the potassium particles were found over the surface in larger clusters, where others were found as smaller particles over the surface. Inside the particles most of the potassium were placed inside pores, smaller voids or elevations on the charcoal. From CT, there is an white edge with potassium to be seen around most of the particles or as some particles inside the impregnated charcoal.

There were only a few particles studied for SEM and CT. The difference between the particles is relatively large, which makes the visual inspection of the carbon materials a temporary result. The results should be examined more in later research.

From CT, both gas and wet K-impregnation resulted in some completely impregnated particles and some particles that had a white line around the edge of the particles. The completely impregnated particles were clearer in the pictures for the Gas K-impregnated particles, where they were very white compared to the other particles. For the wet K-impregnated particles the completely impregnated particles were not as white as the gas impregnated particles. This might imply that particles from the gas K-impregnation have a larger difference in potassium content between the particles, than for wet K-impregnated particles. Since there is so few particles analyzed, the large difference between particles for gas K-impregnation increases the risk of different potassium content for the batch of carbon material sent for chemical analysis and used for CO_2 reactivity.

For almost all the particles, there is a white edge around the particles. This edge is thicker for the wet K-impregnated particles, than for the gas K-impregnated particles. However, the white edge is brighter for the gas K-impregnated particles, implying that there is more concentrated potassium on the edge than there is for wet K-impregnated charcoal. A reason for this might be that there is a more topochemical reaction for the wet K-impregnated charcoal than for the gas K-impregnated. At the gas impregnated charcoal, the particles seem to either be impregnated throughout the particle or not impregnated at all.

From SEM there is found potassium, and the potassium is placed different than what is

found from the CT pictures. Since there is such difference between the particles analyzed in CT, there is difficult to state which type of particle is analyzed in SEM and therefore the SEM and CT pictures is hard to compare. One aspect that can be seen from both CT and SEM, is that the charcoal particles analyzed have different pore structures, which might affect how the potassium attaches to the particles. However, from SEM there is three main methods found for placement of potassium on carbon materials. First method is that the potassium attaches to the pore walls, covering the pore walls in different degrees. The next method is that the potassium attached to the charcoal as particles, both few or many and large or small particles is found. The last method is that potassium is found as small particles covering the surface of the charcoal. These methods will be discussed below.

Some of the charcoal particles have a visible pore structure in the SEM pictures, where the pore openings can be studied. From Figure 5.2 it can be seen that both the gas and wet K-impregnation might result in pores filled with potassium particles in varying degree. From these pictures, it seems that the potassium from the gas K-impregnated samples have smaller particles more distributed around the pore openings, where the potassium particles from the wet K-impregnation have larger particles filling up some of the pores. From these figures, it seems like the potassium particles from the wet K-impregnation is much larger than the particles from the gas K-impregnation. The difference in size might come be a result of the solution used for the wet K-impregnation and the potassium gas used for gas K-impregnation. There might be a difference in the size of the potassium particles since the gas contains pure potassium where the solution uses potassium carbonate.

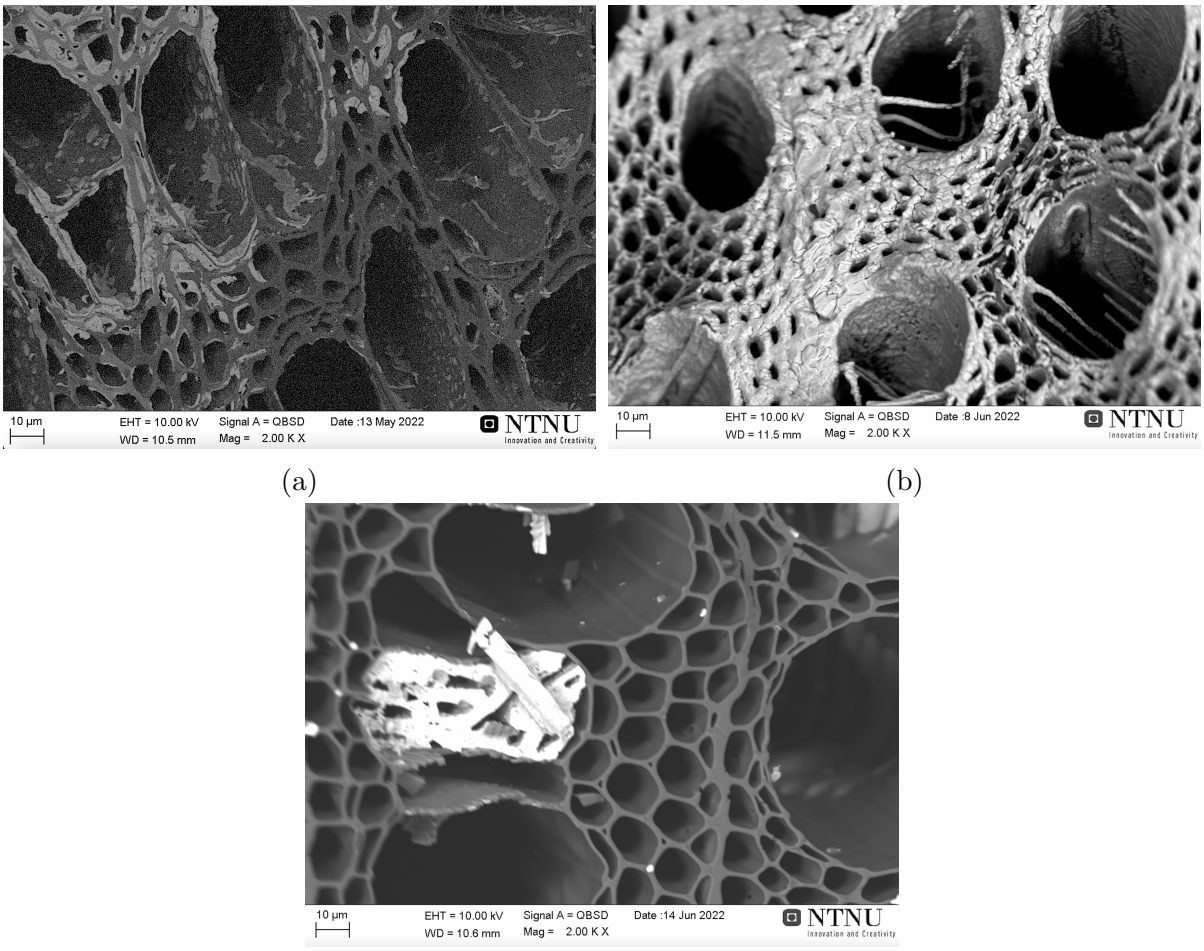

Figure 5.2: Figure (a) is of the middle of CharcoalRM2.95%K_g, Figure (b) is of the middle of CharcoalHT6.86%K_g and Figure (c) is of the middle of CharcoalRM8.71%K_w . All figures using BSE analysis.

The surface of the particles studied in SEM is presented in Figure 5.3, showing pictures from BSE analysis of the surfaces. The two wet K-impregnated particles have a quite similar potassium attachment where there is white particles of potassium, both small and large particles, attached to the surface roughness and pores. For the gas K-impregnated samples there is a larger difference between the surfaces, where Figure 5.3a have a surface almost completely covered with small potassium particles where Figure 5.3b have a few small particles distributed over the surface. Comparing the two gas K-impregnated surfaces with the CT pictures, then Figure 5.3a could be an example on a completely impregnated particle, where Figure 5.3b could be one of the particles where the impregnation could not be seen.

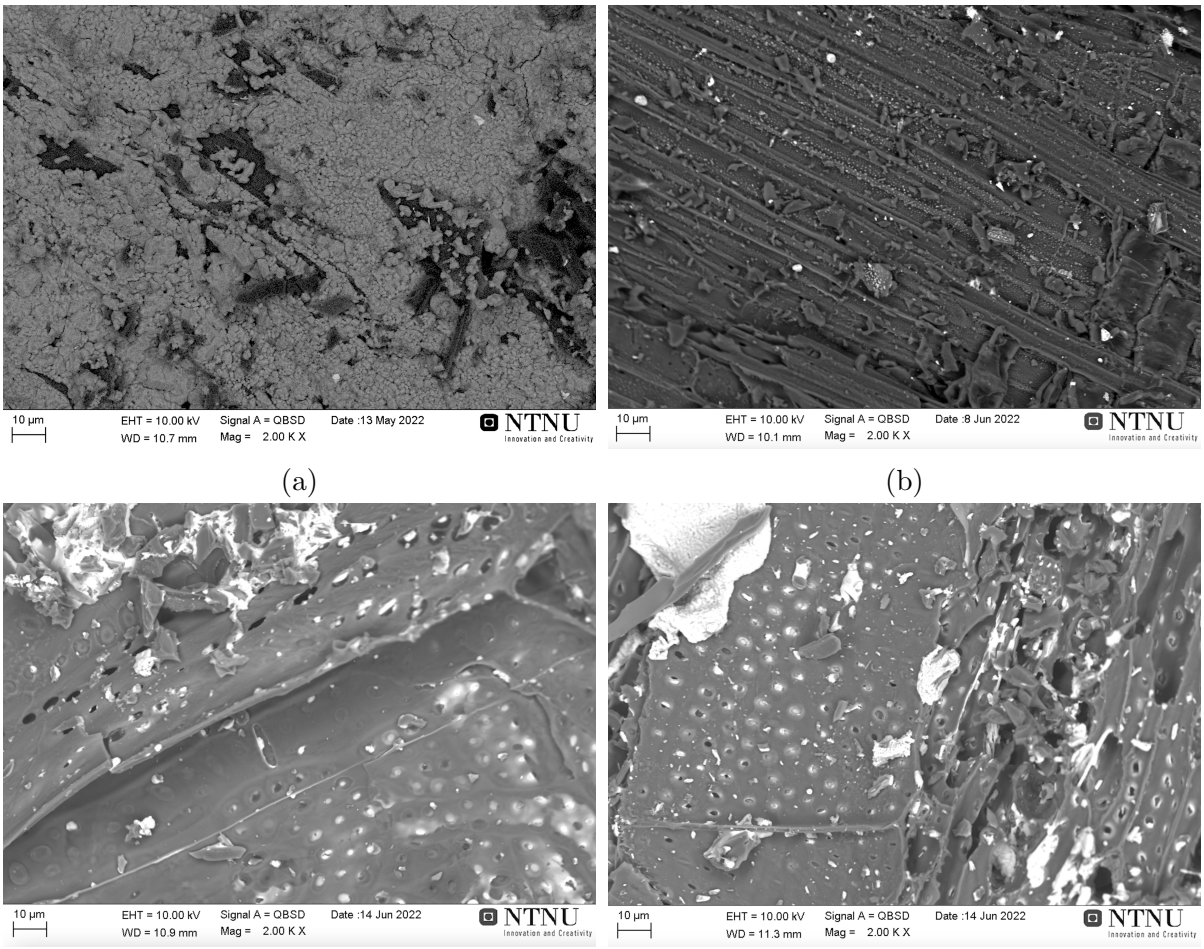

Figure 5.3: Showing the BSE pictures of the surface of: Figure (a) CharcoalRM2.95%K_g, Figure (b) CharcoalHT6.86%K_g, (c) CharcoalRM8.71%K_w and Figure (d) CharcoalHT10.53%K_w.

Both on the surface and in the middle of the particles, there seems to be potassium in all the studied particles. For the wet K-impregnated particles it is mostly attached to the charcoal as large particles distributed in the charcoal. Where the gas K-impregnated particles show a larger variety of potassium attachment, it seems like the completely impregnated charcoal particles both have a completely covered surface with potassium, and that the pores are filled with small potassium particles. The potassium particles with lower potassium content could be understood to have a few small potassium particles placed on the charcoal particle. There is only a few particles analyzed for this thesis, so the results found here is only temporary and there could be other methods for potassium attachment than found here.

5.3 CO_2 reactivity

All the K-impregnated samples were used to measure CO_2 reactivity to see how the potassium content affects the CO_2 reactivity of the carbon materials. What is found in this work will be analyzed with earlier results. The CO_2 reactivity of the charcoal will also be compared to coke since the goal with this project is to see if charcoal could substitute coke in the manganese alloy production.

It is found that the CO_2 reactivity of CharcoalRM is 0.0314 %FixC/s [8], CharcoalHT is 0.0305 %FixC/s and Coke is 0.0014 %FixC/s. From these values, it can be seen that the charcoal CO_2 reactivity is more than 10 times the CO_2 reactivity of coke. Comparing these values with the typical values for charcoal and coke from earlier research, then it can be seen that the charcoal has a 10 times higher CO_2 reactivity there as well. [10]. The rest of this section will focus on the effect potassium have on the measured CO_2 reactivity of the wet and gas K-impregnated carbon materials.

5.3.1 Gas K-impregnation

Compared to the raw materials in this project work, all the gas K-impregnated samples were showed to increase in potassium content, and for all of the samples this resulted in an increase in the CO_2 reactivity as well, Table 4.5. The CO_2 reactivity is measured as the slope of the amount fixed carbon that reacts over time until 20% of the FixC have reacted. For the gas K-impregnated carbon materials, the results from this project is showed in Figure 4.40. While Figure 5.4 show the values for all the results from this project, and compared to earlier projects in Appendix A.1.

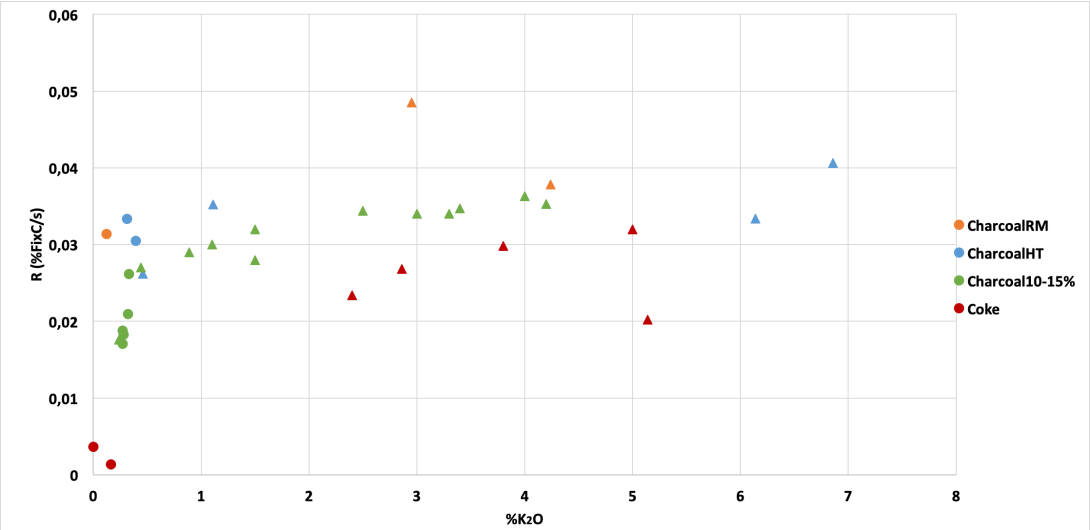

Figure 5.4: CO_2 reactivities versus potassium content for gas K-impregnated carbon materials from this project and earlier projects. The circular points is raw material, where the triangles is the gas K-impregnated samples.

If considering all the charcoal samples in Figure 5.4, there can be seen a tendency that all the raw materials and samples with less than 1%K_2O have a CO_2 reactivity which varies

a lot for the same $\%K_2O$. For charcoal values above $1\%K_2O$, the CO_2 reactivity almost stabilizes between 0.03 %FixC/s to 0.04%FixC/s. For coke, the values seem to increase evenly for the $\%K_2O$ values attained in this work. For the values for coke with around $5\%K_2O$, it is difficult to say something about the tendency, but since theory states that potassium is supposed to increase the CO_2 reactivity of the carbon materials, the deviating lower point will be assumed to be an outlayer for the rest of this report. The reason for why this point is so deviating could be many. One reason might be that the potassium content in the batch for CO_2 reactivity and chemical analysis were different, which is likely since there is a large difference between the particles after gas K-impregnation according to SEM and CT.

Studying the gas K-impregnation of CharcoalRM, it can be seen from Figure 5.4 that an increase from $0.12\%K_2O$ to $2.95\%K_2O$ and $4.24\%K_2O$ results in an increase from 0.0314 %FixC/s to 0.0485 %FixC/s and 0.0378 %FixC/s. The point for $2.95\%K_2O$ and 0.0485 %FixC/s lays almost 0.01 %FixC/s above the rest of the points for CO_2 reactivity for the same amount of potassium. For CharcoalRM there is one upper point where the CO_2 reactivity is significantly higher than for the rest of the charcoal samples. Due to this, the point with $2.95\%K_2O$ for CharcoalRM is assumed to be an outlayer as well. It is not enough points measured for gas K-impregnated CharcoalRM to say anything about the tendencies for the correlation between $\%K_2O$ and CO_2 reactivity for CharcoalRM alone.

If studying CharcoalHT in Figure 5.4, there is no clear tendencies for values below $1.11\%K_2O$. But when increasing the potassium content up to $3\%K_2O$, the CO_2 reactivity stays between 0.035 %FixC/s to 0.041 %FixC/s. For the heat treated charcoal the CO_2 reactivity almost stays constant for increasing potassium content. As the raw material is exposed to 1100 °C during CO_2 reactivity test, this material will also be heat treated before the Boudouard reaction starts, and the two groups of not treated raw materials (CharcoalRM) and heat treated raw materials (CharcoalHT) could be one group, as seen in Figure 5.4.

Lastly, studying the densified materials with densification degree between 10 and 15%, the CO_2 reactivity increases rapidly from around 0.015 %FixC/s to 0.035 %FixC/s for $\%K_2O$ values from 0 to $2\%K_2O$. All the densified materials are from earlier results [8]–[10], but added to be able to see eventual tendencies. For values above $2\%K_2O$ the CO_2 reactivity seems to stabilize around $0.035\%K_2O$ for increasing potassium content. The highest potassium content measured for the densified materials is around $4.25\%K_2O$. For higher values the change in CO_2 reactivity versus $\%K_2O$ is uncertain.

Considering all the points in Figure 5.4 together, the charcoal stabilizes between 0.03 and 0.04 %FixC/s for all $\%K_2O$ attained. Comparing the charcoal values with the values for coke, it can be seen a slower increase in CO_2 reactivity with increasing $\%K_2O$ for coke. Since the highest potassium content for coke is around $5\%K_2O$, there is difficult to say if the values for coke stabilizes around the same CO_2 reactivity as charcoal or not. However, for the highest attained $\%K_2O$ for coke, the value for coke and charcoal is almost the same and within the area of 0.03 to 0.04 %FixC/s.

If the two outlayers from this project work is removed, then the results from this work fits into the development from the points from earlier research. For the values above $6\%K_2O$ for CharcoalHT, it be the tendency where the values for CO_2 reactivity between 0.03 to 0.04 %FixC/s continues for higher potassium levels.

5.3.2 Wet K-impregnation

From the results, Table 4.6, the potassium content increases for all the wet K-impregnated samples compared to the raw materials before impregnation. In Figure 5.5 the values from this work is added with results from earlier research [8], [9]. The earlier research is given in Table A.1. Most of the values for CharcoalRM and CharcoalHT is a part of this work, but some of the points is from earlier.

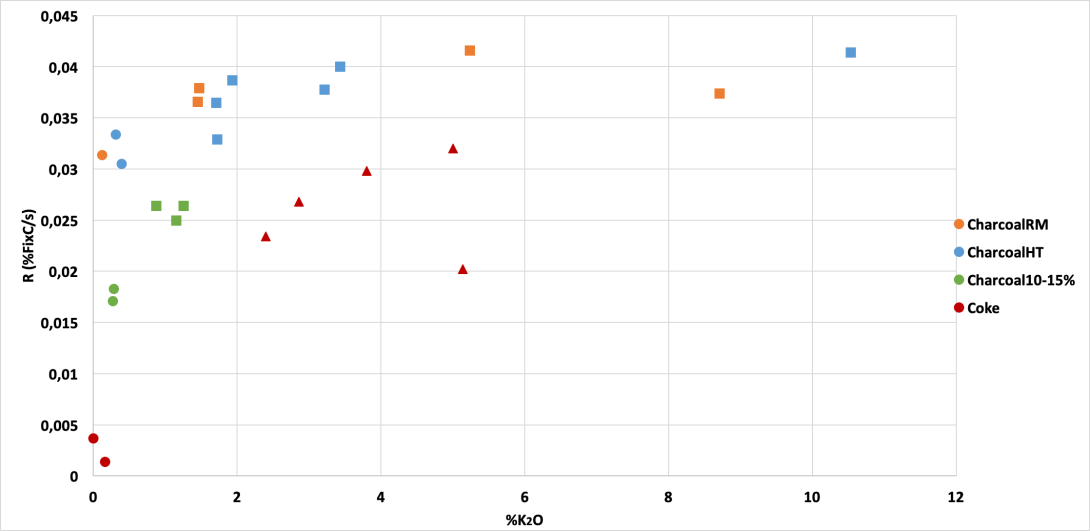

Figure 5.5: CO_2 reactivities versus potassium content for wet K-impregnated charcoal from this project and earlier projects [8], [9]. The circular points is raw material, where the triangles is the gas K-impregnated samples. Coke is added for comparison.

First considering the change in CO_2 reactivity showed in Figure 5.5 for CharcoalRM before and after wet K-impregnation. CharcoalRM have a potassium content of 0.12 and CO_2 reactivity of 0.0314 %FixC/s. After wet K-impregnation the potassium content in the charcoal increases, and for the impregnations using molarities of 2.5 and 5, the potassium content is increased to 5.23%K_2O and 8.71%K_2O. The following increase in CO_2 reactivity is not as immense with an increase from 0.0314 %FixC/s up to 0.0416 %FixC/s. For CharcoalHT the tendencies are quite like CharcoalRM. The increase in CO_2 reactivity relative to potassium content is relatively similar for both raw materials. Only that CharcoalHT achieves a higher potassium value of 10.53 %K_2O.

The last group of charcoals, is the densified charcoals from authors earlier research. All the densified charcoal has a densification degree between 10-15%K_2O. For this group, it can be seen a rapid increase in CO_2 reactivity for potassium content below 1%K_2O. The CO_2 reactivity seems to increase for the values up to 2%K_2O, however there is no measured CO_2 reactivity for potassium values above 2%K_2O.

Comparing all the values for wet K-impregnated charcoal, there seems to be increase in the values for CO_2 reactivity for increasing potassium content up to 2%K_2O. For higher values, it seems that the CO_2 reactivity stabilizes between 0.035 to 0.045 %FixC/s. All the wet K-impregnated measurements is higher than the values for coke, and if coke is to stabilize at the highest measured value, the wet K-impregnated charcoal will have a CO_2 reactivity which is around 0.01 %FixC/s higher.

5.3.3 Temperature drop

The CO_2 reactivity is the measured rate of the Boudouard reaction, Reaction 1.4. In the literature section, there is performed a calculation about the size of the temperature drop when assuming only carbon in the carbon material and a temperature of 1100 °C when the purging of CO and CO_2 starts. The result of this calculation was a temperature drop from 1100 °C to 207 °C if the Boudouard reaction continued until 20% of the carbon had reacted. This will of course be less due to the continued energy input from the furnace in the experiments, however in the industrial furnace the drop may be higher than experienced in the lab scale investigations.

From the CO_2 reactivity measurements, the temperature drop for the carbon materials were measured, given in Figure 4.45 and 4.46. From these figures, the temperature drop increases for most samples with increasing potassium content. And where the calculated temperature drop is around 900 °C, the highest achieved temperature drop during the CO_2 reactivity tests is 207.6 °C, but most of the values lays around 100-150 °C. There might be several reasons for the large difference between the calculated temperature drop and the achieved temperature drop. First the surroundings for the crucible during the CO_2 reactivity test keep a higher temperature through the experiment, which will give a continuous addition to the temperature to the reacting charcoal. Another aspect that contributes to keeping the temperature high is the power in the furnace, because when the temperature decreases, the furnace will automatically increase the power to increase the temperature inside the furnace. The last aspect to be mentioned is that some of the CO_2 reactivity measurements is stopped before 20% of the fixed carbon has reacted. This will cause the temperature drop to be calculated using a temperature that is warmer than the actual temperature. However, since there is only some percent of the charcoal remaining to react, it is possible to assume that the temperature would not decrease enough to change the temperature drop to be more like the calculated temperature drop.

There is no significant difference between the temperature drop caused by the different K-impregnation methods. Therefore, it can be assumed that the method used for potassium impregnation not the be the important factor regarding the temperature drop. However, the higher potassium contents with the highest measured CO_2 reactivity is the samples with the highest temperature drop. This implies that inside the furnace when producing manganese alloys, the temperature drop will be larger when using carbon materials with higher CO_2 reactivity.

5.3.4 Comparing methods

An aspect discovered using CT and SEM, is that the different batches of charcoal analyzed have different amounts of potassium. Also, the particles can vary a lot within the batch. This makes the samples very exposed to differences in the potassium content when dividing the batches for the analyses. This might also explain why some of the measured potassium contents does not seem to correspond with the other results from the batch, like the outliers found when discussing the CO_2 reactivity, since the batch used for the CO_2 reactivity measurements could have a different potassium content than the batch used for the chemical analysis. The difference between each particle seems to be larger with the gas K-impregnated particles, it can explain why there is more outlayers for the gas K-impregnation than for the wet.

From earlier explanations of the curves for CharcoalRM and CharcoalHT, Figure 5.5 and 5.4, the CO_2 reactivity versus $\%K_2O$ is similar. The major difference between the raw materials, is that CharcoalRM have more volatiles than CharcoalHT. During heat treatment, the volatiles will be removed, which is the case for CharcoalHT. Since the CO_2 reactivity for the same potassium contents is similar for both the materials, it can be discussed if there is any difference between impregnating charcoal before or after removing the volatiles. Since the CO_2 reactivity is so similar, it can be assumed that the presence of volatiles does not affect how the potassium contributes to a change in CO_2 reactivity. This also makes it possible to study CharcoalRM and CharcoalHT as one.

To be able to compare the results from gas K-impregnation with the wet K-impregnated samples, all the values are plotted together in Figure 5.6. The first aspect to be noticed is that almost all the CO_2 reactivity increases for increasing potassium content for values up to $2\%K_2O$. Most of the values for both impregnation methods blend together so well that it is difficult to separate between the methods when they are plotted together. However, there is some differences between CharcoalRM versus the densified charcoals. For all the measured values, the densified charcoal is almost 0.005 %FixC/s lower than for CharcoalRM. There are no values to state how the development for densified materials will be for higher values than $4\%K_2O$. The overall increase in CO_2 reactivity for CharcoalRM is small. Compared with the increase in the densified materials, the increase is significantly higher for potassium content below $2\%K_2O$. Coke have the fastest increase in CO_2 reactivity compared to the other carbon materials. These differences in the rate the different materials increases their CO_2 reactivity for increasing potassium content, results in the CO_2 reactivity almost being the same for potassium levels above $3.5\%K_2O$.

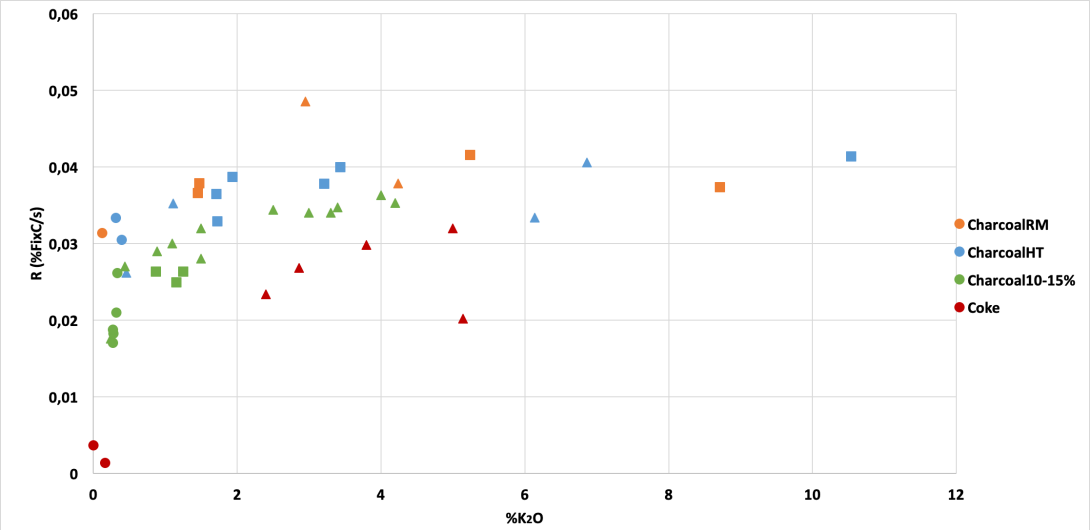

Figure 5.6: CO_2 reactivities versus potassium content for gas and wet K-impregnated charcoal from this project and earlier projects. The circular points is raw material, where the triangles is the gas K-impregnated samples.

Earlier research have used densification as a method for decreasing the CO_2 reactivity of the charcoal [6], [8], [9], [34]. Studying the effect of potassium compared to the effect of densification, there seems to be a higher reduction in CO_2 reactivity after densification than effect of potassium for potassium content below 2%K. There is assumed that the potassium content in the low temperature area in the furnace is above 3.5%K [36]. For values above 3.5%K the potassium increases the CO_2 reactivity of the densified charcoal to the same level as CharcoalRM and CharcoalHT. This might imply that the potassium has a higher effect on the CO_2 reactivity than densification.

The attachment of potassium found in Figure 5.2 and 5.3 showed that the gas K-impregnation had smaller potassium particles covering large areas of the surface or only a few distributed particles in the sample. For the wet K-impregnated samples the larger K-particles were distributed around the charcoal particle. Comparing the potassium attachment to the charcoal particle with the CO_2 reactivity measured for the samples, there is no significant difference between the potassium content or the corresponding CO_2 reactivity. Earlier research showed that there was a larger difference between the size of the particles and the achieved CO_2 reactivity [9]. However, the results found were based on potassium contents up to 2 $\%K_2O$, and for lower potassium contents there can be seen a difference between the CO_2 reactivity here as well.

For the higher potassium contents, the difference between the carbon materials is small. One reason for this might be that a potential driving force for the effect of potassium on the CO_2 reactivity is the partial pressure of potassium. If the potassium is attached as pure potassium, potassium carbonate or KO_2, the Reactions 2.2, 5.1 and 5.2 show possible reactions that could take place during the CO_2 reactivity. The common part between the reactions, is that they all produce potassium gas. The reason for assuming these reactions is first for the gas K-impregnated samples found in Figure 3.8 to be KO_2 or assumed to be pure K, when the temperatures in the CO_2 reactivity test reaches 1100 °C, the potassium and potassium oxides starts to react forming K (g). The same for wet K-impregnation,

where the solution uses K_2CO_3 at lower temperatures than the boiling temperature, which means there most likely will be potassium carbonate on the wet K-impregnated samples. When potassium carbonate reaches 1100 °C, then the oxide also will react with carbon producing K (g). Due to all these reactions producing K (g), the partial pressure of K (g) might be the reason for the placement of potassium at higher potassium values results in the same CO_2 reactivity.

$$K_2CO_3 + 2C = 2K(g) + 3CO(g) \tag{2.2}$$

$$K(s) = K(g)) \tag{5.1}$$

$$KO_2 + 2C = K(g) + 2CO(g) \tag{5.2}$$

Inside the industrial furnace the potassium content was assumed to be above 3.5%, which results with only the potassium content above 3.5%K_2O is interesting for the furnace operations. To show how the CO_2 reactivity changes for potassium levels above 3.5%K_2O, Figure 5.7 shows the relevant points. In this figure it can be seen that all the CO_2 reactivity lays between 0.029 to 0.043 %FixC/s. Which again implies that the differences between gas and wet K-impregnated samples, densified charcoal and coke is quite small, if it exists at all.

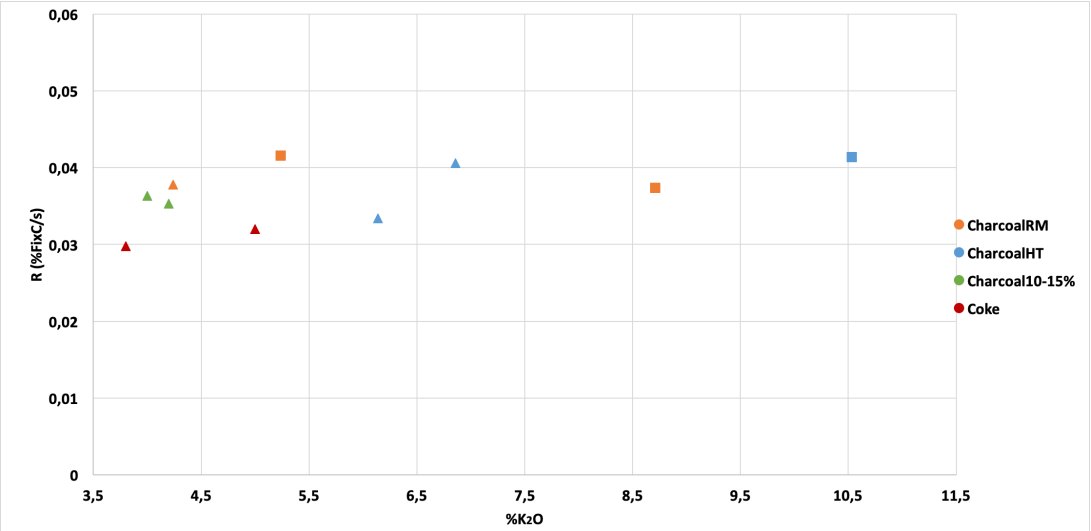

Figure 5.7: CO_2 reactivities versus potassium content for gas and wet K-impregnated charcoal from this project and earlier projects. The circular points is raw material, where the triangles is the gas K-impregnated samples. This figure is adjusted for the potassium content inside the furnace of 3.5%K_2O and points assumed to be outliers is removed.

If the values for densified charcoal and coke continues the tendencies found for higher potassium, then all the carbon materials will have almost the same CO_2 reactivity for the potassium contents found inside the SAF furnace when producing manganese alloys. If the CO_2 reactivity values for all carbon materials is almost the same, then the CO_2

reactivity can be neglected as a difference between charcoal and coke when considering a change of carbon materials in the manganese alloy production.

The temperature drop inside the SAF will be affected by different CO_2 reactivity. But as mentioned above, the materials used have almost the same CO_2 reactivity, and therefore the temperature drop caused by the Boudouard reaction will be almost the same for all the samples. Again, making the difference between the CO_2 reactivity of the different carbon materials being quite similar.

5.4 Industrial relevance

Potassium impregnation of charcoal is done to be able to understand how the carbon materials in the manganese alloy production is affected by potassium. Inside the furnace there is potassium present from the manganese ore and some from the carbon materials, and the K-impregnation is to see how the potassium alone affects the carbon materials. To find out the effect of potassium outside of the furnace, the carbon materials needs to be impregnated with this potassium and then be further analyzed to be able to find the effect of only potassium. This means that the K-impregnation will only be performed on a lab-scale, and not performed in the industry. This also implies that the methods will not need to be adapted to impregnate larger amounts of carbon material at the time.

In the section where the experimental procedure for the gas K-impregnation, there is mentioned that there were two incidents that occurred. These incidents took place because the alkalis on the charcoal auto-ignited. These alkalis will already be present in the industry inside the furnace when producing manganese alloys, and the experiments performed in this thesis is to simulate the effect of these alkalis. Due to this, there will not change anything for the industry, it will only be a risk at lab scale.

As mentioned, the CO_2 reactivity for the relevant $\%K_2O$ values inside the SAF is quite similar for CharcoalRM, CharcoalHT, densified charcoal and coke. This implies that the CO_2 reactivity differences inside the furnace will not be affected in a large degree when changing carbon material from coke to charcoal. There are several other properties that might affect the furnace operations, but according to the results in this project work, there seems to be a small difference if only considering the CO_2 reactivity for the different carbon materials with different potassium contents.

6 Concluding remarks and further work

Charcoal and coke have been impregnated with potassium to understand the effect on the CO_2 reactivity inside the manganese alloy furnace. The K-impregnated materials were analyzed with visual inspection using SEM and CT, and the CO_2 reactivity or the rate of the Boudouard reaction 1.4 were used to compare the impregnation methods.

$$CO_2 + C = 2CO \tag{1.4}$$

Both wet and gas K-impregnation showed an increase in potassium content for all impregnated samples compared to the raw materials. However, the increase during wet K-impregnation with 5 molar solution had the highest achieved potassium content. To be able to study charcoal at higher potassium levels, the cheapest, easiest and most effective method will be the wet K-impregnation method to achieve potassium contents above the level found inside the manganese alloy furnace.

From SEM and CT, it was found a large difference in the amounts of potassium in the different particles analyzed for gas K-impregnated samples, where the charcoal particles were more like each other after wet K-impregnation. This makes the results from each of the wet K-impregnated more comparable, since the potassium content were more similar when the sample were divided into batches for the different analyses. There were also found a difference in how the potassium attached to the charcoal particles, but from the CO_2 reactivity measurements it did not seem to be affecting the rate of the Boudouard reaction.

The CO_2 reactivity was found to increase for increasing potassium content, it was also found to stabilize for potassium values above 3 $\%K_2O$ at a CO_2 reactivity between 0.030 and 0.045 %FixC/s for all the carbon materials tested. Since the alkali content inside the furnace is above 3.5%K, it was assumed that the CO_2 reactivity for both coke and charcoal is between 0.030 and 0.045 %FixC/s inside the furnace. This implies that the difference between the CO_2 reactivity between coke and charcoal is small or none. Densified charcoal also seems to reach the same values for the potassium levels found inside the furnace, resulting in no difference between charcoal and densified charcoal regarding the CO_2 reactivity. These conclusions are made considering the results found for this thesis, but the results are temporary and needs to be researched further to confirm these conclusions.

There is still needed more data on the higher potassium contents and how the CO_2 reactivity changes for high potassium values for the different carbon materials. The tendencies for the CO_2 reactivity in this thesis looks promising for a change from coke to charcoal in the manganese production, but the results are temporary until there is more data on the subject confirming the results found in this thesis. There are also several other properties which are important for the carbon material in the SAF, and they need to be studied as well.

References

[1] Eli Ringdalen. "Reduced CO_2 emissions in metal production". (2019), [Online]. Available: https://www.sintef.no/en/projects/2018/reduced-co2-reduced-co2-emissions-in-metal-production/. (accessed: 07.12.2021).

[2] FN Sambandet. "Parisavtalen". (2020), [Online]. Available: https://www.fn.no/om-fn/avtaler/miljoe-og-klima/parisavtalen. (accessed: 11.05.2022).

[3] European Comission. "Sustainable development goals". (2016), [Online]. Available: https://ec.europa.eu/international-partnerships/sustainable-development-goals. (accessed: 11.05.2022).

[4] Tor Lindstad, "CO_2-emissions and the ferroalloy industry", INFACON 8, Beijing, Mar. 1998.

[5] Bodil Monsen, Merete Tangstad, Ingeborg Solheim, and Martin Syvertsen, "Charcoal for manganese alloy production", INFACON XI, Vol.11, New Delhi, 2007.

[6] Liang Wang, Fredrik Buvarp, Øyvind Skreiberg, Pietro Bartocci, and Francesco Fantozzi, "A study on densification and CO_2 gasification of biocarbon", *AIDIC - associazione italiana di ingegneria chimica*, vol. 65, pp. 145–150, 2018. DOI: https://doi.org/10.3303/CET1865025.

[7] Nicholas Smith, "Properties of carbon reductants for Si and ferroalloy production", *SINTEF*, 2019.

[8] Emma Solhaug, "Different methods for k-impregnation of charcoal and the effet on the CO_2 reactivity", *Summer project, NTNU, Faculty of Natural Sciences, Department of Material Science and Engineering*, 2021.

[9] ——, "Densified biocarbon and the effect of potassium on the CO_2 reactivity", *Specialization project, NTNU, Faculty of Natural Sciences, Department of Material Science and Engineering*, 2021.

[10] Hamideh Kaffash, Gerrit R. Surup, and Merete Tangstad, "Densification of biocarbon and its effect on CO_2 reactivity", *Process*, vol. 9, p. 193, 2021. DOI: https://doi.org/10.3390/pr9020193.

[11] Merete Tangstad, *Metal production in Norway*. Akademika Publishing, 2013, ISBN: 978-82-321-0241-9.

[12] Emma Solhaug, "Introduction to manganese ferroalloys production (lecture notes)", *Norwegian University of Science and Technology, Department of Material Science and Engineering*, 2021.

[13] Merete Tangstad, Johan Paul Beukes, Joalet Steenkamp, and Eli Ringdalen, in *New Trends in Coal Conversion*, Isabel Suáres-Ruiz, Maria Antonia Diez, and Fernando Rubiera, Eds. Woodhead Publishing, 2019, ch. 14. Coal-based reducing agents in ferroalloys and silicon production, pp. 405–438, ISBN: 9780081022016. DOI: https://doi.org/10.1016/B978-0-08-102201-6.00014-5.

[14] Sverre E. Olsen, Merete Tangstad, and Tor Lindstad, *Production of Manganese Ferroalloys*. Tapir Academic Press, 2007, ISBN: 978-82-519-2191-6.

[15] Merete Tangstad, in *Handbook of Ferroalloys*, Ed. Butterworth-Heinemann, 2013, ch. 7. Manganese Ferroalloys Technology, pp. 221–266, ISBN: 9780080977539. DOI: https://doi.org/10.1016/B978-0-08-097753-9.00007-1.

[16] R. K. Pachauri, M. R. Allen, V. R. Barros, *et al.*, *Synthesis report; Intergovernmental Panel on Climate Change*. Climate change 2014: 2014, ISBN: 978-92-9169-143-2.

[17] United States Environmental Protection Agency. "Overview of greenhouse gases". (2021), [Online]. Available: https://www.epa.gov/ghgemissions/overview-greenhouse-gases. (accessed: 14.02.2022).

[18] Marcus Sommerfeld and Bernd Friedrich, "Replacing fossil carbon in the production of ferroalloys with a focus on bio-based carbon: A review", *Minerals*, vol. 11, no. 11, p. 1286, 2021. DOI: https://doi.org/10.3390/min11111286.

[19] Tor Lindstad, Sverre E. Olsen, Gabriella Tranell, Tor Færden, and Jonathan Lubetsky, "Greenhouse gas emissions from ferroalloy production", INFACON XI, Vol. 2, New Delhi, 2007, ISBN: 978-0230-63070-3.

[20] Bodil Monsen, Merete Tangstad, and H. Midtgaard, "Use of charcoal in silicomanganese production", Thenth International Ferroalloys Congress, Cape Town, South Africa, 2004, pp. 392–404, ISBN: 0-9584663-5-1.

[21] University of Alaska Fairbanks. "Underground mining methods handout (lecture notes)". (2009), [Online]. Available: https://web.archive.org/web/20090326053910/http://www.faculty.uaf.edu/ffrg/min454/Handout2_UMM.doc. (accessed: 20.05.2022).

[22] Anton Dilo Paul, "Coal, fuel and non-fuel uses", *Encyclopedia of Energy*, vol. 118, Cutler J. Cleveland, Ed., pp. 435–444, 2004. DOI: https://doi.org/10.1016/B0-12-176480-X/00290-4.

[23] Bodil Monsen, Tor Lindstad, and Johan K. Tuset, "CO_2 emissions from the production of ferrosilicon and silicon metal in norway.", Electric Furnace Conference, Vol. 56, New Orleans, 1998, ISBN: 9781886362291.

[24] Wei Huo, Zhijie Zhou, Xueli Chen, and Z. Guangsuo Yu, "Study on co2 gasification reactivity and physical characteristics of biomass, petroleum coke and coal chars", *Bioresource thechnology*, vol. 159, no. 5, pp. 143–149, 2014, ISSN: 0960-8524. DOI: https://doi.org/10.1016/j.biortech.2014.02.117.

[25] Hamideh Kaffash and Merete Tangstad, "The effect of densification on compressive strength of charcoal", INFACON XVI, Trondheim, 2020.

[26] A. Abánades, E. Ruiz, E. M. Ferruelo, *et al.*, "Experimental analysis of direct thermal methane cracking", *International journal of hydrogen energy*, vol. 36, no. 20, pp. 12 877–12 886, 2011, ISSN: 0360-3199. DOI: https://doi.org/10.1016/j.ijhydene.2011.07.081.

[27] International Carbon Black Association. "What is carbon black?" (2006), [Online]. Available: https://web.archive.org/web/20090401121937/http://www.carbon-black.org/what_is.html#. (accessed: 11.12.2021).

[28] Meng-Jiao Wang, Charles A. Gray, Steve A. Reznek, Khaled Mahmud, and Yakov Kutsovsky, "Carbon black", 2003. DOI: https://doi.org/10.1002/0471238961.0301180204011414.a01.pub2.

[29] A. Dufour, A. Celzard, E. Martin, F. Broust, V. Fierro, and A. Zoulalian, "Catalytic decomposition of methane over a wood char concurrently activated by pyrolysis gas", *Applied Catalysis: General*, vol. 346, no. 1-2, pp. 164–173, 2008, ISSN: 0926-860X. DOI: https://doi.org/10.1016/j.apcata.2008.05.023.

[30] Marius Larsen, "Densification of charcoal", 2021.

[31] ——, "Densification of charcoal and its characterization", *Summer project, NTNU, Faculty of Natural Sciences, Department of Material Science and Engineering*, 2021.

[32] Hamideh Kaffash and Merete Tangstad, "The effect of densification on compressive strength of charcoal", INFACON XVI, Trondheim, 2021. DOI: http://dx.doi.org/10.2139/ssrn.3926700.

[33] "Hsc chemistry". (), [Online]. Available: http://www.hsc-chemistry.net. (accessed: 11.05.2022).

[34] ——, "CO_2 gasification of densified biomass: The influence of K on reaction rate", *JOM*, vol. 74, pp. 1900–1907, 2022. DOI: https://doi.org/10.1007/s11837-021-05150-7.

[35] Kira Turkova, Dmitry Slizovskiy, and Merete Tangstad, "CO reactivity and porosity of manganese materials", *ISIJ International*, vol. 54, no. 5, pp. 1204–1208, 2014. DOI: https://doi.org/10.2355/isijinternational.54.1204.

[36] Merete Tangstad, *Conceptual tapping model of mn-ferroalloy furnaces (powerpoint presentation)*, (accessed: 20.05.2022).

[37] M. Alam and T. DebRoy, "The effects of CO and CO_2 on the Na_2CO_3 catalyzed boudouard reaction", *Metallurgical Transactions B*, vol. 15.2, pp. 400–403, 1984.

[38] Y. K. Rao, A. Adjorlolo, and J. H. Haberman, "On the mechanism of catalysis of the boudouard reaction by alkali-metal compounds", *Carbon*, vol. 20, pp. 207–212, 1982, ISSN: 0008-6223. DOI: https://doi.org/10.1016/0008-6223(82)90022-7.

[39] T. Lindstad, M. Syvertsen, R. J. Ishak, and H. B. Arntzen, "The influence of alkalis on the boudouard reaction", 2004.

[40] Kawnish Kirtania, Joel Axelsson, Leonidas Matsakas, Paul Christakopoulos, Kentaro Umeki, and Erik Furusjö, "Kinetic study of catalytic gasification of wood char impregnated with different alkali salts", *Energy*, vol. 118, no. C, pp. 1055–1065, 2017.

[41] Alfa Aesar. "12609 potassium carbonate, acs, 99.0% min". (), [Online]. Available: https://www.alfa.com/en/catalog/012609/. (accessed: 11.12.2021).

[42] Engineering Toolbox. "Fuels and chemicals - autoignition temperatures". (2003), [Online]. Available: https://www.engineeringtoolbox.com/fuels-ignition-temperatures-d_171.html. (accessed: 16.05.2022).

[43] Nicholas Smith, SINTEF, *Personal communication through project work*, (accessed: 19.04.2022).

[44] Jarle Hjelen, *Scanning elektron-mikroskopi*. Metallurgisk institutt, NTH, 1986.

A Appendix

A.1 Calculations for temperature balance using HSC for the CO_2 reactivity

	A	B	C	D	E
1	INPUT SPECIES (1) Formula	Temper. °C	Pressure bar	Amount kmol	Amount kg
2	CO2(g)	1100,000		0,002	0,070
3	CO(g)	1100,000		0,002	0,045
4	C	1100,000		0,002	0,028
5	C	1100,000		0,001	0,007

Figure A.1: Input parameters into the heat and material balance function in HSC

	A	B	C	D	E
1	OUTPUT SPECIES (1) Formula	Temper. °C	Pressure bar	Amount kmol	Amount kg
2	CO(g)	25,000		0,004	0,101
3	C	25,000		0,002	0,028
4	CO2(g)	25,000		0,001	0,026

Figure A.2: Output parameters into the heat and material balance function in HSC

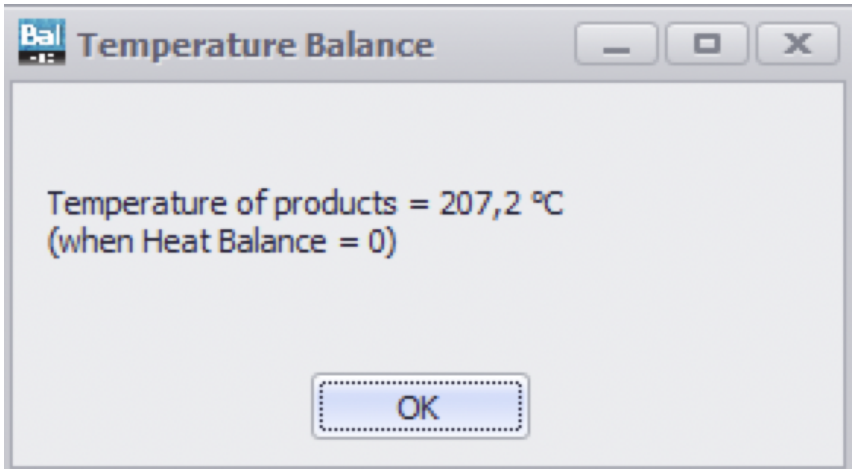

Figure A.3: Calculated temperature balance in the heat and material balance function in HSC

A.2 Calculations of the reaction enthalpy for HMS case

Reaction Equations

File Edit Format Sheet Options Help

Specifications

Reaction Equation or Chemical Formula | Smallest Coefficient: 1 | Balance

2KO2 + H2O(g)= 2KOH + 3/2 O2(g)

	From (°C)	To (°C)	Step (°C)		
Temperature	0,000	100,000	5,000	Browse...	Calculate

	A	B	C	D	E	F	G	H
1	**Reaction Equation**							
2	**2KO2 + H2O(g)= 2KOH + 3/2 O2(g)**							
3								
4	**Reaction Data**							
5	**T**	**ΔH**	**ΔS**	**ΔG**	**K**		**Log K**	
6	**°C**	**kJ**	**J/K**	**kJ**				
7	0,000	-40,060	30,848	-48,486	1,874E+009		9,273	
8	5,000	-40,062	30,841	-48,640	1,365E+009		9,135	
9	10,000	-40,070	30,809	-48,794	1,005E+009		9,002	
10	15,000	-40,086	30,756	-48,948	7,479E+008		8,874	
11	20,000	-40,107	30,682	-49,102	5,622E+008		8,750	
12	25,000	-40,134	30,591	-49,255	4,265E+008		8,630	
13	30,000	-40,170	30,470	-49,407	3,265E+008		8,514	
14	35,000	-40,212	30,334	-49,559	2,521E+008		8,402	
15	40,000	-40,258	30,185	-49,711	1,962E+008		8,293	
16	45,000	-40,309	30,025	-49,861	1,538E+008		8,187	
17	50,000	-40,363	29,857	-50,011	1,215E+008		8,085	
18	55,000	-40,420	29,681	-50,160	9,662E+007		7,985	
19	60,000	-40,480	29,500	-50,308	7,735E+007		7,888	
20	65,000	-40,542	29,315	-50,455	6,230E+007		7,795	
21	70,000	-40,606	29,127	-50,601	5,049E+007		7,703	
22	75,000	-40,671	28,938	-50,746	4,115E+007		7,614	
23	80,000	-40,738	28,748	-50,890	3,372E+007		7,528	
24	85,000	-40,806	28,557	-51,034	2,778E+007		7,444	
25	90,000	-40,874	28,368	-51,176	2,300E+007		7,362	
26	95,000	-40,943	28,180	-51,317	1,913E+007		7,282	
27	100,000	-41,011	27,995	-51,458	1,599E+007		7,204	

Figure A.4: Calculations of the reaction between water vapor and KO_2 at 25 °C using HSC.

A.3 CO_2 reactivity from earlier research

Table A.1: A overview over the results from the CO_2 reactivity test, which shows the potassium content (%K_{20}) and the reaction rate, R. The different treatments performed is either untreated (none), heat treated (HT), densified (dens), K-impregnated using gas (gas) or using wet K-impregnation (wet).

Sample name	**Treatment**	**%FixC**	**%K_{20}**	**R (%FixC/s)**	**Ref.**
CharcoalRM	None	85.2	0.12	0.0314	[8]
CharcoalRM1.47%K_w	None	79.7	1.47	0.0379	[8]
CharcoalHT (350 g)	HT	96.9	0.30	x	[8]
CharcoalHT (750 g)	HT	94.6	0.39	x	[8]
Charcoal15%	Dens	96.7	0.27	0.0171	[8]
Charcoal15%0.24K_g	Gas	95.5	0.24	0.0176	[8]
Charcoal15%1.50K_g	Gas	94.6	1.50	0.0280	[8]
Charcoal15%3.40K_g	Gas	88.5	3.40	0.0347	[8]
Charcoal15%0.87K_w	Wet	94.3	0.87	0.0264	[8]
Charcoal-2%	Dens	96.7	0.27	0.0334	[9]
Charcoal-2%0.40K_g	Gas	95.5	0.24	x	[9]
Charcoal-2%0.46K_g	Gas	94.6	1.50	0.0262	[9]
Charcoal-2%6.14K_g	Gas	88.5	3.40	0.0334	[9]
Charcoal-2%1.71K_w	Wet	93.0	1.71	0.0365	[9]
Charcoal-2%1.93K_w	Wet	92.9	1.93	0.0387	[9]
Charcoal-2%1.72K_w	Wet	92.9	1.72	0.0329	[9]
Charcoal11%	Dens	96.9	0.28	0.0183	[9]
Charcoal11%1.15K_w	Wet	94.9	1.15	0.0250	[9]
Charcoal11%1.25K_w	Wet	87.8	1.25	0.0264	[9]
CharcoalA	Dens	98.1	0.27	0.0188	[10]
CharcoalA14.2%0.44%K_g	Gas	x	0.44	0.0270	[10]
CharcoalA14.2%1.10%K_g	Gas	x	1.10	0.0300	[10]
CharcoalA14.2%3.00%K_g	Gas	x	3.00	0.0340	[10]
CharcoalB	Dens	96.5	0.33	0.0262	[10]
CharcoalB13%1.50%K_g	Gas	x	1.50	0.0320	[10]
CharcoalB13%3.30%K_g	Gas	x	3.30	0.0340	[10]
CharcoalB13%4.20%K_g	Gas	x	4.20	0.0353	[10]
CharcoalC	Dens	96.7	0.32	0.0210	[10]
CharcoalC15%0.89%K_g	Gas	x	0.89	0.0290	[10]
CharcoalC15%2.50%K_g	Gas	x	2.50	0.0344	[10]
CharcoalC15%4.00%K_g	Gas	x	4.00	0.0363	[10]
Met.Coke	None	x	0	0.0037	[10]
Met.Coke	Gas	x	2.4	0.0234	[10]
Met.Coke	Gas	x	3.8	0.0298	[10]
Met.Coke	Gas	x	5	0.0320	[10]

A.4 Results from Proximate and Ash analysis from SINTEF Norlab

Table A.2: Proximate analysis of the different samples made and analyzed for this thesis.

Sample name	**Volatiles**	**%FixC**	**Ash**
CharcoalRM	12.7	85.2	2.1
CharcoalRM1.45K$_w$	16.12	79.13	4.75
CharcoalRM5.23K$_w$	15.80	71.80	12.40
CharcoalRM8.71K$_w$	16.72	65.03	18.25
CharcoalRM02.95K$_g$	5.65	80.87	13.48
CharcoalRM4.24K$_g$	4.7	85.92	9.38
CharcoalRM1.77K$_g$	2.0	94.65	3.35
CharcoalHT	2.41	94.90	2.69
CharcoalHT3.21K$_w$	5.07	87.77	7.16
CharcoalHT3.43K$_w$	6.54	82.75	10.71
CharcoalHT10.53K$_w$	8.63	71.32	20.05
CharcoalHT6.68K$_g$	4.81	82.17	13.02
CharcoalHT1.11K$_g$	2.13	94.72	3.15
CharcoalHT0.27K$_g$	1.59	95.5	2.91
Coke	2.05	86.65	11.3
Coke0.38K$_g$	1.17	88.90	9.93
Coke5.14K$_g$	0.62	87.77	11.61
Coke2.86K$_g$	2.62	78.58	18.8

Table A.3: Ash analysis of the different samples made and analyzed for this thesis. The oxides is given as a percentage of the ash given in Table A.2.

Sample name	**K_2O**	**SiO_2**	**TiO_2**	**Al_2O_3**	**Fe_2O_3**	**CaO**	**MgO**	**MnO**	**P_2O_5**
CharcoalRM	5.6	23.4	0.1	2.4	1.1	37.4	5.4	2.8	6.4
CharcoalRM1.45K_w	30.48	44.5	0.01	1.2	0.9	18.9	1.6	0.81	1.35
CharcoalRM5.23K_w	42.20	43.5	0.01	0.6	0.3	11.5	0.8	0.40	0.65
CharcoalRM8.71K_w	47.71	47.1	0.01	0.1	0.4	3.6	0.4	0.23	0.43
CharcoalRM2.95K_g	21.90	70.0	0.004	0.1	0.1	6.6	0.4	0.51	0.31
CharcoalRM4.24K_g	45.20	28.2	0.007	0.1	0.4	22.5	1.5	1.00	0.89
CharcoalRM1.77K_g	25.00	17.2	0.009	0.1	0.7	48.5	3.7	2.00	2.66
CharcoalHT	14.63	x	0.01	0.2	1.6	55.8	5.6	2.46	4.20
CharcoalHT3.21K_w	44.80	36.7	0.007	0.2	0.2	14.1	1.6	0.81	1.23
CharcoalHT3.43K_w	32.00	58.9	0.004	0.1	0.1	7.0	1.0	0.28	0.48
CharcoalHT10.53K_w	52.50	40.4	0.002	0.2	0.1	5.5	0.5	0.32	0.35
CharcoalHT6.68K_g	52.70	33.0	0.003	0.1	0.1	11.7	1.1	0.42	0.72
CharcoalHT1.11K_g	35.10	26.0	0.010	0.2	0.9	29.4	3.6	1.80	2.76
CharcoalHT0.27K_g	9.40	19.8	0.023	0.2	0.8	60.3	4.6	2.30	2.31
Coke	1.42	42.3	0.95	19.5	10.7	14.3	7.9	0.14	1.25
Coke0.38K_g	3.85	48.1	1.47	29.7	6.8	3.1	1.4	0.03	0.48
Coke5.14K_g	44.30	24.6	0.76	15.0	4.6	1.7	0.8	0.03	0.30
Coke2.86K_g	15.20	38.0	1.18	23.2	5.8	2.9	1.1	0.02	0.50

A.5 Temperature and measured weight with calculations of slope from CO_2 reactivity tests.

The CO_2 reactivity curves measured in this work. Here the part from the purging of CO_2 (g) and CO (g) during the CO_2 reactivity measurements. The orange curve is the measured weight, and the slope of the linear part of the curve is given as the function y. The slope of this curve is the CO_2 reactivity for the different samples.

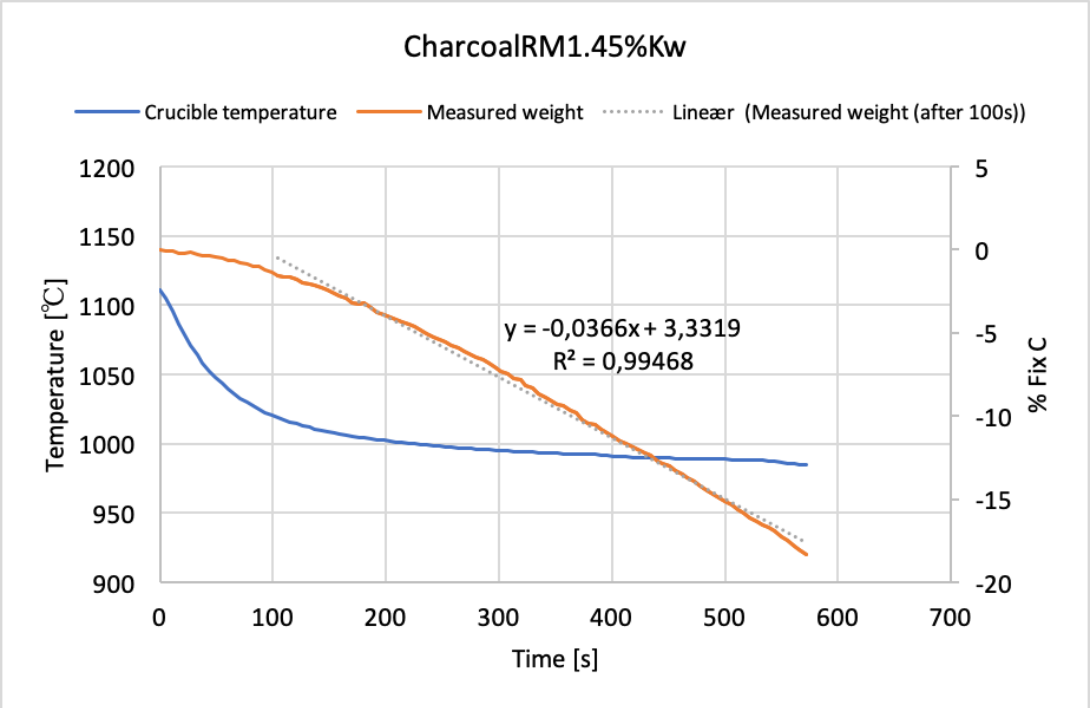

Figure A.5: CO_2 reactivity for the wet K-impregnated CharcoalRM using a 1 molar solution. The measured CO_2 reactivity is 0.0366 %FixC/s.

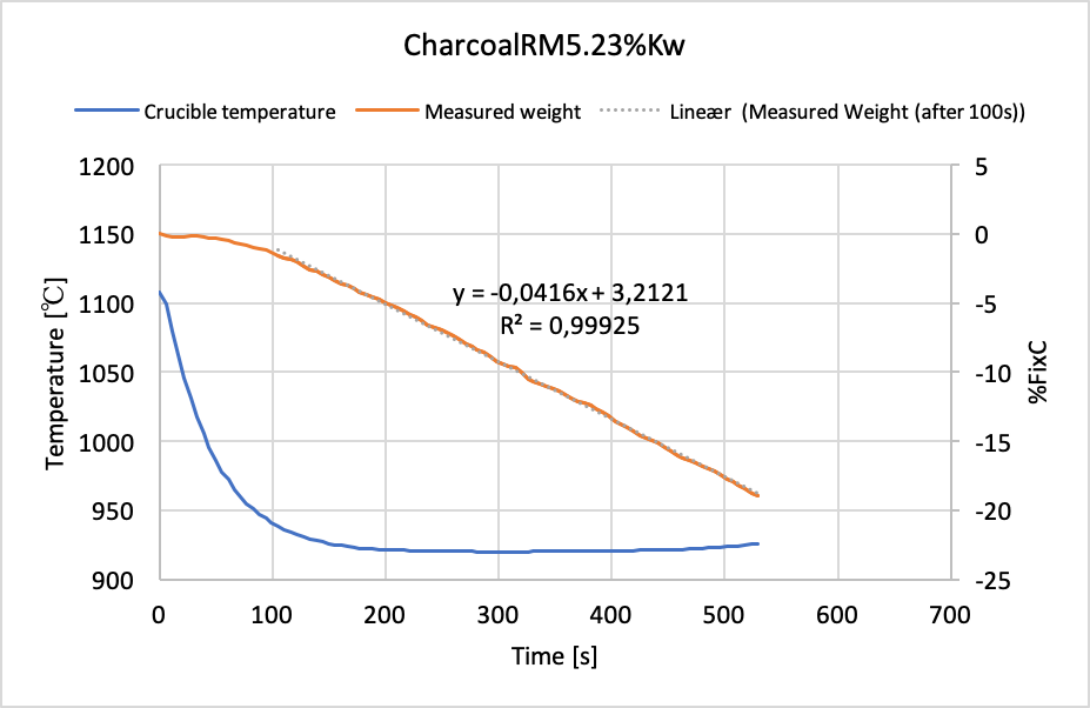

Figure A.6: CO_2 reactivity for the wet K-impregnated CharcoalRM using a 2.5 molar solution. The measured CO_2 reactivity is 0.0416 %FixC/s.

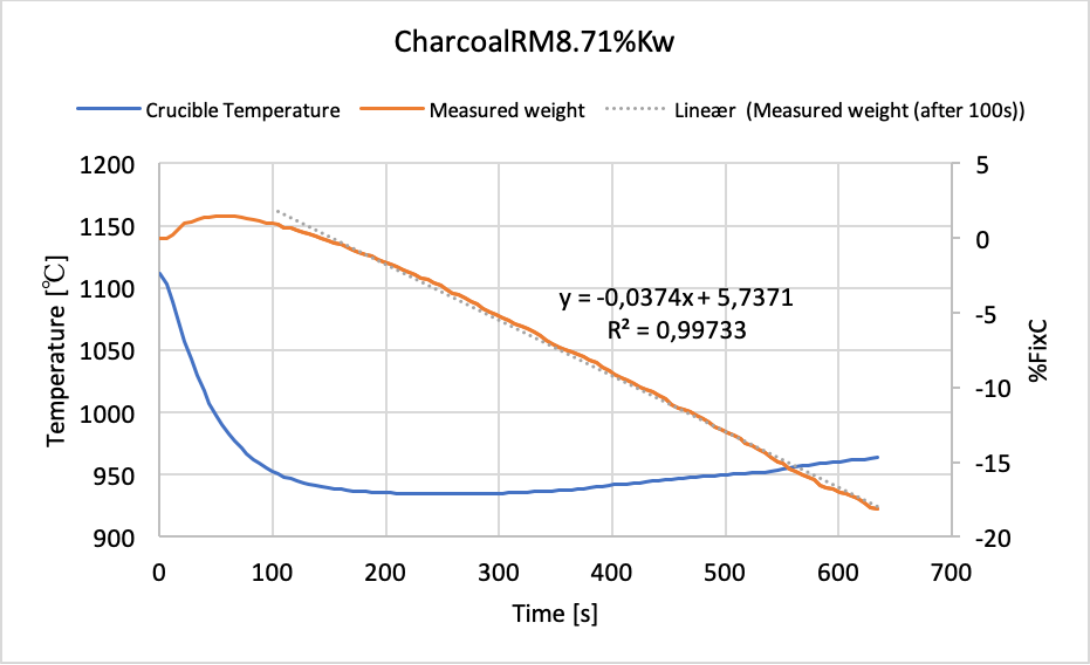

Figure A.7: CO_2 reactivity for the wet K-impregnated CharcoalRM using a 5 molar solution. The measured CO_2 reactivity is 0.0374 %FixC/s.

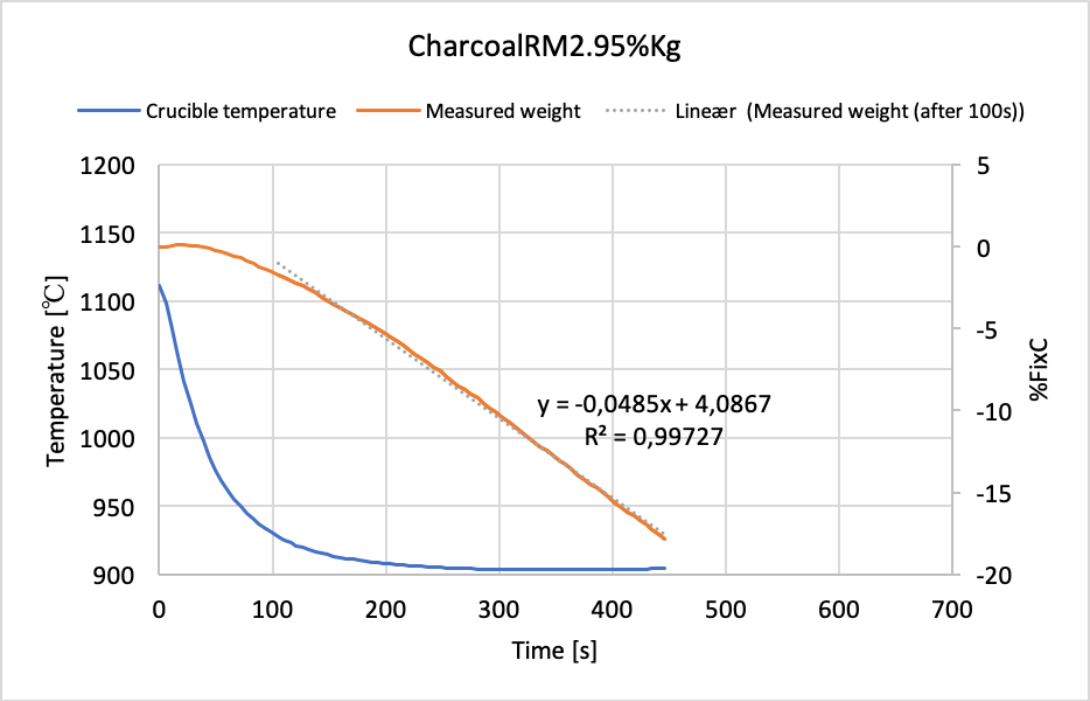

Figure A.8: CO_2 reactivity for bottom layer from the gas K-impregnated CharcoalRM. The measured CO_2 reactivity is 0.0485 %FixC/s.

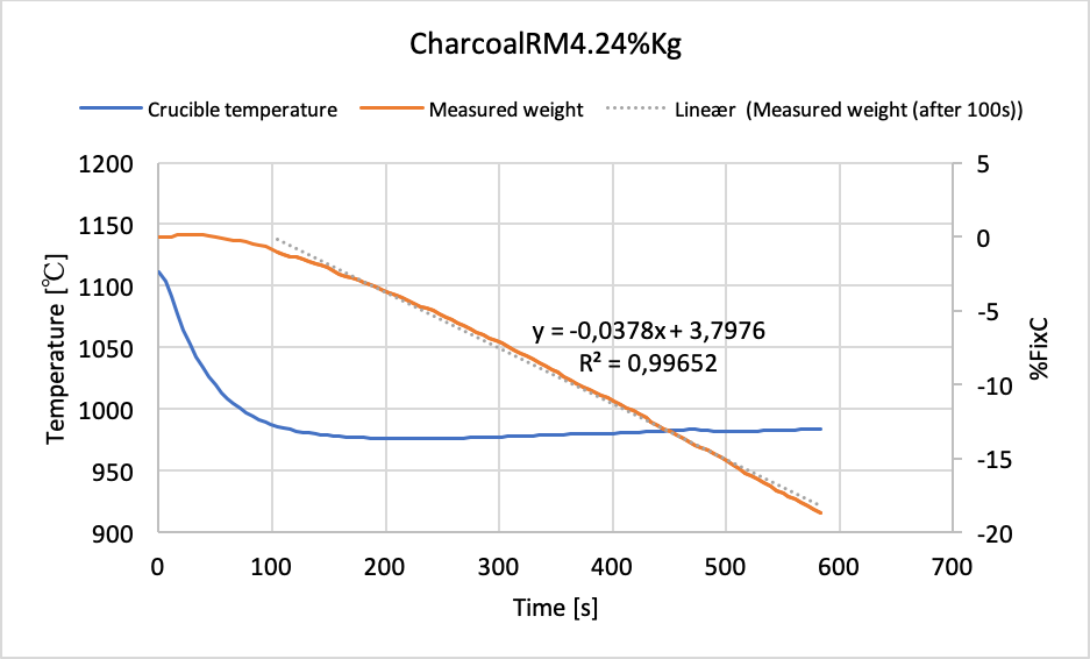

Figure A.9: CO_2 reactivity for middle layer from the gas K-impregnated CharcoalRM. The measured CO_2 reactivity is 0.0378 %FixC/s.

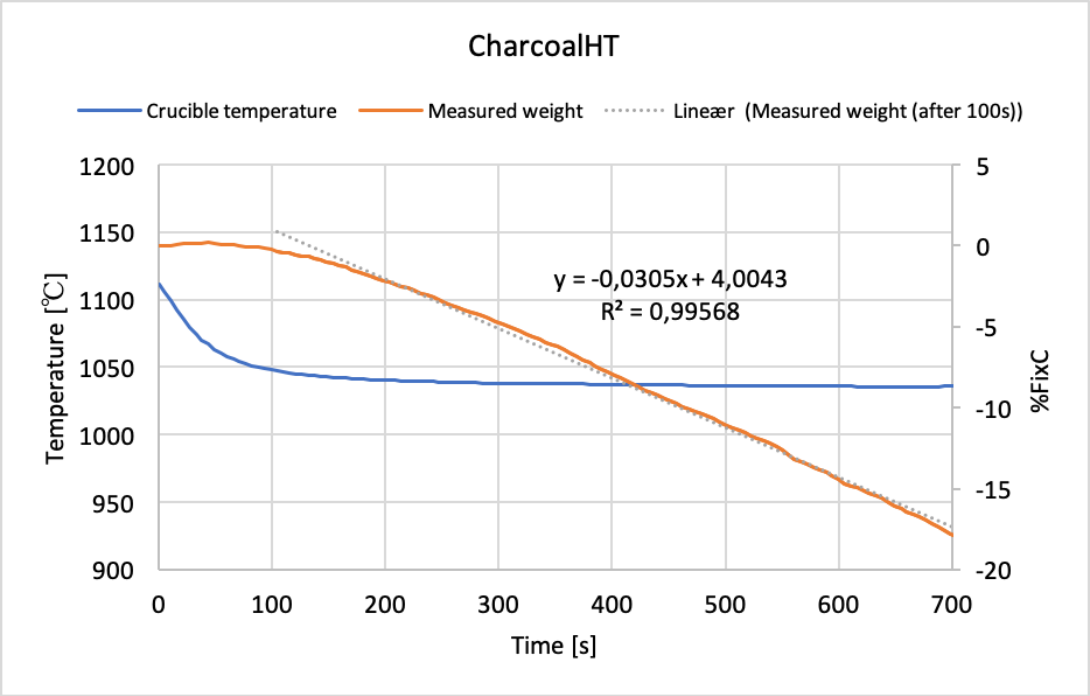

Figure A.10: CO_2 reactivity of CharcoalHT. The measured CO_2 reactivity is 0.0305 %FixC/s.

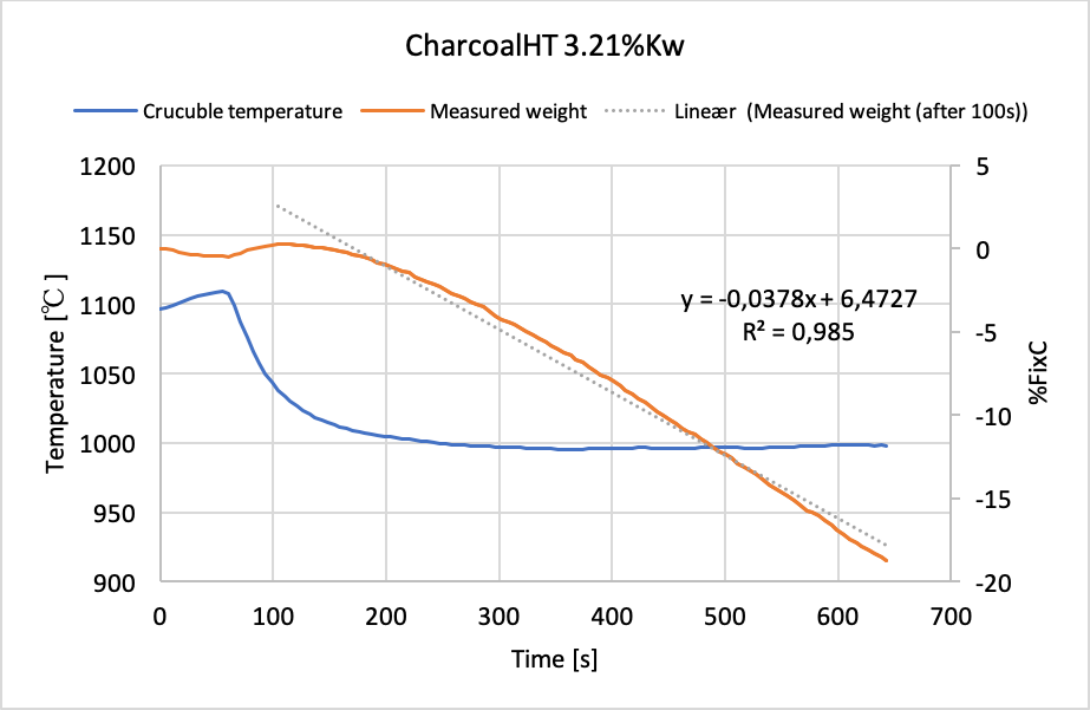

Figure A.11: CO_2 reactivity for the wet K-impregnated CharcoalHT using a 1 molar solution. The measured CO_2 reactivity is 0.0378 %FixC/s.

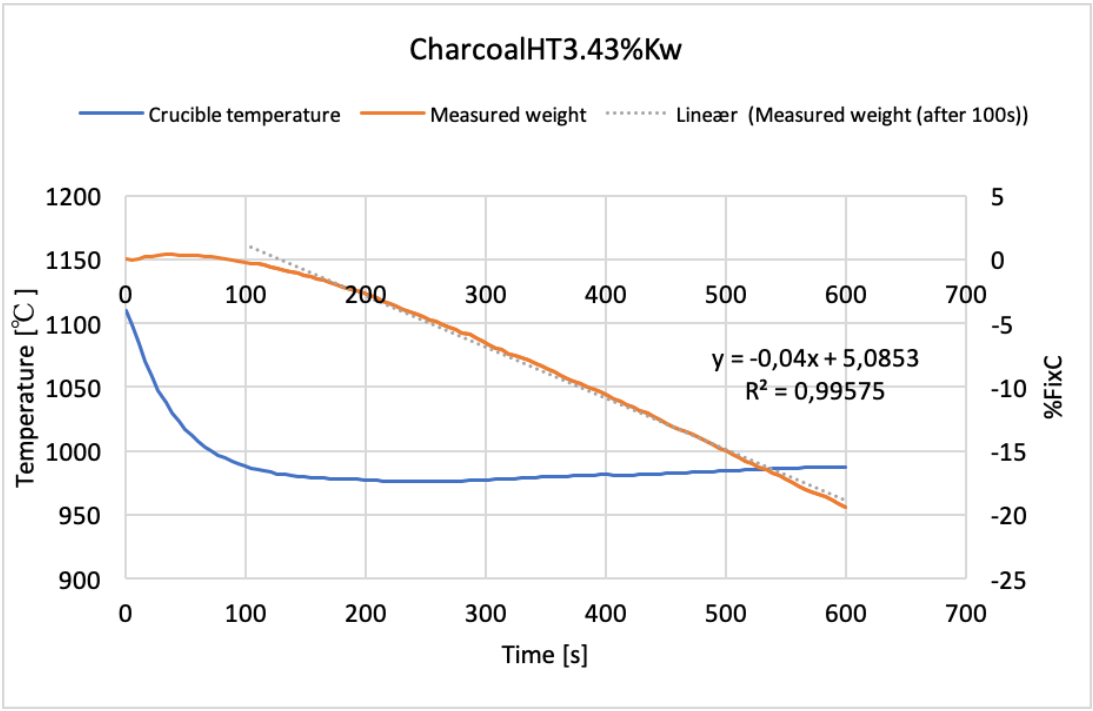

Figure A.12: CO_2 reactivity for the wet K-impregnated CharcoalHT using a 2.5 molar solution. The measured CO_2 reactivity is 0.0400 %FixC/s.

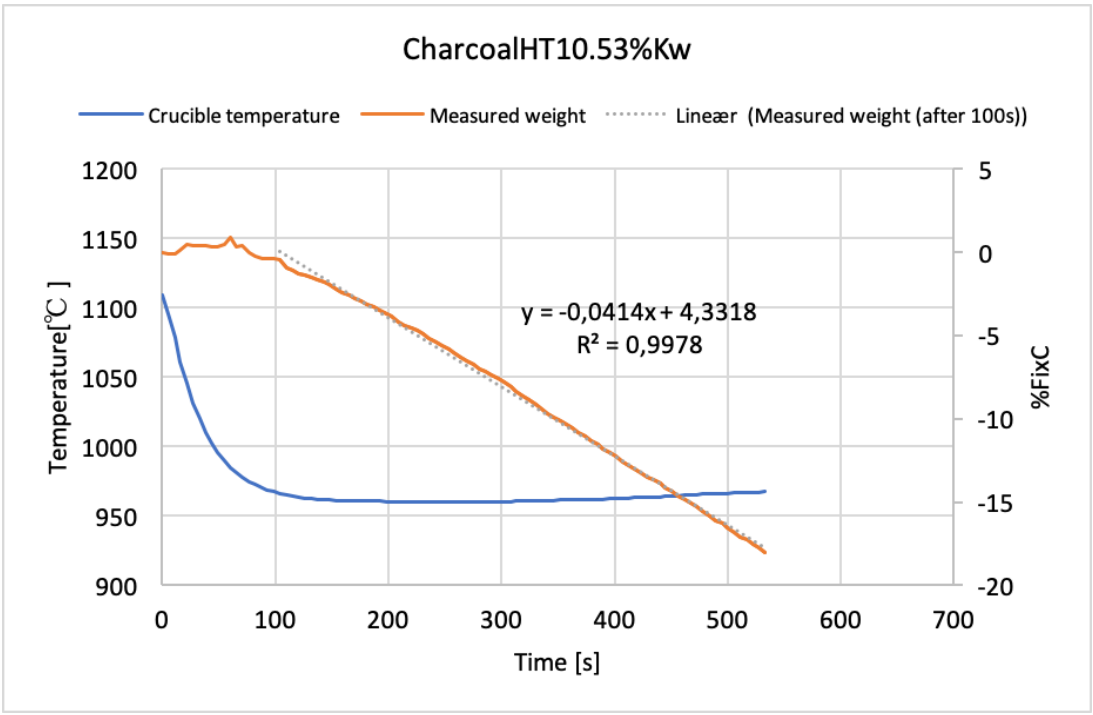

Figure A.13: CO_2 reactivity for the wet K-impregnated CharcoalHT using a 5 molar solution. The measured CO_2 reactivity is 0.0414 %FixC/s.

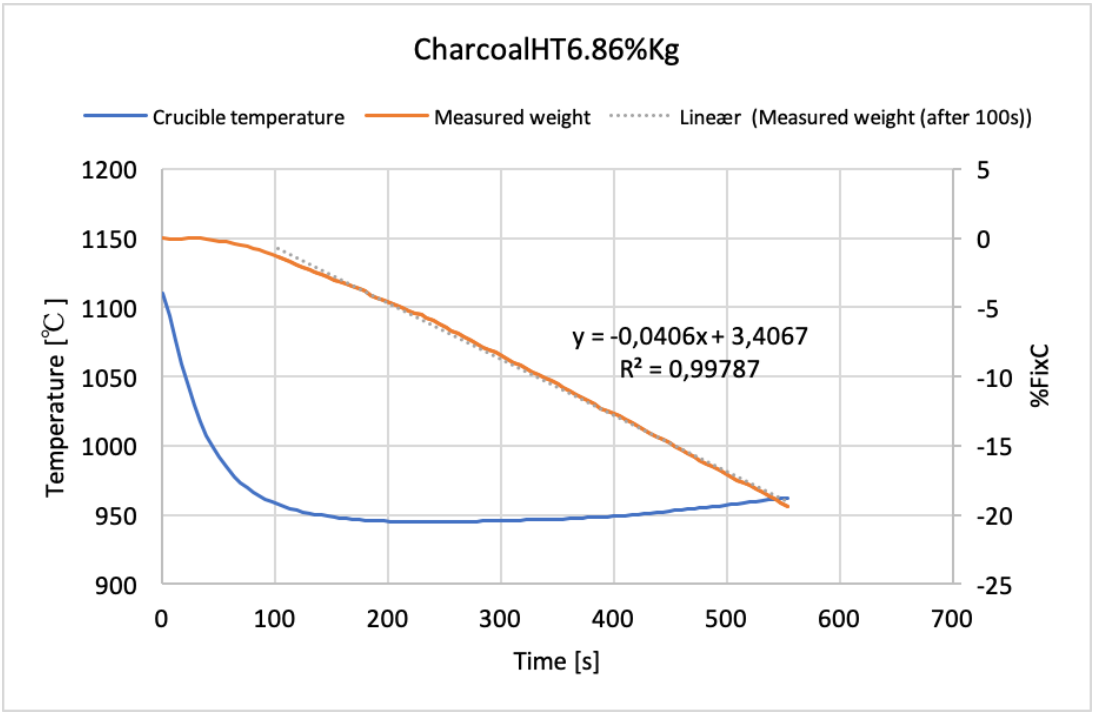

Figure A.14: CO_2 reactivity for bottom layer from the gas K-impregnated CharcoalHT. The measured CO_2 reactivity is 0.0406 %FixC/s.

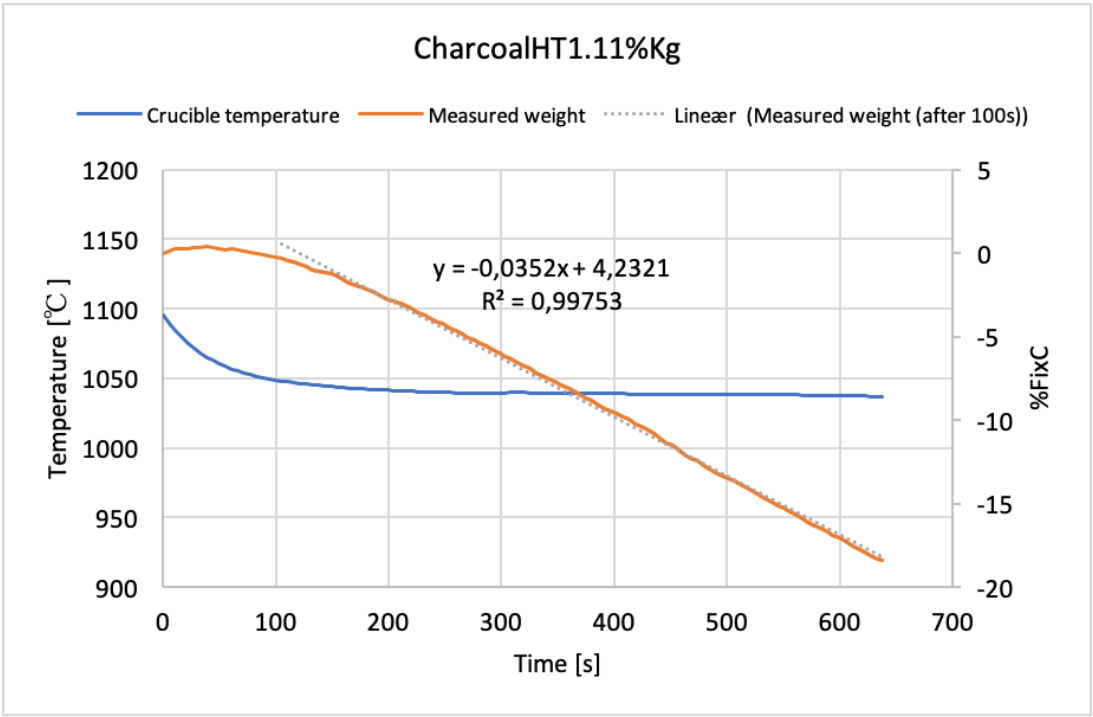

Figure A.15: CO_2 reactivity for middle layer from the gas K-impregnated CharcoalHT. The measured CO_2 reactivity is 0.0352 %FixC/s.

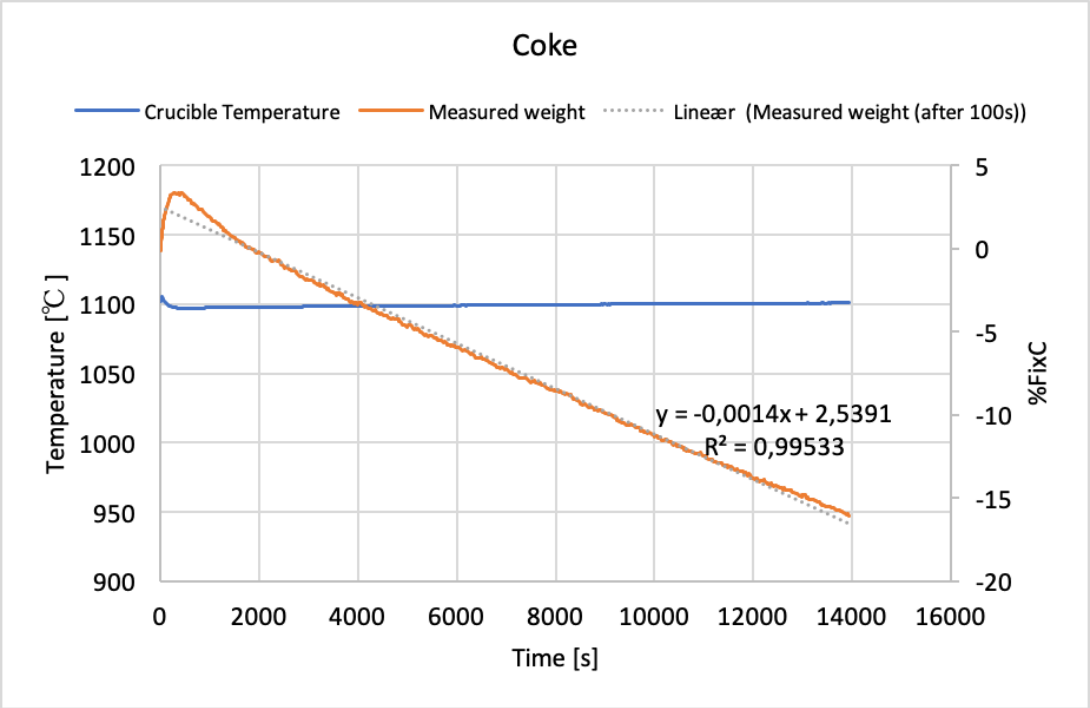

Figure A.16: CO_2 reactivity of Coke. The measured CO_2 reactivity is 0.0014 %FixC/s.

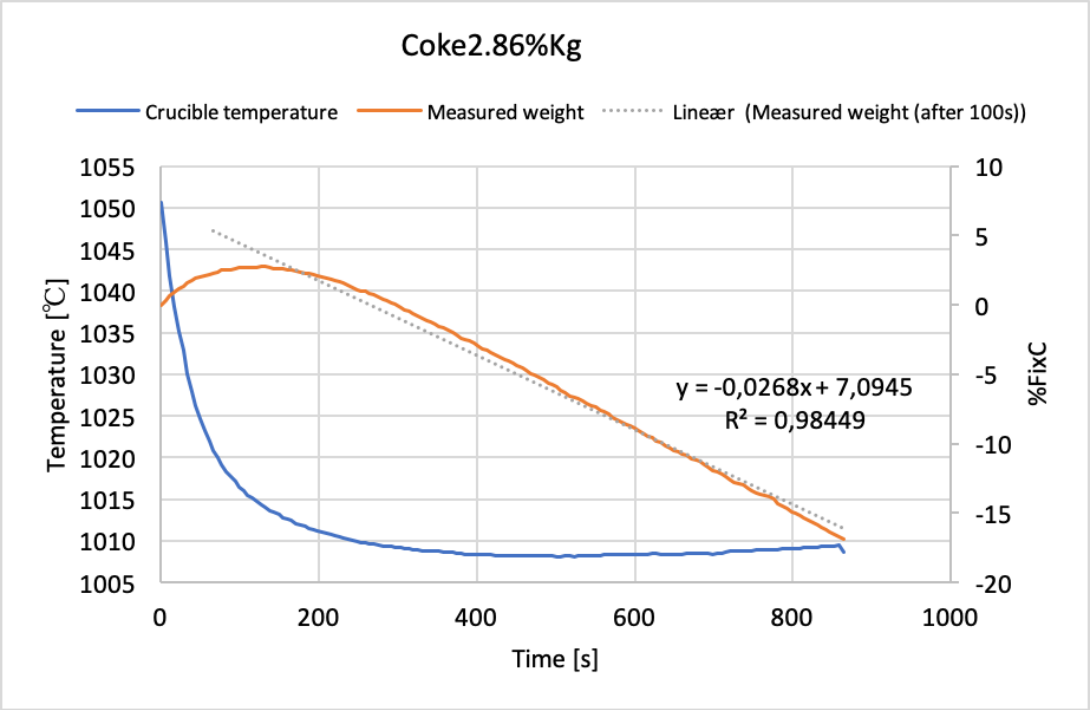

Figure A.17: CO_2 reactivity for bottom layer from the gas K-impregnated Coke. The measured CO_2 reactivity is 0.0268 %FixC/s.

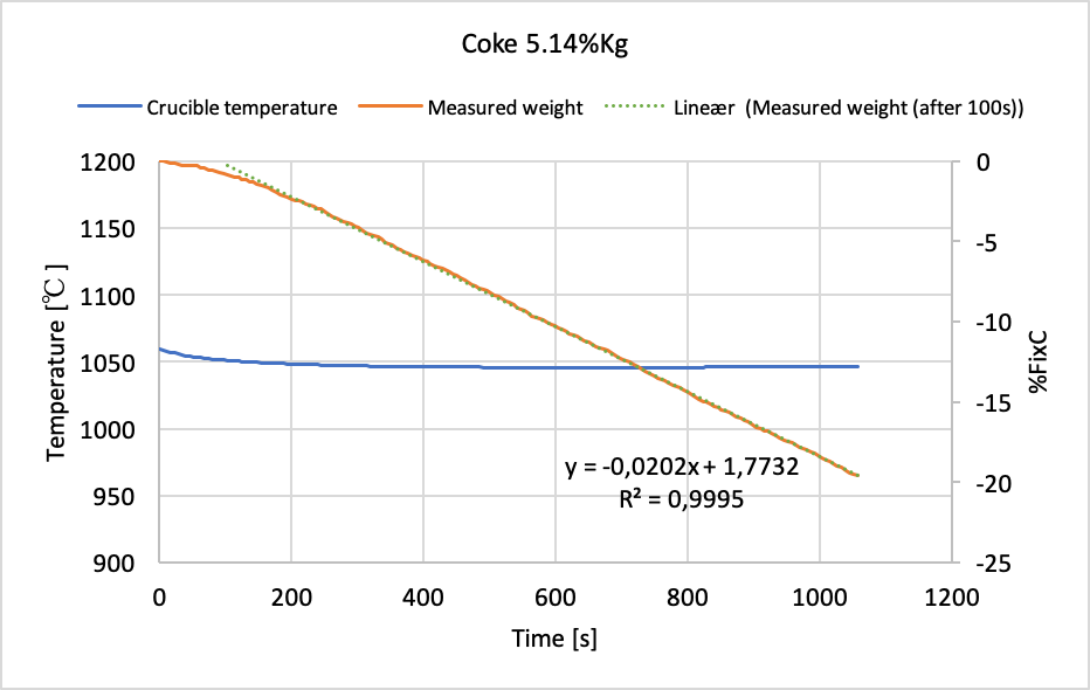

Figure A.18: CO_2 reactivity for middle layer from the gas K-impregnated Coke. The measured CO_2 reactivity is 0.0202 %FixC/s.

Emma Solhaug

Methods for K-impregnation of carbon materials and their effect on the CO_2 reactivity

NTNU
Norwegian University of
Science and Technology